Universität Karlsruhe (TH)

Institut für Zoologie II

Institutsleitung: Prof. Dr. Doris Wedlich

Function of *Xenopus* Cadherin-6

in Neural Development

Zur Erlangung des akademischen Grades eines

DOKTORS DER NATURWISSENSCHAFTEN

(Dr. rer. nat.)

der Fakultät für Chemie und Biowissenschaften der

Universität Karlsruhe (TH)

vorgelegte

DISSERTATION

von

Gui Ruan

aus Anshan, Liaoning Province, P.R.China

2004

Function of *Xenopus* Cadherin-6

in Neural Development

Zur Erlangung des akademischen Grades eines

DOKTORS DER NATURWISSENSCHAFTEN

(Dr. rer. nat.)

der Fakultät für Chemie und Biowissenschaften der

Universität Karlsruhe (TH)

vorgelegte

DISSERTATION

von

Gui Ruan

aus Anshan, Liaoning Province, P.R.China

2004

Dekan: Prof. Dr. Manfred Kappes

Referent: Prof. Dr. Doris Wedlich

Korreferent: PD. Dr. Jonathan P. Sleeman

Tag der mündlichen Prüfung: 19-23.07.2004

献给母亲，
铭记您的教诲"努力成为最好的！"

Dedicated to my mother,

who always said to me "Do your best to be the best!"

Abstract

Cadherins, **Ca²⁺** dependent cell to cell a**dhe**sion molecules, are crucial for cell sorting and tissue integrity during embryogenesis. Numerous cadherins are expressed in the developing brain. They are involved in compartmentalization of the early embryonic central nervous system (CNS) and in establishment and stabilization of the interneuronal connections. More recently, transcripts of *Xenopus* cadherin-6 (Xcad-6), a member of classical type II cadherins, were shown in the CNS, the developing eye and strongly in the peripheral nervous system (PNS), the placode-derived cranial nerves (David and Wedlich, 2000).

In an attempt to clarify the function of Xcad-6 during embryonic development, Xcad-6 expression pattern was first analyzed with the aid of a polyclonal antibody directed against the extracellular domain. Xcad-6 proteins appear from late neurula of stage 20 embryos onwards and gradually increase until tadpole of stage 40. A soluble isoform of Xcad-6 (sXcad-6), originating from alternatively splicing was proved to be present along with an integral full-length Xcad-6 during embryonic development. Cell transfections assays revealed that sXcad-6 is secreted into the supernatant. Whether sXcad-6 is of physiological significance in embryogenesis remains open.

In *Xenopus* development Xcad-6 is localized in the subpopulations of the CNS, where only the neurites and axons are Xcad-6 positive. Xcad-6 was also found predominantly expressed in the PNS including lateral line nerves. In the developing eye, Xcad-6 is initially confined to the inner- and outer limiting membrane, the interface between the invaginating optic vesicle and the surrounding tissues. Later, Xcad-6 expression extends to the other parts of the retina but still demarcates the neurites and axons of the neural retinal cells.

Microinjection of anti-sense Xcad-6 morpholino oligonucleotides (MO) led to reduced eye, abnormal eye and missing eye phenotypes observed in tadpole of stage 40 embryos. Murine cadherin-6 was able to rescue these eye defects. By RT-PCR and *in situ* hybridization, a role of Xcad-6 was excluded either for induction or separation of the eye field although Xcad-6 is exclusively expressed in the anterior neural plate of stage 13 embryos, which gives rise to eye field. However, histological examination revealed disrupted epithelial structure of the neural and pigmented retina in tailbud stage 27 embryos. Transplantation of MO-injected eye field further confirmed these defects in the polarized epithelia of the retina. In contrast, the reverse transplants proved a cell autonomous function of Xcad-6 during eye development. Phosphohiston3-detection and TUNEL assay revealed a reduction of mitosis and an increase of apoptosis in the developing eye after microinjection of Xcad-6 MO, which probably contribute to smaller eye, missing eye and degradation of Xcad-6 MO transplants. Thus, it is

concluded that Xcad-6 preserves epithelial structure and promotes growth of the presumptive neural and pigmented retina during the invagination of the optic vesicle.

Animal cap (AC) cultivation and N-CAM immunostaining revealed that Xcad-6 is involved in neurite formation and fiber fasciculation during interneuronal connection. Xcad-6 MO injected neuralized AC cells could not form neurites and a fiber network. Also, in *in vivo* embryos, cranial fibers deficient for Xcad-6 could not bundle properly. This suggests a role of Xcad-6 in interneuronal connections.

Zusammenfassung

Cadherine sind Ca^{2+}-abhängige Zell-Zell-Adhäsionsmoleküle, die während der Embryogenese an der Zellerkennung und Zelladhäsion beteiligt sind und auf diese Weise die Gewebeintegrität vermitteln. Zahlreiche Cadherine werden im Gehirn exprimiert und sind in die Kompartimentierung des zentralen Nervensystems (ZNS) und die Bildung und Stabilisierung interneuronaler Verknüpfungen involviert. *Xenopus* Cadherin-6 (Xcad-6), ein Mitglied der klassischen Typ II Cadherine, wird im ZNS, im sich entwickelnden Auge und in den, aus den Plakoden des peripheren Nervensystems (PNS) hervorgehenden cranialen Nerven exprimiert (David und Wedlich, 2000).

Ziel dieser Arbeit war die Untersuchung der Funktion von Xcad-6 während der Embryonalentwicklung. Dazu wurde das Expressionsmuster mit Hilfe eines polyklonalen Antikörpers analysiert. Xcad-6 Protein wird zuerst bei Embryonen des späten Neurulastadiums (St. 20) gebildet und nimmt quantitativ bis zum Schwanzknospenstadium (St. 40) zu. Dabei konnte neben dem vollständigen Xcad-6 eine trunkierte, nur aus der extrazellulären Domäne bestehende Form (sXcad-6) nachgewiesen werden. welches parallel zum membranständigen Xcad-6 exprimiert wird. Mittels Zelltransfektion konnte die Translation und Sekretion von sXcad-6 gezeigt werden. Ungeklärt ist, welche Rolle die kurze Form in der Embryonalentwicklung spielt.

Es wird dabei vornehmlich in den Neuriten und Axonen von Nervenzellen in Subpopulationen des ZNS exprimiert. Außerdem ist es im PNS, inklusive den Laterallinien-Nerven nachweisbar. Im Auge beschränkt sich die Expression zunächst auf die innere und äußere limitierende Membran, die Schnittstelle zwischen dem invaginierenden Augenvesikel und dem umgebenden Gewebe. Später sind auch andere Bereiche der Retina Xcad-6-positiv, die Expression bleibt aber beschränkt auf die Neuriten und Axone der neuralen Retinazellen.

Mikroinjektion von anti-sense Xcad-6 Morpholino Oligonukleotiden (MO) resultiert in Embryonen mit verschiedenen Augen-Defekten, u.a. reduzierte Augen oder ein völliger

Verlust von Augenstrukturen. Diese Defekte können über eine Co-Injektion von murinem Cadherin-6 zusammen mit MO verhindert werden. Obwohl Xcad-6 spezifisch in der anterioren Neuralplatte des St. 13 exprimiert wird, kann eine Beteiligung an den Prozessen der Induktion und der Separation des Augenfeldes ausgeschlossen werden.

Histologische Untersuchungen zeigen in den Augen unterbrochene epitheliale Strukturen in der neuralen und pigmentierten Retina in Embryonen ab dem St. 27. Transplantationen von MO-injizierten Augenfeldern in unbehandelte Embryonen resultieren in Defekten in der Polarisierung des Retina-Epithels. Umgekehrte Transplantationen verdeutlichen, dass es sich dabei um eine Zell-autonome Funktion von Xcad-6 handelt. Mittels des PhosphoH3 Nachweises und dem TUNEL-Assay kann eine verminderte Mitose und eine verstärkte Apoptose in MO-injizierten Augen nachgewiesen werden. Diese Kombination kann zu dem MO-Phänotyp, der Ausbildung der reduzierten oder fehlenden Augen, beitragen. Nach diesen Untersuchungen dient Xcad-6 der Aufrechterhaltung epithelialer Strukturen und des Wachstums der neuralen und pigmentierten Retina während der Invagination des Augenvesikels.

Xcad-6 unterstützt zudem die Bildung von Neuriten und die Faser-Bündelung bei interneuronalen Verbindungen, wie in Experimenten mit animalen Kappen (AC) gezeigt werden kann. Xcad-6 MO injizierte, neuralisierte AC-Zellen sind nicht in der Lage, Neuriten und Fasernetze auszubilden. Zudem ist die Bündelung der cranialen Fasern in Xcad-6 MO-injizierten Embryonen in vivo unvollständig. Dies deutet auf eine Beteiligung von Xcad-6 an der Bildung interneuronaler Verbindungen hin.

Contents

4. Results

Abbreviations

AC: animal cap
AP: alkaline phosphatase
APBS: amphibian phosphate buffer solution
APS: ammonium peroxodisulfate

BSA: bovine serum albumin

°C: degrees Celsius
Cad: cadherin
CAMs: cell adhesion molecules
Cad-6:   cadherin-6
C-cad-6B: chicken cadherin-6B
cDNA: complementary deoxyribonucleic acid
CMZ: ciliary marginal zone
CNR: cadherin-related neuronal receptor
CNS: central nervous system
Con A: Concanavalin A
CoMO: control MO

DAPI: 4'.6-diamidino-2-phenylindol-dihydrochloride
DEPC: diethylpyrocarbonate
DIG: digoxingenin
DNA: deoxyribonucleic acid
DP: desmoplakin
DSC: desmocollin
DSG: desmoglein
DXD: calcium-binding amino acid residues of type II cadherins
DXNDN: calcium-binding amino acid residues of type II cadherins

EC domain: extracellular domain
EC1-5:   5 extracellular repeats of cadherins

g: gram

e.g.:   for example
EDTA: ethylenediaminetetraacetic acid

FCS: fetal calf serum
FN: fibronectin

GAM: goat anti-mouse IgG
GAR: goat anti-rabbit IgG
GFP: green fluorescent protein
GPI: glycosylphosphatidylinositol anchor

HAV: His-Ala-Val, homophilic binding amino acid residues of classical cadherins
HCG: human chorionic gonadotropin

IC domain: intracellular domain
IgG: immunoglobin G

INL:	inner nuclear layer
IPL:	inner plexiform layer
kb:	kilo base pairs
kD:	kilo Dalton
LN:	laminin
LTP:	long-term potentiation
M:	molar
MBSH:	Modified Barth's Saline buffer
MBT:	midblastula transition
mcad-6.	murine cadherin-6
MEMFA:	fixative
min:	minute
MO:	anti-sense morpholino oligonucleotide
N:	nano
NC:	neural crest
ng:	nanogram
nm:	nanometer
NHS:	N-hydroxysuccinimide
NOP:	Nonidet lysis buffer
NR:	neural retina
OCM:	oocyte culture medium
OD:	optical density
ONL:	outer nuclear layer
OPL:	outer plexiform layer
PBS:	phosphate buffer solution
PCR:	polymerase chain reaction
PFA:	paraformaldehyde
PG:	plakoglobin
PH 3:	phospho Histone 3
PNS:	peripheral nervous system
POD:	horseradish peroxidase
PSD:	postsynaptic density
QAI:	homophilic binding amino acid residues of type II cadherin
QAL:	homophilic binding amino acid residues of type II cadherin
QAV:	homophilic binding amino acid residues of type II cadherin
RGCs:	retinal ganglion cells
RNA:	ribonucleic acid
RPE:	retinal pigmented epithelium
rpm:	revolutions per minute
RT:	room temperature
RT-PCR:	reverse transcription RCR
SAP:	shrimp alkaline phosphatase
SDS-PAGE:	sodiumdodecylsulphate-polyacrylamide gel electrophoresis
sXcad-6:	soluble isoform of Xcadherin-6

tBR:	truncated BMP receptor
TdT:	terminal deoxynucleotidyl transferase
TM domain:	transmembrane domain
TNT:	*in vitro* transcription and translation
μ:	micro
UTR:	untranslated regions
UV:	ultra violet
V:	volt
WM:	whole mount
wt:	wild type
XAV:	homophilic binding amino acid residues of type II cadherin
Xcad-6:	*Xenopus* cadherin-6
XE-cad:	*Xenopus* E-cadherin

1 Introduction

1.1 Cell Adhesion Molecules

The formation of different tissues and organs in multicellular organisms is based on cell sorting, aggregation and communication processes mediated by cell adhesion molecules. Cells first contact weakly with one another and, after recognizing the correct partner cell they strengthen adhesiveness by clustering the adhesion molecules. In many tissues cell junctions are formed at the end of this process which functionally specify subcellular membrane compartments. Cell adhesion is conferred in molecular terms by various integral membrane proteins, the so-called cell adhesion molecules (CAMs). Nowadays, CAMs are divided into five major classes, cadherins, immunoglobulin (Ig) superfamily, selectins, mucins and integrins (Alberts et al., 1994; Lodish et al., 1999).

A subgroup of cell junctions is established by clustered adhesion molecules. According to their cell type specificity and subcellular localization, these junctions are subdivided into

- adherens junctions (zonula adherens) which are located at the apical-lateral border of epithelial cells (Mooseker et al., 1984; Madara, 1987; Madara et al., 1988);
- adhesive junctions in synapses (synaptic adherens junctions) of neurons (Fannon and Colman, 1996; Uchida et al., 1996; Kohmura et al., 1998);
- autotypic junctions between the layers of glial cells in the axon myelin sheath (Fannon et al., 1995);
- desmosomes (intermediate disks) found in epithelial cells and between cardiomyocytes (Volk and Geiger, 1986; Garrod et al., 2002);
- hemidesmosomes, the cellular contact sites to the basal lamina in epithelia (Alberts et al., 1994).

Cadherin-mediated Ca2+-dependent homophilic cell adhesions participate in specifying adherens junctions and desmosomal junctions. These junctions are linked to the cytoskeleton via α–, β- and γ-catenin (plakoglobin) (Lodish et al., 1999).

1.2 Cadherins

Cadherins, a group of calcium-dependent transmembrane glycoproteins mediating homophilic interaction between neighboring cells, were initially identified in the mid-eighties, e.g. E-cadherin (uvomorulin) and N-cadherin (Vestweber and Kemler, 1985; Takeichi et al., 1988; Kemler et al., 1989; Takeichi, 1991). Since then, especially in the last decade more and more cadherins have been discovered. Cadherins are confirmed to play a key role in cell

sorting and tissue maintenance during embryonic development and organogenesis (Takeichi, 1988; Broders and Thiery, 1995a; Ruan et al., 2004). Also, it has been demonstrated that the cadherin superfamily is involved in multiple biological processes, including cell recognition, cell signalling, cell communication, morphogenesis and synaptic activity (Tanaka et al., 2000; Ivanov et al., 2001; Angst et al., 2001). Based on sequence alignment, cadherins are grouped into subfamilies: classical (type I and type II) cadherins, protocadherins including CNR (cadherin-related neuronal receptor), desmosomal cadherins (desmocollins and desmogleins), and cadherin-related proteins (e.g., the FAT family, seven transmembrane-cadherins and T-cadherin) (reviewed in Broders and Thiery, 1995b; Kühl and Wedlich, 1996; Suzuki, 1996; Yagi and Takeichi, 2000; Ivanov et al., 2001; Angst et al., 2001). All members of the cadherin superfamily possess a common structure: an extracellular portion (EC) displays repeats of 4 up to 34 conserved calcium-binding domains of approximately 110 amino acid residues in length; a transmembrane region passing once or 7 times through the cell membrane, except for T-cadherin which anchors to cell membrane by GPI (glycosylphosphatidylinositol anchor); and an intracellular tail which interacts with numerous cytoplasmic partners (Angst et al., 2001). In addition to vertebrates, cadherins have also been detected in invertebrates, e.g. *Drosophila* and *Caenorhabditis elegans* (Sano et al., 1993; Oda et al., 1994; Yagi and Takeichi, 2000). Thus, cadherins are evolutionarily conserved molecules (Pouliot, 1992; Grunwald, 1993).

Classical (Type I and Type II) Cadherins

The classical cadherins are single-span transmembrane glycoproteins, and share a common molecular mass of 120-140kD. Structurally, the classical cadherin consists of a signal peptide and prosequence, which are required for membrane targeting of the cadherin and both of which are removed by proteolytic cleavage; a long extracellular domain (EC) subdivided in 5 repeats (EC1-EC5) of 110 amino acids, the so-called cadherin repeats; a transmembrane hydrophobic region (TM) and a relatively short and highly conserved intracellular tail (IC) (Kemler, 1992; Broders and Thiery, 1995b; Yagi and Takeichi, 2000; Ivanov et al., 2001; Angst et al., 2001). After a series of post-translational modifications, such as glycosylation, phosphorylation and proteolytic cleavage, the precursors of cadherins turn into mature proteins (Kemler, 1992; Suzuki et al., 1991; Shimoyama et al., 2000).

A 40 amino acid residue containing a well-conserved sequence HAV (His-Ala-Val) located in the C-terminal region of EC1 seems important for homophilic binding between classical type I cadherins (Blaschuk et al., 1990; Nose et al., 1990; Ivanov et al., 2001). Cadherin adhesion activity is important in morphogenesis (Takeichi, 1995; Gumbiner, 1996). The following binding behaviors between neighboring cells were observed. First, homophilic binding

induces aggregation and separation of cells expressing different types of cadherins (Takeichi, 1995). Second, heterophilic binding sometimes emerges but generally shows weak adhesiveness. Third, two subpopulation expressing the same cadherin but in different amounts also segregate from each other (Steinberg and Takeichi, 1994). The presence of calcium ensures stable cadherin-mediated cell-to-cell adhesion and prevents the proteolytic cleavage of cadherins. The putative and highly conserved calcium binding motifs (DXNDN and DXD) are distributed over the region from EC1 to EC4, except for the amino-terminus of EC1 and the carboxy-terminus of EC5 (Kemler et al., 1989; Takeichi, 1990; Ruan et al., 2004).

The intracellular domain (IC) of classical cadherins can bind to cytoplasmic proteins, the catenins, and in turn they link the cadherins to cytoskeleton-actin filaments, thereby forming cadherin-catenin complexes which are required for stable cell-cell adhesion (Nagafuchi and Takeichi, 1988; Stappert and Kemler, 1994; Takeichi, 1995; Ozawa et al., 1990; Rimm, 1995; Brieher et al., 1996). To date, four catenins have been identified, $\alpha-$, $\beta-$ and $\gamma-$catenin (plakoglobin) as well as the c-src kinase substrate p120[cas] (Knudsen and Wheelock, 1992; Kemler, 1993; Reynolds et al., 1994; Daniel and Reynolds, 1995; Shibamoto et al., 1995). X-ray analysis of N-cadherin (N-cad), E-cadherin (E-cad) and C-cadherin (C-cad) have shown that classical cadherins form lateral dimers (Shapiro et al., 1995; Nagar et al., 1996; Brieher et al., 1996) (See Fig. 1.1).
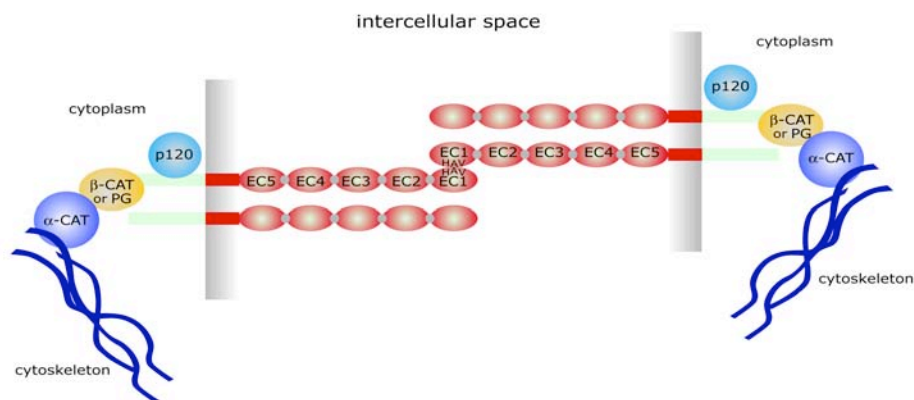
Fig. 1.1 Structure of a classical cadherin and cadherin dimers. The five extracellular domains (EC1-EC5) are colored in red. The grey spots in between indicate the calcium binding sites. The intracellular domain is linked to the cytoskeleton via cytoplasmic partners, such as b-catenin and a-catenin. P120 binds to the juxtamembrane region of the intracellular domain (IC). Cadherin dimers in the "molecular zipper" model are formed by head-to-head contacts between two neighboring cadherins at the homophilic binding site (HAV).

Using the polymerase chain reaction (PCR) technique, numerous classical type II cadherins have been identified in *Xenopus*, rat, mouse, chicken and human and have been designated by the numbers 5, 6, 7, 8, 9, 10, 11, 12, 14 and 15. Classical type II cadherins are characterized by sharing higher homology amongst themselves, more than 40% identity (in human, ranging from 58-76%) versus less than 35% in type I cadherins (Suzuki et al., 1991; Shimoyama et al., 2000). In contrast to type I cadherins, type II family members contain a QAV, QAI, QAL or XAV tripeptide instead of the HAV motif in the EC1 domain (Broders and Thiery, 1995b; Shimoyama et al., 2000; Blaschuk et al., 1990; Nose et al., 1990; Ivanov et al., 2001). Moreover, the transmembrane (TM) domain of type II cadherins is highly conserved, both in length and in amino acid sequence, which indicates that type II cadherins have more in common concerning the extracellular (EC) domain and the transmembrane (TM) part (Shimoyama et al., 2000).

The classical type I cadherins are extensively studied, especially E- and N-cad. E-cad (cadherin-1), as a molecular marker for non-neuronal tissues, is generally expressed by all types of epithelial cells, and is indispensable for the compaction process of cells early in mouse embryogenesis (Kemler et al., 1977; Hyafil et al., 1980). Moreover, E-cad has been found to serve as an invasion suppressor in experimental tumor cell lineages (Frixen et al., 1991; Vleminckx et al., 1991) and *in vivo* human tumors (Berx et al., 1995). In contrast, N-cad (cadherin-2), as a molecular marker for the neuronal tissues, is expressed mostly embryonically. In adults N-cad is restricted to neural and muscle cells (Hatta et al., 1988; Miyatani et al., 1989; Redies and Takeichi, 1993). While type I cadherins are well understood, little is known about the specific molecular interaction partners and functional properties for classical type II cadherins. Surprisingly, type II cadherins are expressed in loosely associated migrating cells. Cadherin-11 has been found in the cranial neural crest (NC) during migration (Simonneau et al., 1995; Kimura et al., 1995; Hoffmann, 1995; Hadeball et al., 1998). Cadherin-6B in chicken is persistingly expressed in the fusing neural folds before NC migration, whereas it decreases in NC domain as soon as migration starts (Takeichi, 1995; Nagakawa and Takeichi, 1998).

The Protocadherin Family

The protocadherins including CNRs, as a relatively new and dramatically growing family of cadherins have been characterized in mammal, amphibian, *Drosophila* and *Caenorhabditis elegans* species (Sano et al., 1993; Kohmura et al., 1998; Nollet et al., 2000; Yagi and Takeichi, 2000; Hilschmann et al., 2001). Protocadherins contain up to seven calcium binding EC domains homologous to those of classical cadherins, a TM region and a specific IC tail exhibiting no identity with the well characterized classical cadherins. They do not

associate with catenins (Broders and Thiery, 1995b; Yagi and Takeichi, 2000; Angst et al., 2001). To date, at least 52 protocadherins have been identified on protein level by the immunoglobulin domain like structures and on DNA level by the genomic organization (Wu and Maniatis 1999; Hilschmann et al., 2001). They have been grouped into three subclasses: 15 α-, 15 β-, and 22 γ-protocadherins depending on the variable (V) part of the gene similar to immunoglobulins and T-cell-receptor. A tissue-specific expression of protocadherins has been found, e.g., human protocadherins PC42 (PCDH1), PC43 in brain (Broders and Thiery, 1995a), Arcadlin (PCDH8) in rat synapses (Yamagata et al., 1999), NF-protocadherin (NFPC) in *Xenopus* neural fold (Bradley et al., 1998), axial protocadherin (AXPC) in *Xenopus* (Kuroda et al., 2002) and paraxial protocadherin (PAPC) in *Xenopus* and zebrafish (Kim et al., 1998; Yamamoto et al., 1998). Protocadherins normally confer moderate adhesive interaction mostly in the absence of calcium (Sano et al., 1993). More recently, many protocadherins, particularly the CNRs were discovered in synaptic structures in the developing mammalian brain (Arndt and Redies, 1998; Kohmura et al., 1998). For instance, CNRs are localized by antibody detection in the pre- and postsynaptic membrane of restricted subpopulations of the same type of neurons, suggesting that similar to classical cadherins, protocadherins are also involved in the formation of synapses in brain.

Desmosomal Cadherins

The desmosomal cadherins are the components of desmosomes, which are located mainly in tissue subject to mechanical stress, e.g. epidermis and myocardium. They consist of two subfamilies, the desmocollins (DSC) and desmogleins (DSG), both of which have cell- and differentiation-specific expression patterns (King et al., 1997). Desmosomal cadherins have 5 cadherin repeats (EC) in the extracellular part similar to the classical cadherins, the lateral dimers consisting of a DSC and a DSG can mediate strong cell-cell adhesion by homophilic/heterophilic binding between opposed cells in the presence of plakoglobin (PG) (Marcozzi et al., 1998; Chitaev and Troyanovsky, 1997). Moreover, desmosomal cadherins have a specific cytoplasmic region containing a catenin-binding domain, where they can bind PG intracellularly. PG in turn interacts with desmoplakin (DP), which associates with intermediate filaments, thereby forming cadherin-mediated adhesion (Angst et al., 2001).

1.3   Cadherin-6

The full-length cadherin-6 (K-cadherin) was isolated from a carcinoma cell line (Shimoyama et al., 1995; Xiang et al., 1994). Cadherin-6 (cad-6) has been shown to be mainly expressed in the developing kidney (Paul et al., 1997; Cho et al., 1998), the nervous system (Inoue et al., 1997; Suzuki et al., 1997; Inoue et al., 1998; David and Wedlich, 2000; Inoue et al.,

2001), the neural retina (Faulkner-Jones, 1999; Honjo et al., 2000b) and in bones (Mbalaviele et al., 1998) of human, mouse, rat, chicken, and *Xeponus laevis*. It has also been detected abundantly in hepatocellular and renal cell carcinoma (Shimoyama et al., 1995). During kidney development, cad-6 protein is detectable in the induced mesenchyme and in proximal tubule, suggesting that it plays a role in the polarization of epithelium derived from mesenchyme (Cho et al., 1998; Paul et al., 1997). In mouse, cad-6 was found to be restricted to subregions of the brain and the retina, especially to neurons and their precursors. Cad-6 is also expressed in the synapses of the central (CNS) and peripheral (PNS) nervous system and in migratory NC cells (Inoue et al., 1997; Suzuki et al., 1997; Inoue et al., 1998; Faulkner-Jones et al., 1999; Honjo et al., 2000b). Cad-6B is confined to a subpopulation of the tectofugal fiber connecting the tectum with the target in the chicken brain (Redies, 1997). However, the expression pattern of cad-6 in *Xenopus laevis* differs to some extent from that of other species. Cad-6 transcripts are present in the developing eye, the CNS and PNS, predominantly in the neurogenic placode-derived cranial ganglia and cranial nerves including lateral line nerves, suggesting that *Xenopus* cad-6 may be important in establishing the interneuronal connection between CNS to PNS during development (David and Wedlich, 2000). Apart from the expression pattern, both function and gene regulation of cadherin-6 in embryonic development remain poorly understood.

1.4   Cadherins during Neural Development

The vertebrate neural tube initially consists of numerous transverse and longitudinal neuromeres of primordial neuroepithelium. Primordial fiber tracts lie between the neuromeres. With further development, the proliferative cells in the ventricular zone of each neuromere migrate towards the mantle zone as postmitotic neuroblasts. Later neuroblasts accumulate forming either laminae in the cerebral and cerebellar cortices or brain nuclei in the gray matter area of the CNS. In order to form different functional systems within the nervous system, particular nuclei and laminae are selectively connected to one another by fiber tracts in a highly precise and orderly way. There are even connections to the peripheral sensory and motor organs over a long distance. Each functional system of the CNS specifically processes a certain type of information, such as vision, audition co-ordination or emotion. Functionally, each system is subdivided into several individual neural circuits performing different tasks, like the analysis of movement and color in the visual system (Gänzler and Redies 1995; Redies, 1997; Rubenstein et al., 1999; Redies, 2000). Although protocadherins were identified to play a role during neural development of the brain (Wu and Maniatis 1999; Hilschmann et al., 2001), at least 17 classical cadherins (Redies 1997) are also expressed in the CNS in a spatiotemporally restricted pattern and may provide guidance

cues for morphogenesis in the CNS. For example, N-cad has a role in neurulation, neuroeptithelial morphogenesis, axon elongation, and axon fasciculation and most likely also in synaptogenesis, e.g. at neuromuscular junctions (Redies et al., 1992; Wöhrn et al., 1999; Nollet et al., 2000). Based on expression patterns and experimental results, cadherins have been found to play a role in the following processes (Wöhrn et al., 1999): first, in the formation and maintenance of early embryonic CNS compartmentalization, like neuromeres, brain nuclei, and cortical laminae; second, in the establishment and stabilization of interneuronal connections, including axon elongation and navigation, neurite sorting and fasciculation, and neural circuits and synaptogenesis.

1.4.1 Morphogenesis of Early Embryonic CNS Subdivisions

Establishment of early embryonic CNS subdivisions is the process of transformation of neuromeres to functional domains, such as brain nuclei, cortical regions and laminae (reviewed in Redies, 1995; Redies and Takeichi, 1996). Cadherins were detected in this process. For instance, R-cadherin (R-cad) is expressed in several forebrain neuromeres in a stripe-like or patchy fashion. Later, most of these regions give rise to R-cadherin-positive nuclei and fiber tracts in chicken (Gänzler and Redies 1995). N-cad, cadherin-6 and cadherin-8 expression are restricted to specific regions in the brain of *Xenopus* tadpole and neonatal mouse (Simonneau et al., 1992; Rubenstein et al., 1999). *Xenopus* F-cadherin and murine cadherin-11 demarcate boundaries between neuromeres and brain nuclei in the developing brain (Espeseth et al., 1995; Kimura et al., 1996). AXPC is exclusively expressed in the notochord and distinct parts of the brain. Loss-of-function study by microinjection of morpholino showed a phenotype of curved axes and unclosed neural tube, which is probably due to the defect in cell-sorting revealed by *in vitro* dissociation and reaggregation assays (Kuroda et al., 2002). These data indicate that cadherin-mediated morphological organization via homophilic adhesion contributes to the formation of functional compartments in the developing brain.

1.4.2 Interneuronal Connections

Axon Elongation and Path-Finding

The role for cadherins in axon outgrowth was found by expression patterns and *in vitro* and *in vivo* experimental data. N-cad is localized to the growth cone of sensory neurons (Letourneau et al., 1990). R-cad (cadherin-4) is downregulated within fiber tracts at late stages of development when axon outgrowth has subsided (Arndt and Redies, 1996). In vitro, N- and R-cad are excellent substrates for the elongation of neurites from retinal, sensory ganglionic, and other neurons (Bixby et al.,1988; Matsunaga et al., 1988b;

Neugebauer et al., 1988; Bixby and Zhang, 1990; Redies et al., 1992; Redies and Takeichi, 1993). *In vivo*, combined antibody application against N-cad and b1-integrin leads to pathfinding errors in the retinotectal projections, while each antibody injected individually is insufficient to cause such errors (Stone and Sakaguchi, 1996). This supports a role of N-cad both in axon elongation and navigation. Pax6 mutants lose R-cad and meanwhile display pathfinding errors of forebrain pioneer axons. *In vivo*, R-cad applied by electroporation can rescue this pathfinding error in Pax6 mutants. This indicates that R-cad is a growth-promoting cue for pioneer axon (Andrews and Mastick, 2003). T-cad is an inhibitory substrate for the outgrowth of T-cad-positive neurons from motor neurons in vitro. In vivo, motor axons avoid T-cad-expressing areas, such as the caudal sclerotome (Fredette at al., 1996).

Cadherins play a role in neurite outgrowth and pathfinding most likely also through homophilic adhesion mechanisms which exist when cells sort and aggregate by a homophilic binding during morphogenesis of tissues and organs. *In vitro* assays showed that N-cad provides a guidance cue for sensory axon migration within the CNS by a homophilic adhesion mechanism. N-cad-expressing ganglial neurons send out axons on N-cad transfected neuroblastoma cells and axons navigate closely along N-cad-expressing boundaries between transfected cells. This suggests that N-cad does not merely stimulate neurite outgrowth, but may also provide directional cues for axon pathfinding via a homophilic adhesion mechanism (Redies et al., 1992).

Neurites Sorting and Fasciculation

Neurite aggregation (fasciculation) often goes hand in hand with the sorting of different neurite populations. The tectofugal fibers comprise several populations that originate in the tectum and project to different targets in the brain (Hunt and Künzle, 1976). The neurons giving rise to these projections are mixed and dispersed throughout the deeper layers of the tectum. At least four cadherins, N-, R-cad, cadherin-6B and cadherin-7 are expressed in these neurons in a restricted fashion and with partial overlap. These neurons send out different cadherin-positive neurite populations to form a thick fiber bundle. Immunostaining of this fiber bundle can discern several thick fascicles which differentially express cadherins in chicken (Redies, 1997; Wöhrn et al., 1999). Similarly, N-cad-expressing sensory neurites and R-cad-expressing motor neurites were found in different courses within the brain, both giving rise to a common sensory and motor root of the vagus nerves in chicken (Redies et al., 1992). *In vitro* findings revealed a role for N-cad in axon fasciculation. N-cad antibody can defasciculate neurites of retinal ganglion cells (RGCs) growing on laminin (Drazba and Lemmon, 1990). These data suggest that cadherin-mediated sorting and fasciculation are

closely related processes and that they are regulated by adhesive homophilic binding activity (Redies, 1997, 241; Wöhrn et al., 1999).

Neural Circuitry, Target Recognition and Synaptogenesis

Cadherin-induced different adhesiveness of cells regulates the formation of brain nuclei in the CNS (Redies, 1995). This mechanism may also apply to the formation of neural circuitry and synapses (Redies, 1997).

Immunohistochemical and *in situ* hybridization data showed cadherin expression in fiber connection and their target areas. E-, N-, R-, T-, P-cad, cadherin-6B and cadherin-7 were found to be restricted to subsets of fiber tracts or fascicles in CNS. Each cadherin displays a distinct expression pattern although partial overlay between the expression patterns of cadherins has been observed. One of the catenins associated with cadherins in the CNS, aN-catenin, is widely expressed in most fiber tracts (Hirano et al., 1992; Redies et al., 1993; Hirano and Takeichi, 1994; Uchida et al., 1994; Arndt and Redies, 1996; Wöhrn et al., 1999). It is reasonable to assume that the preferentially homophilic binding between cells expressing the same cadherin also plays a role in axonal target recognition (Redies, 1997).

The synaptic complex is first and foremost built around an adhesive junction, and the complex is quite similar to the desmosome and the adherens junction of epithelia (Peters et al., 1991). Although the molecular mechanisms underlying the early morphogenesis in the CNS have been under intensive scrutiny, the function of the integral membrane proteins in the final step has surprisingly remained unclear. As adherent junctions, synaptic junctions are assembled with cadherins, structurally, an N- and E-cad-mediated organelle also emerges in the synaptic junction (Fannon and Colman, 1996). N-cad is concentrated in the isolated postsynaptic densities (Beesley et al., 1995). Using antisera raised against E- and N-cad EC domain, these two proteins were found to be distributed along the axonal and dendritic plasma membranes in a mutually exclusive pattern and ultimately form cadherin self-association locks in nascent synaptic connections. They neither co-localize nor overlay at the same synaptic complexes. M-cadherin (cadherin-15), associated with glomeruli, a specialized synaptic structure of the cerebellum is restricted to a subset of synapses (Bahjaoui-Bouhaddi et al., 1997). It therefore seems reasonable to propose that members of the cadherin family of adhesion molecules are primary mediators of the events in the laying-in of synaptic specificity during development, such as apposition and lock-in of presumptive synaptic membranes in the final step of the formation of nerve connection (Spacek and Harris, 1998; Fannon and Colman, 1996). Functionally, cadherin-mediated synaptic junctions also provide a nexus for cell-cell communication (Fannon and Colman, 1996; Uchida et al., 1996; Inoue and Sanes, 1997). N-cad becomes restricted to excitatory synapses, while

inhibitory synapses, sites of GABAergic synapses lack N-cad but are associated with clusters of b-catenin. This suggests that the cadherin pattern systematically reflects functionally (excitatory and inhibitory) and spatially distinct synaptic sites on single neurons (Benson and Tanaka, 1998). Loss-of-function studies either for cadherin-11 or cadherin-6 in mice result in neural connection defects. The cadherin-11 knockout mice exhibit an enhancement of long-term-potentiation (LTP) in the hippocampus (Manabe et al., 2000), while the antibody against cadherin-6B affects the distribution of PSD-95, a postsynaptic scaffold protein (Honjo et al., 2000). Two classical type I molecules, E- and N-cad have also been reported to be involved in LTP (Tang et al., 1998). These data suggest that classical cadherins play a role in synaptic activity and synaptic structure organization. Two cadherin-associated intracellular molecules, aN- and b-catenin were found in the synaptic complex (Uchida et al., 1996). This indicates that the cadherin/catenin system is widespread within the CNS and PNS as it is found in synapses and in fiber tracts (Redies, 1997).

1.5   The Aim of This Work

The aim of this work is to clarify the function of the *Xenopus laevis* homologue of classical type II cadherin-6. The previous experimental data in *Xenopus laevis* revealed that Xcad-6 transcripts are present in the CNS, PNS and the developing eye, particularly predominantly in neurogenic placode-derived cranial ganglia and cranial nerves (David and Wedlich, 2000). To support the functional studies the Xcad-6 protein expression pattern should first be examined using a polyclonal anti-peptide antibody raised against the first extracellular domain (EC1). Gain-of-function and loss-of-function analysis were planned to elucidate the role of Xcad-6 in embryogenesis. Therefore, Xcad-6 or deleted forms of Xcad-6 should be overexpressed by injection of *in vitro* synthesized RNA. Alternatively, a knockdown approach using anti-sense morpholino oligonucleotides was entertained. According to the Xcad-6 expression profile the phenotypes arising in gain and loss of function experiments should be scored for defects in ganglia, nerve and eye development. This included a detailed *in situ* hybridization analysis of specific marker genes present in these tissues and organs. In addition, further experimental data should be collected in transplantation assays and explant cultures of wildtype and anti sense morpholino injected embryos. Finally, based on the identification of two isoforms of Xcad-6 cDNAs, a membrane integrated and a putative soluble form, the presence of a soluble isoform of Xcad-6 and its possible function should be analyzed in *Xenopus* development.

2 Materials

2.1 Biological Materials

2.1.1 Animals

Xenopus laevis were purchased from the NASCO, the U.S.A, and were housed in the standard water tanks in Zoologisches Institut II, Universität Karlsruhe (TH). The tank water quality was monitored with pH value, carbonate, conductivity once a week. The frogs were fed with pellet food twice a week and bovine heart tissue once a week *ad libitum*.

2.1.2 Antibodies

Primary Antibodies

- Xcad-6 antibody: rabbit polyclonal antibody raised against the first extracellular domain (EC1) of *Xenopus* cadherin-6 (AG Wedlich, Universität Ulm, Germnay and Eurogentec, Seraing, Belgium)

- 10 H3: mouse monoclonal antibody against *Xenopus* Ecadherin (AG Hausen, MPI, Tübingen, Germany)

- Anti-HA: mouse anti-hemaglutinin (HA) monoclonal antibody (Roche, Mannheim, Germany)

- Anti-phospho-Histone H3: rabbit anti-phospho-Histone H3 polyclonal antibody (Upstate, distributed by BIOMOL GmbH, Hamburg, Germany)

- Anti-flag antibody: rabbit anti-flag polyclonal antibody (Sigma, Deisenhofen, Germany)

- Anti-Digoxigenin-AP: Alkalinephosphatase (AP)-conjugated anti-digoxingenin Fab fragments (Boehringer, Mannheim, Germany)

- Anti-Fluorescein-AP: Alkalinephosphatase (AP)-conjugated anti-fluorescein Fab fragments (Boehringer, Mannheim, Germany)

- m9E10: mouse monoclonal antibody whose epitope corresponds to amino acids 408-439 within the carboxyterminal domain of human c-Myc (Behrens, J., MDC, Berlin, Germany)

- Anti-GFP: mixture of two mouse monoclonal antibodies to the Green Fluorescent Protein (GFP) and a GFP fusion protein (Boehringer, Mannheim, Germany)

- N-CAM: mouse monoclonal antibody against *Xenopus* N-CAM (Henke and Fahle, MPI, Tübingen, Germany)

Secondary Antibodies

- GAM-POD: horseradish-peroxidase conjugated goat anti-mouse IgG (Dianova, Hamburg, Germany)

- GAR-POD: horseradish-peroxidase conjugated goat anti-rabbit IgG (Dianova, Hamburg, Germany)

- GAM-AP: Alkaline phosphatase-conjugated goat anti-mouse IgG (Dianova, Hamburg, Germany)
- GAR-AP: Alkaline phosphatase-conjugated goat anti-rabbit IgG (Dianova, Hamburg, Germany)
- GAR-Cy2: Cy^{TM}-2-conjugated goat anti-rabbit IgG (Amersham Life Science, Arlington, USA)
- GAR-Cy3: Cy^{TM}-3-conjugated goat anti-rabbit IgG (Dianova, Hamburg, Germany)
- GAM-Cy2: Cy^{TM}-2-conjugated goat anti-mouse IgG (Dianova, Hamburg, Germany)
- GAM-Cy3: Cy^{TM}-3-conjugated goat anti-mouse IgG (Dianova, Hamburg, Germany)

2.1.3 cDNA Clones and Vectors

- Full-length Xcad-6 GFP in pCDNA 3.1/CT-GFP (David R., University of Ulm, Germany)
- Short-form Xcad-6 GFP in pCDNA 3.1/ CT-GFP (David R., University of Ulm, Germany)
- Murine full-length cadherin-6 in pCA-pA vector (Inoue T., Kansas City, USA)
- XRx1 in PGEM3 (Vignali R., University of Pisa, Italy)
- XNeuroD in pBSK+ (Schlosser G., University of Bremen, Germany)
- XMyT1 in pCS2+ (Schlosser G., University of Bremen, Germany)
- XDelta1 in pSp72 (Schlosser G., University of Bremen, Germany)
- XOtx2 in pBSKS (Cho K.W., University of California, USA)
- XPax2 in pBSK+ (Heller N., Swiss Federal Institute of Technology, Switzerland)
- XEya1 in pTAdv (David R., University of Ulm, Germany)
- EGFP in pCS2 (David R, University of Ulm, Germany)
- DsRed2-N1 in pCS2-flag (Ruan, G., University of Karlsruhe (TH), Germany)
- Truncated BMP receptor (tBR, dominant negative BMP-receptor) in pSP64T3 (KüzÜkieylan N., University of Ulm, Germany)
- pCS2-flag (Köbernick K., University of Karlsruhe (TH), Germany)
- pCDNA 3.1/CT-GFP (Invitrogen, Groningen, Netherlands)
- DsRed2-N1 plasmid (Clontech, Palo Alto, USA)

2.1.4 Cell Line

H293: a permanent cell culture of primary human embryonic kidney cell line (Gradl D., University of Karlsruhe (TH), Germany)

2.1.5 Genotypes of Bacterial Host Strains

- *XL-1-blue*: recA1, gyr A96, thi, hsdR17 (rk-, m k+), supE44, l-, lac-, [F', proAB, lacqZDM15, TN10, (tetr)] (Bullock et al., 1987)

- *Sure*: e14–(McrA–) Δ(mcrCB-hsdSMR-mrr)171 endA1 supE44 thi-1 gyrA96 relA1 lacrecB recJ sbcC umuC::Tn5 (Kanr) uvrC [F´ proAB lacIqZΔM15 Tn10 (Tetr)] (Stratagene, Amsterdam, Netherlands)

2.1.6 Oligonucleotides

Cloning Primers

Xcad-6/1, forward: 5'-CCTATCAGTTGCGAGCACTG-3'
    reverse: 5'-CCAAGTCCAGAAATCGTGGG-3'
    fragment size: 269bp

Xcad-6/2, forward: 5'-AGTCTTCCCCTGTGGGTTCT-3'
    reverse: 5'-CTGGGCCAAAACTGTTCCTA-3'
    fragment size: 389bp

Xcad-6/3, forward: 5'-CGGATTACTGTAGATGATGTGG-3'
    reverse: 5'-ACGCGGGTGATTTGTTTAGG-3'
    fragment size: 304bp and 165bp

Histone 4, forward: 5'-CGGGATAACATTCAGGGTATCACT-3'
    reverse: 5'-ATCCATGGCGGTAACTGTCTTCCT-3'
    fragment size: 200bp

XMyT-1, forward: 5'-CTCCAAGAGAAAATCCCACCC-3'
    reverse: 5'-GAGAGTTGGCTATGATTTCGTG-3'
    fragment size: 302bp

XDelta-1, forward: 5'-CTCTGCCAGATATCCTGCTC-3'
    reverse: 5'-GGCAAGGCGACTTATCAGAC-3'
    fragment size: 395bp

XNeuroD, forward: 5'-CAATGGAGAGGAGAACGAGG-3'
    reverse: 5'-GAGTAGCAGGGCACAACTTTG-3'
    fragment size: 251bp

XEya1, forward: 5'-CAGCCAGGACAGCCTTATGG-3'
    reverse: 5'-AGTGGTAGGGCTGGTGTTAC-3'
    fragment size: 363bp

DsRed2-N1, forward with EcoR I: 5'-CAAGAATTCCATGGCCTCCTCC-3'

reverse with Xho I: 5'-GAACTCGAGCTACAGGAACAGGTG-3'

fragment size: 703bp

XET1, forward: 5'-CCTATCCTTGACTTGCTACA-3'

reverse: 5'-GTTTTGGGGAAGGAGGGTAT-3'

fragment size: 255bp

XRx1, forward: 5'-CCCCAACAGGAGCATTTAGAAGAC-3'

reverse: 5'-AGGGCACTCATGGCAGAAGGTT-3'

fragment size: 416bp

b-actin, forward: 5'-GCGTACCTCATGAAGATCCT-3'

reverse: 5'-GCGGATGTCCACGTCACACT-3'

fragment size: 110bp

Morpholinos (GeneTools Philomath, USA)

Xcad-6 Morpholino: 5' – CTAAAAGTTCTCATGGTGCAGTAAG – 3'

Control Morpholino: 5' – CCCCAGCTCAAGAGACCTGACGCAT – 3'

2.2   Non-biological Materials and Distributors

2.2.1   Chromatography Matrices

Hi Trap NHS-activated Sepharose Columns (Pharmacia, Freiburg, Germany)

Hi Trap Protein A Sepharose Columns (Pharmacia, Freiburg, Germany)

Hi Trap Protein G Sepharose Columns (Pharmacia, Freiburg, Germany)

2.2.2   Filters and Carriers

DE 81 filter paper (Whatman, London, Great Britain)

MicroSpin G-50 Columns (Amersham, Braunschweig, Germany)

Nitrocellulose BA 45 (Schleicher & Schüll, Dassel, Germany)

Sterile Filter (Millipore, Eschborn, Germany)

X-OMAT AR 5 Film (Kodak AG, Stuttgart, Germany)

2.2.3   Kits

Ambion in vitro transcription kit (Ambion, Huntingdon, Great Britain)

DIG RNA Labeling Mix, 10x conc. (Roche, Mannheim, Germany)

ECL^{TM} Western Blotting Detection Reagent (Amersham, Braunschweig, Germany)

Fluorescein RNA Labeling Mix, 10x conc. (Roche, Mannheim, Germany)

Qiagen EndoFree^{TM} *Plasmid* Kit (Qiagen, Hilden, Germany)

TNT^{TM} *in vitro* Transcription and Translation Kit (Promega, Mannheim, Germany)

Stratagene's QuikChange^{TM} site-directed mutagenesis kit (Stratagene, La Jolla, USA)

Trizol Reagent (*Gibco* BRL, Karlsruhe, Germany)

2.2.4 Radioactivity

35S-Methionine (1000 Ci/mmol) (Amersham, Braunschweig, Germany)

2.2.5 Equipments

- Agarose-Gel-Electrophoresis-Apparatus (Pharmacia, Freiburg, Germany)
- Binocular Fluorescence Microscope (MZFLIII, Leica, Benzheim, Germany)
- Brightfield Microscope (Axiovert200, Zeiss, Oberkochen, Germany)
- Centrifuges: Heraeus Biofuge (fresco, 1387 Rotor, Heraeus-Christ, Hanau, Germany), Heraeus Multifuge 3 S-R (3046 and 6441 Rotor, Kendro, Langenselbold, Germany)
- Color Digital Camera (12 bit, Qimaging, Burnaby, Canada)
- Confocal Laser Microscope TCS SP (Leica, Heidelberg, Germany)
- Diana Camera Detection System (Raytest, Straubenhardt, Germany)
- Electrophoresis PAGE and Protein Transblot system: Trans-Blot Protean II, Protein-Electrophoresis and Tankblot-System (Biorad, Munich, Germany); Mini Protean II and Mini Fluorescence Microscope (Leica, Benzheim, Germany)
- Gel Dryer Model 583 (Biorad, Munich, Germany)
- Trans Blot (Bio-Rad, Munich, Germany)
- Hyperprocessor (Amersham, Braunschweig, Germany)
- Incubator and Orbital Shaker (Thermo Forma, Marietta, USA)
- Injection Capillary (Outer Diameter 1.0 mm, H. Saur Laborbedarf, Reutlingen, Germany)
- Microinjection System (H. Saur Laborbedarf, Reutlingen, Germany)
- Micromanipulator (Bachhofer, Reutlingen, Germany)
- Micropipette Puller (Model P-97, Sautter Instruments, Novato, USA)
- Microwave R-2j28 (Sharp, Japan)
- PCR System: PCR Cycler UNO II and Personal Cycler (Biometra, Göttingen, Germany)
- Photometers: Biophotometer (Eppendorf, Hamburg, Germany); Ultrospec 2100pro (Amersham, Cambridge, Great Britain)
- Pneumatic Pico Pump PV 820 (Bachhofer, Reutlingen, Germany)
- Power Supply 200/2.0 (Biorad, Munich, Germany)
- Power Supply ST 3002 (Life, Eggenstein, Germany)

- Sequencer ABI 377A and 373 (Applied Biosystems Inc.,Weiterstadt, Germany)
- Software: Illustrator (Adobe Systems Inc., USA), Leica Scanware (Leica, Heidelberg, Germany), Mac Molly Tetra (Softgene, Berlin, Germany), Photoshop (Adobe Systems Inc., USA), Openlab 3.1.1 (Openlab, Heidelberg, Germany)
- Ultra Low Temperature Freezer (New Brunswick Scientific GmbH, Nürtingen, Germany)
- Vibratome Sectioning System (VT 1000S, Leica, Benzheim, Germany)

2.2.6 Chemicals

- 1-Butanol (Merck, Darmstadt, Germany)
- L-15 Leibovitz Medium (*Gibco* BRL, Karlsruhe, Germany)
- 2-Mercaptoethanol (Serva, Heidelberg, Germany)
- 5-Bromo-4-chloro-3-indolyl-β-D-galactopyranosid (X-Gal) (Roche, Mannheim, Germany)
- 100bp Ladder (Roche, Mannheim, Germany)
- Acetic Acid (Merck, Darmstadt, Germany)
- Acrylamide (Serva, Heidelberg, Germany)
- Agar (Bacteriological Grade, *Gibco* BRL, Karlsruhe, Germany)
- Agarose (*Gibco* BRL, Karlsruhe, Germany)
- Ampicillin, Sodium-Salt (Sigma, Munich, Germany)
- Ammonium Peroxodisulfate (Merck, Darmstadt, Germany)
- Aprotinin (Sigma, Munich, Germany)
- L-Arginin (Sigma, Munich, Germany)
- Bisacrylamide (Serva, Heidelberg, Germany)
- Borat (Sigma, Munich, Germany)
- Bovine Serum Albumin (BSA, Sigma, Munich, Germany)
- Bromophenol Blue (Sigma, Munich, Germany)
- Carmin (Sigma, Munich, Germany)
- Casein-Hydrolysate (*Gibco* BRL, Karlsruhe, Germany)
- CHAPS (AppliChem, Darmstadt, Germany)
- Chloroform (Merck, Darmstadt, Germany)
- Con A Sepharose (Sigma, Munich, Germany)
- Coomassie Brilliant Blue G-250 (Serva, Heidelberg, Germany)
- L-Cysteine Hydrochloride (Sigma, Munich, Germany)
- DAPI (4'.6-Diamidino-2-phenylindol-dihydrochloride, Merck, Darmstadt, Germany
- Deoxynucleotides dATP, dCTP, dGTP and dTTP (Amersham, Braunschweig, Germany)
- DEPC (Diethylpyrocarbonate, Sigma, Munich, Germany)
- DIG-coupled UTP (Roche, Mannheim, Germany)

- DNase I, RNase free 5 U/ μl (Roche, Mannheim, Germany)
- EDTA (Ethylenediaminetetraacetic Acid, Titriplex, Life, Eggenstein, Germany)
- Elvanol (Polyvinylalcohol 25/140, Serva, Heidelberg, Germany)
- Ethidium Bromide (Sigma, Munich, Germany)
- *Fast Red* Tablets (Roche, Mannheim, Germany)
- Fibronectin (Roche, Mannheim, Germany)
- Ficoll (Sigma, Munich, Germany)
- Fetal Calf Serum (FCS, Roche, Mannheim, Germany)
- Freon 113 (1.1.2-Trichlorotrifluoroethane, Aldrich, Steinheim, Germany)
- Formaldehyde (Merck, Darmstadt, Germany)
- Geneticin (G418 sulfate, an aminoglycoside related to Gentamycin; Invitrogen, Karlsruhe, Germany)
- L-Glutamine (Sigma, Munich, Germany)
- Glycerol (Merck, Darmstadt, Germany)
- Glycin (AppliChem, Darmstadt, Germany)
- HEPES (4-(2-Hydroxyethyl)-piperazine-1-ethanesulfonic acid, Serva, Heidelberg, Germany)
- HMW Marker (Sigma, Munich, Germany)
- Human Chorionic Gonadotropin (Schering, Berlin, Germany)
- λ-Hind III Marker (Roche, Mannheim, Germany)
- Klenow Fragment (Roche, Mannheim, Germany)
- Lamb Serum (*Gibco* BRL, Karlsruhe, Germany)
- Laminin (Kemler R., University of Freiburg, Germany)
- Leupeptin (Roche, Mannheim, Germany)
- Lysozyme (Sigma, Munich, Germany)
- Milk, Nonfat Powdered (Nestle, Frankfurt, Germany)
- MS 222 (Aminobenzoic Acid Ethyl Ester, Sigma, Munich, Germany)
- NBT/BCIP (Roche, Mannheim, Germany)
- Nonidet P40 (Ethylphenyl-Polyethylene Glycol, Sigma, Munich, Germany)
- Nystatin (Sigma, Munich, Germany)
- Paraformaldehyde (Merck, Darmstadt, Germany)
- Penicillin/Streptomycin stock solution: 10000 U penicillin/ml, 10 mg streptomycin/ml from Life, Eggenstein, Germany)
- Pepstatin A (Sigma, Munich, Germany)
- Phenol (Sigma, Munich, Germany)
- PMSF (Phenylmethylsulfonylfluorid, Sigma, Munich, Germany)

- Polyvinylpyrrolidone (PVP, Sigma, Munich, Germany)
- Ponceau S (Sigma, Munich, Germany)
- Proteinase K (Merck, Darmstadt, Germany)
- Restriction Endonucleases (Roche, Mannheim, Germany; Stratagene, Hamburg, Germany; MBI Fermentas, Wilna, Lithuania)
- Reverse Transcriptase (Superscript II, *Gibco* BRL, Karlsruhe, Germany)
- Ribonucleotides ATP, CTP, GTP, UTP (Roche, Mannheim, Germany)
- RNase Inhibitor (40 U/ μl) (Life, Eggenstein, Germany)
- Select Yeast Extract (*Gibco* BRL, Karlsruhe, Germany)
- Shrimp Alkaline Phosphatase (SAP, Amersham, Braunschweig, Germany)
- Sodium Deoxycholate (Merck, Darmstadt, Germany)
- Sodium Lauryl Sulfate (Sodium Dodecyl Sulfate, SDS, Serva, Heidelberg, Germany)
- SP6 RNA Polymerase (10 U/ μl) (Roche, Mannheim, Germany)
- T4 DNA Ligase (Roche, Mannheim, Germany)
- T4 DNA Polymerase (*Gibco* BRL, Karlsruhe, Germany)
- T7 RNA Polymerase (10 U/ μl) (Roche, Mannheim, Germany)
- Taq DNA Polymerase (5 U/ μl) (Amersham, Braunschweig, Germany)
- TdT (Terminal deoxynucleotidyl Transferase, *Gibco* BRL, Karlsruhe, Germany)
- TEMED (N, N, N', N'-Tetramethylethylenediamine, Merck, Darmstadt, Germany)
- Tetracycline (Sigma, Munich, Germany)
- Torula RNA (Sigma, Munich, Germany)
- Tris (Tris-hydroxymethyl-aminomethane, Merck, Darmstadt, Germany)
- Triethanolamine (Sigma, Munich, Germany)
- Triton X-100 (Serva, Heidelberg, Germany)
- Trypsin (Sigma, Munich, Germany)
- Tryptose Phosphate Broth (*Gibco* BRL, Karlsruhe, Germany)
- *Turbo* Pfu DNA Polymerase (Stratagene, Amsterdam, Nederlands)
- Tween 20 (Polyethylensorbitanmonolaurate, Sigma, Munich, Germany)
- Urea (Merck, Darmstadt, Germany)

All other basic chemicals were purchase from Fluka (Neu-Ulm, Germany), Merck (Darmstadt, Germany), Roth (Karlsruhe, Germany), Serva (Heidelberg, Germany) or Sigma (Munich, Germany)

3   Methods

3.1   Cultivation and Manipulation of Embryos

3.1.1   *In vitro* Fertilization and Microinjection

***In vitro* Fertilization**

Buffers and Solutions

- 10x MBSH (Modified Barth's Saline): 880 mM NaCl, 100 mM HEPES, 10 mM KCl, 24 mM NaHCO$_3$, 8 mM MgSO$_4$, 4 mM CaCl$_2$, 3.3 mM Ca(NO3)$_2$ (pH 7.3)
- Cysteine solution: 2% (w/v) L-Cysteine Hydrochloride in 0.1x MBSH (pH 8.2)
- Human Chorionic Gonadotropin (HCG): 3300 IU/mg; stock solution: 1 mg/ml in sterile 0.5% NaCl
- OCM-Medium (Oocyte Culture Medium): 15 mM HEPES (pH 7.8), 0.4 mg/ml L-Glutamine, 50 μg/ml Gentamycin sulfate, 1 μg/ml BSA, 50 U/ml Nystatin, 50% Liebovitz, 10% FCS (pH 7.8), filter sterile

The dorsal lymph sacs of *Xenopus laevis* adult females were subcutaneously injected with 600-800 IU HCG which induces egg maturation within 14-18 hours. On the following day, an adult male was sacrificed and the testes were isolated and stored in OCM medium at 4°C for one week. A piece of testis was washed and macerated in 1-1.5 ml 1x MBSH. 100-200 μl of this testis stock suspension was diluted to 0.1x MBSH and distributed over the eggs which was manually squeezed from the female oviducts into a petri dish. Five min later, the petri dish was filled with 0.1x MBSH and stored at 14-16°C. Success of fertilization is determined by the upward turning of the pigmented animal pole. Approximately 90-120 min after fertilization, the embryos started cleavage. The jelly coat was removed by gently spinning the embryos in cysteine solution for 4 min. Afterwards the eggs were intensively rinsed with 0.1x MBSH to remove the cysteine. The embryos were staged according to Nieuwkoop and Faber protocol (1975).

Microinjection

Solutions and Equipment

- Agarose-coated dishes: 3% agarose in 0.1x MBSH coated dishes with holes for holding the embryos were generated using a plastic Pingpang grid.
- Glass needles: the microinjection glass needles were prepared by pulling autoclaved thin glass tubes (O.D: 1.0 mm, I.D.: 0.5 mm, 10 cm length) with a micropipette puller (Sautter Instruments, Novato, USA), the needle tip was small enough to prevent cytoplasmic leakage during injections (Zoology Institute II, University of Karlsruhe (TH), Germany)

The glass needle was fixed onto a micromanipulator that was connected to an air pump. The injection volume was determined by measuring the diameter of the water droplet expelled into the mineral oil from the glass needle tip using a standard square meter. For injection the embryos were transferred into the agarose-coated dishes and fixed in the holes by removing

the buffer. DNA or RNA was injected in a volume of 4-10 nl into one or two blastomeres of 2- or 4-cell stage embryos. Dorsal and ventral blastomeres can be distinguished at the cell stage by their size and pigmentation: dorsal blastomeres being less pigmented and smaller than ventral ones. After injection, the embryos were kept in 1x MBSH for about 1-1.5 hours healing at room temperature (RT), and then cultured in 0.1x MBSH at 14-18°C.

3.1.2 Anaesthetization, Fixation and Storage

Solutions and Fixatives:

- 20x MS 222 (stock solution): 4 mg/ml in 0.1x MBSH
- 3.7% MEMFA: 100 mM MOPS (pH 7.4), 2 mM EGTA, 1 mM $MgSO_4$, 3.7% Paraformaldehyde
- 3.7% PFA: 3.7% paraformaldehyde in APBS/Ca^{2+}

For documentation, the embryos were anaesthetized in 1X MS200. They were reactivated by transferring into 0.1x MBSH.

For whole mount *in situ* hybridization, whole mount immunostaining as well as histology, embryos were placed in fixatives for 2 hours at RT or overnight at 4°C. For whole mount *in situ* hybridization, the embryos were fixed in 3.7% MEMFA, while for whole mount immunostaining or histology 3.7% PFA was used as fixative. After fixation, the embryos were transferred into either 100% ethanol or 100% methanol and stored at –20°C.

3.1.3 Transplantation

Transplantation of the eye field of *Xenopus laevis* embryos was developed according to the previously described method with some modifications (Borchers et al., 2001). Briefly, donor embryos were injected with either a combination of 8 μM Xcad-6 morpholino and 200 pg GFP-myc mRNA or 400 pg DsRed2-flag mRNA into 2 dorsal blastomeres of 4-cell stage embryos, while the host embryos were prepared either by co-injection of 8 μM Xcad-6 morpholino and 200 pg GFP-myc mRNA into 1 dorsal blastomere of 4-cell stage embryos or remained uninjected. Using hair as a cutting needle, the anteriormost part of the neural plate, the so-called presumptive eye field was dissected from stage 13 donor embryo and transferred into the corresponding cavity of an host embryo The eye field of stage 13 embryo is determined according to the expression region of the eye field gene, XRx (Casarosa et al., 1997). For healing, the transplanted embryos were kept in 1x MBSH under a cover glass for 1.5 hours at 20°C. After the cover glass was removed carefully, the medium was changed to 0.1x MBSH. The embryos were cultivated until stage 31/32 for analysis. Following documentation of the graft with a fluorescence microscope, the embryos were fixed for histological analysis.

3.1.4 Cultivation of Neuralized Animal Caps and N-CAM Immunostaining

Solutions and Medium

- Fibronectin and Laminin solution: 100 ng/μl fibronectin and 100 ng/μl laminin were mixed in PBS
- Geneticin (G418 sulfate, an aminoglycoside related to Gentamycin) stock solution: 100 mg/ml Geneticin dissolved in 4 times distilled H_2O
- Dissociation buffer: 50.3 mM NaCl, 0.67 mM KCl, 18.42 mM Na_2HPO_4, 0.85 mM KH_2PO_4, 2.38 mM $NaHCO_3$, and 1.8 mM EDTA, pH 7.3, sterilized by a 0.22 μm filter
- 1x MBSH + Penicillin/Streptomycin: penicillin/streptomycin (1:100) in 1x MBSH
- 1x MBSH/2 mM Ca^{2+} + Penicillin/Streptomycin: 2 mM Ca^{2+}, penicillin/streptomycin (1:100) in 1x MBSH
- Amphibian Leibovitz Medium: 30 ml L-15 Leibovitz medium, 4 ml FCS (fetal calf serum), 2.5 ml Tryptose phosphate broth, 0.5 ml Penicillin/steptomicin, 0.4 ml L-arginin (40 mg/ml in 4 times distilled H_2O), 0.5 ml L-glutamin (2.9 g/ml in 4 times distilled H_2O), finally filled up to 50 ml with 4 times distilled H_2O
- APBS/Ca^{2+}: 2 mM $CaCl_2$, 103 mM NaCl, 2.7 mM KCl, 0.15 mM KH_2PO_4, 0.7 mM NH_2PO_4 (pH 7.5)
- Elvanol: 3 g Elvanol was dissolved in 40 ml APBS pH 7.2 or PBS pH 7.2; after being stirred for 16 hours, 15 ml glycerol was added, and after stirring for an additional 16 hours the mixture solution was centrifuged at 9000xg; the supernatant was transferred into a fresh container. 1.2-phenylene diamine was added at a concentration of 1 mg/ml. The mixture was stirred in the dark until it was completely dissolved; and the pH value was adjusted to 8.0. Finally, 2-mercaptoethanol was added to the solution until it became clear, and then it was stored as aliquots of 2 ml at -20°C.

The neuralized animal caps were obtained by microinjecting 100 pg truncated BMP-receptor (tBR) into 2 animal poles of 2-cell stage embryos which were cultivated until the mid-blastula-transition of stage 8 at 15°C. After removing the vitelline membrane, the neuralized animal caps (ACs) were dissected with forceps. 10 ACs were dissociated in dissociation buffer for 40 min. Meanwhile, the cover glass, which was coated overnight at 4°C with 50 μl of fibronectin (FN) and laminin (LN) mixture in PBS was blocked with 50 μl of 1% BSA for 5 min at RT. After washing in 1x MBSH/Ca2+ plus penicillin/streptomycin, the ACs were seeded on a cover glass in 3 ml 1x MBSH/Ca2+ plus penicillin/streptomycin in a petri dish. The AC explants were kept untouched for 3 hours until the explants adhered to the FN/LN coated glass. To investigate the function of Xcad-6, co-injection of 4 μM Xcad-6 MO and tBR was performed and the co-injected ACs were isolated and cultivated as described above. Geneticin was supplemented into the medium (1:1000) every 6 hours per day. Starting from the second day, 1ml medium was replaced by the same amount of amphibian Leibovitz medium every 6 hours per day. After 56-hour cultivation, equivalent to stage 40 noninjected embryos, the AC-containing cover glasses were taken out and put on a clean slide for further N-CAM immunostaining. After washing the medium with APBS/Ca^{2+}, the AC samples were fixed with 3.7% PFA for 10 min at RT followed by 8 min incubation in APBS/Ca^{2+} plus 0,1%

Triton. After 3 times washing with APBS/Ca^{2+} for 20 min, the AC cells were incubated in 1% BSA for 30 min at RT to block unspecific binding before the N-CAM antibody (1:100 in APBS/Ca^{2+}) was added and incubated overnight at 4°C. The cells were washed 3 times with APBS/Ca^{2+} for 20 min each before the AC explants were incubated for 2 hours at RT with the secondary antibody, goat-anti-mouse conjugated with Cy2 (GAM-Cy2, 1:200 in APBS/Ca^{2+}). After 4 times rinsing with APBS/Ca^{2+} for 20 min, the specimen were embedded in Elvanol by reversing the cover glass and placing it on a clean slide. The AC cells were analyzed with a fluorescence microscope.

3.2   Cellular Biological Methods

3.2.1   Cell Culture

Buffers and Solutions

- Trypsin/EDTA in Puck's solution: 0.5 g Trypsin, 0.2 g EDTA
- DMEM basic medium: DMEM powder for 10 liter medium was dissolved in 9 liter 4 times distilled H$_2$O together with 37g NaHCO$_3$, 100 ml penicillin/streptomycin and sterilized by a 0.22 μm filter. Prior to use, the medium should be tested for contamination
- DMEM supplementary medium for amphibian cells: 300 ml DMEM basic medium, 50 ml heat-inactivated FCS, 5 ml glucose solution (350 mg/ml D-glucose), 5 ml glutamine solution (29 mg/ml L-glutamine), 5 ml pyruvat solution (5 mg/ml) and 5 ml penicillin/streptomycin filled up to 500 ml with 4 times distilled H$_2$O

The cells were cultivated in DMEM supplementary medium under 7% CO$_2$ at 24°C. The confluent cells were dissociated with Trypsin/EDTA in Puck's solution in a culture flask. 1 min later the dissociated single cells were spread in a fresh culture flask in an appropriate dilution.

3.2.2   Transfection of H293 (Human Embryonic Kidney Cell Lineage)

Buffers and Solutions

- 10x HeBS: 1.36 M NaCl, 0.05 M KCl, 7 mM Na$_2$HPO$_4$, 1% (w/v) glucose, 0.2 M Hepes, pH 7.0 adjusted with NaOH
- 1x HeBS: 1: 10 dilution of 10x HeBS, pH 7.12 adjusted with NaOH

Transfection to H293 cell lineage was carried out by calcium phosphate precipitation as described earlier (Gorman, 1985). 5 μg of plasmid DNA were mixed with 1ml HeBS (pH 7.12) by pipetting in a 1.5 ml reaction tube. After adding 50 μl of 2.5 M CaCl$_2$, the mixture was gently pipetted up and down, and incubated at RT for 30 min. The DNA/CaCl$_2$ solution was then added to a flask of semi-confluent grown cells which were seeded 1 day before and incubated in 5 ml fresh DMEM supplementary medium at 37°C for 4 hours before. After 4

hours incubation at 37°C, the medium was changed with 5 ml fresh medium for further cultivation. The cells were harvested 2 days after transfection.

3.3 Microbiological Methods

3.3.1 Bacterial Cultures

- Growth Media and Solutions
- 2TY medium: 1.6% tryptone, 1% yeast extract, 0.5% NaCl, autoclaved; for selective medium antibiotic was added
- LB medium: 1% tryptone, 0.5% yeast extract, 1% NaCl, autoclaved; for selective medium antibiotic was added
- Agar plates: 2TY or LB medium plus 15 g/l agar, autoclaved; for selective plates antibiotics were added at 55°C and the liquid is filled into sterile petri dishes
- Ampicillin stock solution: 50 mg/ml in distilled water (working concentration: 50 μg/ml), stored at –20°C
- Tetracycline stock solution: 5 mg/ml in ethanol (working concentration: 30 μg/ml)

Single bacterial colonies picked from a selective plate or 10 μl of a glycerol culture (frozen culture at –70°C by mixing 700 μl fresh culture with 300 μl autoclaved glycerol) were taken for bacterial cultures. For transformation of bacteria a medium containing an appropriate antibiotic is used. First a starter culture of 10 ml (termed pre-culture) was cultivated at 270-280 rpm in a shaker overnight at 37°C. After diluting the starter culture in selective medium in a range of 1:100 to 1:1000, it was incubated for a further 12-16 hours under the same conditions until the solution reached an optical density (OD600$_{nm}$) of 0.5-0.6. The bacteria were now ready for harvesting and lysis or could be stored as glycerol stocks.

3.3.2 Transformation of Competent *E. coli*

- CaCl$_2$ solution: 100 mM CaCl$_2$

Bacteria cells were made competent by the calcium chloride method. 100 ml 2TY medium with 100-500 μl preculture was cultivated until the OD600$_{nm}$ reached 0.5-0.6 which ensured that the culture was still in the logarithmic growth phase. After centrifugation 5-10 min at 2000g at 4°C in two 50 ml falcon tubes, 1/2 of total volume of 100mM CaCl2 was added to resuspend the pellets. After 30 min of incubation on ice the solution was again centrifuged, resuspended with 1/10 of total volume of 100 mM CaCl$_2$ and incubated on ice for a further 30 min. The competent bacteria were now ready for use or could be stored at 4 °C for 24-28 hours. The efficiency of transformation increased four to six folds during the first 12-24 hours in the state of competence. Less than 50 ng of plasmid were added in 200 μl of competent bacteria medium, gently mixed and incubated on ice for 30 min (maximum until 2 hours). Following a heat-shock for 2 min at 42°C, they were cooled on ice for 5 min. Up to 200 μl of

this bacterial suspension were plated on selective agar plates and incubated at 37°C. Colonies appeared after 12-16 hours.

Transformation of Sure®competent cells was performed according to the "Transformation Guidelines" described in "the Instruction Manual of Competent and Supercompetent Cell" (Stratagene, Heidelberg, Germany).

3.4 DNA Methods

3.4.1 Preparation of Plasmid DNA

Many methods have been developed to purify plasmid DNA from bacteria. This chapter covers the methods that have been proved most suitable for this work. The easiest and quickest method of small scale preparations was the TELT method that was suitable for restriction analysis, subcloning and sequencing. Large scale preparations were done using the *Qiagen*® systems. Finally, plasmids for microinjection into *Xenopus laevis* eggs were prepared with the endotoxin-free *Qiagen*® kit.

TELT Preparation

Buffers and Solutions

- Lysozyme solution: 10 mg/ml in distilled water
- TE buffer: 10 mM Tris/HCl (pH 8.0), 1 mM EDTA
- TELT solution: 2.5 M LiCl, 62.5 mM EDTA, 50 mM Tris/HCl (pH 7.5), 0.4%
- Triton X-100

Bacteria were cultured as described above. 1.5 ml of the culture were centrifuged at 2000g for 5 min, and the supernatant was carefully removed. Following one more centrifugation and decanting, the pellet was resuspended in 150 μl TELT and 15 μl lysozyme solution which disrupts bacterial cell walls by hydrolysing the peptidoglycan. After vortexing and incubation for 5 min at RT the sample was heated for 2 min at 95°C and stored on ice for 5-20 min to inactivate the lysozyme. After centrifugation at 12000g for 20 min at 4°C, the supernatant was transferred to a fresh tube. 150 μl isopropanol was added, the suspension was gently mixed and kept at RT for 5 min. Following centrifugation at 12000g for 10 min, the pellets were washed with 300 μl 70% ethanol, dried at RT, and resuspended in 50 μl TE/RNase (20 μg/ml). Finally, the DNA preparation was stored at –20°C.

Qiagen Preparation

The Qiagen plasmid purification protocols are based on a modified alkaline lysis procedure (Birnboim and Doley, 1979). The genomic DNA was precipitated, and bound to an anion-exchange resin under appropriate low-salt and pH conditions. RNA, proteins, and low-molecular-weight impurities were removed by a medium-salt wash. Plasmid DNA was eluted in a high-salt buffer, and then concentrated and desalted by isopropanol precipitation.

To prepare plasmid DNA for microinjection it is necessary to remove the endotoxins, lipopolysaccharides of Gram-negative bacteria (e. g., *E. coli*), which is accomplished with the *Qiagen EndoFreeTM Plasmid Kit* (see below in 3.4.4).

3.4.2 Polymerase Chain Reaction (PCR)

The polymerase chain reaction (PCR) is a method of *in vitro* amplification of a specific DNA fragment with several millionfolds from a small amount of double-stranded DNA. It is used for *in vitro* cloning, sequencing and mutant generation as well as reverse-transcribed PCR (RT-PCR) to determine whether a specific gene is really transcribed into RNA in a certain cell type or tissue. The success of the PCR reaction depends on the availability of a purified DNA polymerase which must withstand temperature near boiling and two chemically synthesized DNA oligonucleotides serving as primers (each 15-20 nucleotides long) complementary to the flank region of nucleotide sequence at either 5'-terminus of double-stranded DNA. Optimal reaction conditions vary with primer annealing temperature, cycle number, concentration of DNA polymerase, $MgCl_2$, and target DNA fragment size. A standard PCR reaction was carried out in the volume of 50 μl consisting of 1-10 ng template DNA, 25 pmol forward primer, 25 pmol reverse primer, 1.5 mM $MgCl_2$, 5 μl 10x polymerase buffer and 5 U *Taq* DNA polymerase filled with distilled H2O to the final volume. The samples were normally covered with 100 μl mineral oil. The general scheme of PCR reaction includes: denaturing DNA at 94°C for 4 min, and performance of 30-35 cycles of PCR amplification involving denaturing at 94°C for 30 seconds, annealing at 55°C for 1 min, and extending at 72°C for 1 min. Finally, the reaction was incubated at 72°C for 10 min and could be maintained at 4°C overnight.

3.4.3 Site-Directed Mutagenesis PCR

Solution

- NZY+ broth: 1% NZ amine (casein hydrolysate), 0.5% yeast extract, 0.5% NaCl, adjusted to pH 7.5 with NaOH, autoclaved, the following supplements were added prior to use, 1.25 ml of 1M $MgCl_2$ and 1.25 ml of 1 M $MgSO_4$, 1 ml of 2 M filter-sterilized glucose solution or 2 ml of 20% (w/v) glucose, filled up to 100 ml with double-distilled water, finally sterilized by filteration

Using *Stratagene's QuikChange^{TM}* site-directed mutagenesis kit, a site-directed mutagenesis PCR could be performed to make point mutations, switch amino acids, and delete or insert single or multiple amino acids. Compared to other approaches to make *in vitro* site-directed mutagenesis, this site-directed mutagenesis PCR was carried out directly using double-stranded plasmid. 5 μl 10x reaction buffer, 5-50 ng double-stranded DNA plasmid, 5 μl primer

mix containing the desired mutation, 5 μl dNTP mix, 1 μl *PfuTurbo* DNA polymerase (2.5 U/μl), double-distilled water were filled to a final volume of 50 μl. After mixing the components, the reaction was overlaid with 100 μl mineral oil. The cycling parameters were set up in the following way: denature DNA at 95°C for 30 seconds, anneal primers at 55°C for 1 min, extend fragments at 68°C for 2 min per kb of plasmid length, run 12-18 cycles. After cooling to 4°C for 2 min, 1 μl *Dpn* I restriction enzyme (10 U/μl) was added and incubated at 37°C for 1 hour to digest the methylated, nonmutated parental DNA template. For transformation, the *Dpn* I treated DNA reaction was transferred to 50 μl *E. Coli* XL1-Blue supercompetent cells. After heat-shock, 0.5 ml NZY+ broth preheated to 42°C was added. The transformation reaction was incubated at 37°C for 1 hour with shaking at 225-250 rpm just before plating onto agar plates.

3.4.4 Purification of DNA

A basic way to purify the DNA fragment from PCR and other enzymatic reactions is extraction with phenol/chloroform to remove proteins. Additionally, agarose gel electrophoresis is a standard method to separate, identify, as well as to purify DNA fragments from primers, nucleotides, polymerases, and salts which are involved in the reactions.

Extraction with Phenol/Chloroform

- Solutions
- Phenol: TE saturated (pH 8.0) from distributor
- 3 M NaAC, pH 5.2

An equal volume of phenol was added to the sample, mixed thoroughly for 30-60 seconds on the vortex until an emulsion formed. After centrifugation at 12000g for 3 min at RT, the aqueous phase was transferred to a fresh tube. To remove the phenol residues, 2 volumes of chloroform and 1 volume of H_2O were added. The mixture was again vortexed 30-60 seconds until an emulsion form, and then centrifuged at 12000g for 3 min at RT. After transferring to a fresh tube, the aqueous phase was mixed with 1/10 volume of NaAC and 3 volumes of 96% ethanol by vortexing for 10-30 seconds, and then incubated at –70°C for at least 30 min. The reaction was centrifuged at 12000g for 20 min at 4°C. After discarding the supernatant, the pellet was washed with 500 μl of 96% ethanol. Following 2 times centrifugation at 12000g for 5 min at RT and drying in the air for 5 min, the pellet was finally resuspended with 10 μl H_2O. The purified DNA fragment was available for further use.

Agarose Gel Purification

Separation of DNA fragments by Agarose Gel Electrophoresis

Buffers and Solutions

- Ethidium bromide stock solution: 10 mg/ml in TAE (working concentration: 0.5 µg/ml)

- 10x Loading buffer: 0.25% bromphenol blue, 30% glycerine

- 50xTAE buffer: 2 M Tris (pH 8.0), 1 M glacial acetic acid, 50 mM EDTA

Based on the size of the DNA fragment, 1-2% agarose in TAE buffer was melted using a microwave. After adding ethidium bromide to the solution, it was poured into a mould and allowed to polymerize. DNA samples were mixed with 1/10 loading buffer, and loaded onto the slots using a micropipette. A voltage of 60-80V was applied. The negatively charged DNA migrates to the anode, and the migrating distance depends on the size and conformation of the DNA.

Because ethidium bromide intercalates with the DNA, the DNA bands in the gel can be visualized with ultraviolet light at 302 nm which can then be documented. Determination of DNA fragment size and quantity is achieved by comparison with a standard marker. The λ-Hind marker used in this work indicates the following fragment sizes (kb) and quantities (µg or ng): 23.1 kb (0.47 µg), 9.4 kb (0.19 µg), 6.6 kb (0.136 µg), 4.6 kb (94.5 ng), 2.3 kb (47.2 ng), 2.0 kb (41.1 ng), 0.56 kb (11.5 ng), 0.12 kb (2.5 ng). A 100bp ladder is also used, and its fragment sizes in bp are 100; 200; 300, 400; 500; 600; 700; 800; 900; 1000; 1500, respectively.

Extraction of DNA Fragments with the *Endotoxin-Free Qiagen* Kit

The genomic DNA is precipitated, and bound to an anion-exchange resin under appropriate low-salt and pH conditions, while RNA, proteins, and low-molecular-weight impurities are removed by a medium-salt wash. Plasmid DNA is then eluted in a high-salt buffer, and finally concentrated and desalted by isopropanol precipitation. To prepare plasmid DNA for microinjection, it is necessary to remove the endotoxins, lipopolysaccharides coming from Gram-negative bacteria (e. g., *E. coli*). Using the *Qiagen Endotoxin-Free*^{TM} Plasmid Kit, the endotoxin is removed by an endotoxin removal buffer, which yields purified DNA plasmid containing less than 0.1 unit endotoxin per µg DNA plasmid. All steps were done as stated in the manual of *Qiagen* Plasmid Purification Handbook.

After separation on a 1% agarose gel, the DNA-containing band of interest was excised using a clean scalpel under ultraviolet light and placed into an autoclaved microfuge tube. The remnant agarose around the DNA band was cut off as much as possible. 3 volumes of buffer *QG* were added to 1 volume of gel (100 mg equivalent to 100 µl). The reaction was incubated at 50°C until the gel slice dissolved completely. 1 volume of isopropanol was added to the sample and mixed. The sample was loaded to the *QIAquick* spin column

standing in a 2 ml collection tube. After centrifugation at 10000g for 1 min, the flow-through was discarded. Optionally, 0.5 ml of buffer *QG* was added to the *QIAquick* column to remove traces of agarose. Following centrifugation for 1 min, the *QIAquick* column was washed with 0.75 ml of buffer *PE* and centrifuged for 1 min. One more centrifugation was needed to completely remove ethanol from buffer *PE*. To elute DNA, the *QIAquick* column was placed in a clean 1.5 ml microfuge tube and 30 μl buffer *EB* or H_2O were added to the center of the *QIAquick* membrane. After standing for 1 min at RT, the column was centrifuged at a maximum speed for 1 min to collect the purified DNA.

3.4.5 Enzymatic Modifications of DNA

For cloning, the plasmid DNA of a vector has to be cleaved with restriction enzymes and incorporated with a foreign DNA fragment by ligation. The recombinant DNA plasmid can then be applied to transform bacteria.

Digesting DNA with Restriction Enzymes

DNA digestion was done using restriction enzymes which bind to and cleave double-stranded DNA at specific site within or close to a recognition sequence. 5-10 U restriction enzyme effectively digested up to 1 μg DNA. The reaction could be done in 20-80 μl. The standard reaction in a total volume of 20 μl consisted of 2 μl DNA dissolved in H2O, 2 μl 10x restriction buffer or as stated in the manufacturers manual, 2 μl of appropriate restriction enzyme and H_2O filled up to the final volume. If two restriction enzymes are used, 1 μl of each is added. The reaction mixture was incubated at 37°C for at least one hour or at 4°C overnight. To monitor the process, small aliquots could be taken out during the reaction and analyzed on a gel.

Ligation

A standard ligation reaction mixture with a total volume of 10 μl was done by adding 2 μl 10x ligase reaction buffer, 20-200 ng total DNA of digested vector and insert, 0.1 U T4 DNA ligase and H2O filled up to 10 μl. The optimal molar ratio of insert to vector is 3-5:1 for sticky ends or 5-10:1 for blunt ends. The mixture was incubated at 14°C overnight.

Dephosphorylation of DNA Fragments

To avoid re-ligation of DNA vector that is digested only with one restriction enzyme, and has complementary protruding termini, the vector DNA was dephosphorylated. Dephosphorylation was performed with Shrimp alkaline phosphatase (SAP) which removed the 5' terminal phosphate. For 1.0 pmol of DNA termini (similar to 2.5 μg of a 3 kb plasmid), 0.1-0.5 U SAP were sufficient. After adding reaction buffer, the mixture was incubated at 37°C for 1 hour. SAP was inactivated by heating at 65°C for 10 min. All reagents of this

reaction were purchased from *Amersham*. Before the sample can be used for ligation, it must be purified by extraction with phenol/chloroform.

Generating Blunt Ends

Filling the Recessed 3' Termini Using the Klenow Fragment

The Klenow fragment, which consists of the C-terminal portion of *E. coli* DNA polymerase I, is used to fill the recessed 3' termini created by restriction enzymes during DNA digestion and thereby to generate blunt ends. This could be done directly after digesting with restriction enzymes. A standard reaction mixture in a total volume of 10 μl consisted of up to 2 μg DNA, 1 μl 10 mM dNTP mix, 1 μl 10x buffer, and 1 μl Klenow fragment (3-5 U) (all materials from Roche, Mannheim, Germany). The mixture was incubated at 37°C for 30 min, and the Klenow fragment was inactivated by heating at 75°C for 10 min or by adding 1 μl of 0.5 M EDTA. The DNA can be purified by phenol/chloroform extraction and used for ligation.

Cleaving the Overhanging 3' Termini Using T4 DNA Polymerase

T4 DNA polymerase can cleave nuclear acids from the 3' termini to 5' termini at a low concentration of the dNTP mix. For 2 μg DNA in TE buffer, 5 mM MgCl2 as a final concentration, 1 μl 10 mM dNTP mix and 4 U T4 polymerase were added. The mixture was incubated at 12°C for 15 min. By adding 2 μl of 0.5 M EDTA the reaction was inactivated.

3.4.6   DNA Determination

Sequencing

DNA sequencing was done using the enzymatic method of Sanger et al. in 1977 which is based on *in vitro* DNA synthesis carried out in the presence of chain-terminating nucleoside triphosphates. The method was performed automatically. It used standard primers (T3, T7, SP6, M13) or gene specific primers and four dideoxyribonucleoside triphosphates as terminators in separate DNA synthesis reactions on the same primed single-stranded DNA template. These four dideoxyribonucleoside triphosphates were covalently linked to different fluorescing dyes and capable of blocking the addition of the next deoxyribonucleoside triphosphate during their incorporation into a DNA chain due to the absence of a 3' hydroxyl group. As a result, the chain-extension reaction yielded a series of DNA fragments in the four separate tubes. These fragments were then separated in four parallel lanes of a polyacrylamide gel by electrophoresis. This led to a series of bands, each with the fluorescence spectrum indicating a successive base in the DNA being sequenced. The final sequence of DNA was analyzed by a computer using the MacMolly software (Soft Gene GmbH, Berlin, Germany).

Quantification of DNA and RNA

Due to their characteristic absorption maximum at $\lambda=260$ nm, nucleic acids can be photometrically quantified. Contaminations with proteins which have an absorption maximum at ultraviolet wavelengths of $\lambda= 280$ nm can influence the result. Therefore, the ratio of absorptions at both $\lambda= 260$ nm to absorption at $\lambda= 280$ nm should be in a range of 1.6:1 to 2.0:1. For uncontaminated nucleic acid solutions the law of Lambert-Beer is applied: 50 μg/ml double-stranded DNA has an OD 260 of 1.0, 40 μg/ml single-stranded DNA or RNA has an OD 260 of 1.0.

3.5   RNA Methods

- DEPC: 0.1% (v/v) DEPC in distilled water, stirred and incubated overnight to make it dissolved completely, finally autoclaved

Skin and lab ware are often a source of RNases. Therefore to avoid contamination by RNase, it is necessary to wear disposable gloves while working with RNA and to treat all the sterile plastic lab ware with DEPC water and autoclave all plastic dishes. For buffers RNase free chemicals must be used.

3.5.1   Isolation of RNA

Solutions

- Magnesium sulphate: 25 mM $MgSO_4$ in DEPC H_2O
- Sodium acetate: 0.1 M NaAc (pH 5.5) in DEPC H_2O

Total RNA from whole embryos was isolated using *TRIzol* Reagent (Gibco R BRL, Karlsruhe, Germany). The collected embryos were immediately used for RNA isolation or immediately frozen with liquid nitrogen and stored at -70°C for later use.

1 ml of *TRIzol* Reagent is sufficient for the total RNA isolation from 10-20 embryos, equivalent to 50-100 mg of tissue. *TRIzol* Reagent is a mixture of phenol and guanidine isothiocyanate, and is able to dissociate nucleotide from proteins and maintain the RNA integrity. The sample of whole embryos was rapidly homogenized in *TRIzol* Reagent with an ultrasonic homogenizer. For removal of proteins, 200 μl chloroform was added to the homogenate. The mixture was shaken vigorously in the tubes by hand for 15 seconds, and incubated at RT for 2-3 min. After centrifugation for 15 min at 12000g (maximum) at 4°C, the upper aqueous phase was transferred into a sterile tube. 500 μl isopropanol was added, and the mixture was vortexed thoroughly. The pellet was precipitated by centrifuging at 12000g at 4°C for 10 min, and washed with 70% ethanol. Afterwards, the pellet was redissolved in an appropriate volume of DEPC H_2O. 3 μl DEPC H_2O was normally added for 1 embryo, equivalent to 4-5 μg total RNA. To avoid DNA contamination, the RNA should have been treated with DNase I prior to RT-PCR, e.g., 4 μl NaAc, 5 μl MgSO4 and 1μl DNase I were

added in 25 μl RNA solution. The reaction was incubated at RT for 10 min at 37°C for 20 min, and inactivated at 70°C for 5 min. After extraction with phenol/chloroform, the pellet was washed with ethanol and resuspended in DEPC H_2O.

3.5.2 *In vitro* Transcription of RNA

The reverse transcriptase, a retroviral DNA polymerase, takes RNA as a template to transcribe isolated mRNA into cDNA which can be later used for PCR. This RT-PCR allows analysis of expression of RNAs of interest semi-quantitatively during embryonic development when compared to a standard housekeeping gene.

3.5.2.1 *Reverse Transcribed PCR*

First Strand cDNA Synthesis

The reaction was performed in a standard volume of 20 μl suitable for 1-5 μg of total RNA. 1μl Random Hexamer (500 μg/ml), 1-5 μg total RNA, and up to 7 μl DEPC H_2O were added to a nuclease-free microcentrifuge tube. After mixed by pipetting, the mixture was heated at 70°C for 10 min and quickly chilled on ice to allow Random Hexamer to bind to mRNA. The sample was shortly centrifuged and 4 μl 5x *first strand* buffer, 2 μl 0.1 M DTT, and 4 μl 2.5 mM dNTP mix were added to the sample. After gently mixing the mixture, 1 μl (200 U) of reverse transcriptase (Superscript II from Gibco BRL) was added. The reaction was incubated at 42°C for 50 min, then inactivated by heating at 70°C for 15 min. The volume was doubled with 20 μl DEPC H_2O, and the cDNA was stored at -70°C or used directly for PCR. To control specificity of reverse transcription, RT- was also performed using all the other components together with DEPC H_2O instead of the reverse transcriptase.

Analyse of Marker Genes by RT-PCR Semi-Quantitatively

Buffers and Solutions

- 10x TBE: 890 mM Tris Borate (pH 8.0), 2 mM EDTA
- (radioactive) 30% Acrylamide: acrylamide/bisacrylamide = 30:1
- (radioactive) Polyacrylamide gel: 6 ml 30% acrylamide, 1.8 ml 10x TBE, 2.1 ml 87% glycerine, 140 ul 10% ammonium peroxodisulfate, 45 ul TEMED filled up to 36 ml with H_2O

When a cDNA fragment is available by reverse transcription, it can be amplified with a pair of specific primers by PCR. After agarose gel electrophoresis, the intensity of bands on the gel is proportional to the quantity of the amplified transcript if the cycle number is not beyond the saturation point of reaction. A stable and ubiquitously expressed housekeeping gene like histone 4 or EF1 serves as an internal standard because the bands of the housekeeping gene are expected to be equal in the group of compared samples. The sample can be amplified within 26-35 cycles depending on the different purposes. The standard reaction for

RT-PCR was performed with the volume of 20 μl consisting of 2 μl cDNA from the first-stand reaction, 2 μl 2.5mM amplification primers mix, 2 μl PCR buffer, 0.5 μl 10mM dNTP mix, 0.6 μl 50mM MgCl2, 0.4 μl Taq DNA polymerase (5 U/μl) and H_2O filled up to 20 μl. After adding 4 μl 5x loading buffer, an aliquot of reaction was analyzed on 2% agarose gel and finally documented. To avoid DNA contamination, H_2O control PCR was also carried out with all the other components along with H_2O replacing the cDNA.

3.5.2.2 Preparation of RNA for Injections

Preparation of Linearized DNA from Plasmid

To synthesize the capped run-off transcripts of defined size, the double-stranded DNA template which contains a polyA tail or parts of the human globin gene necessary for higher RNA stability *in vivo*, should be completely digested with a suitable restriction endonuclease that cleaves distal to the promoter. This standard reaction mixture with a total volume of 80 μl consisted of 8 μl (5-8 μg) plasmid DNA, 8 μl 10x specific restriction buffer, 8 μl appropriate restriction enzyme, and DEPC H_2O up to 80 μl. The reaction mixture was incubated at 37°C for at least 2 hours or overnight. The linearized DNA was purified by agarose gel extraction.

In vitro Transcription of Capped RNAs

The *in vitro* transcription of capped RNAs was performed in a standard reaction volume of 20 μl using the *Ambion in vitro* transcription kits as stated in the instruction manual. The mixture contained 2 μl 10x transcription buffer, 10 μl 2x ribonucleotide mix, 1 μl (optional) [α-32P]-labeled ribonucleotide, 1 μg linearized template DNA, 2 μl RNA polymerase (T3, T7 or SP6), nuclease-free DEPC H_2O filled up to 20 μl. After gently mixing the components, the reaction mixture was incubated at 37°C either 1 hour for T3, T7 or 2 hours for SP6. To remove DNA template, 1 μl RNAse-free DNase I (2 U/μl) was added and incubated at 37°C for 15 minutes. The reaction was terminated by adding 115 μl nuclease-free DEPC H_2O and 15 μl ammonium acetate stop solution. An equal volume of buffer-saturated phenol/chloroform was added to the reaction mixture. After vortexing and centrifuging at 12000g for 5 min, the upper phase was transferred into a fresh tube. An equal volume of chloroform was added to completely remove phenol. Following centrifugation, the upper phase was transferred to another fresh tube and an equal volume of isopropanol was added. Following vortexing, the reaction was chilled at –20°C for at least 15 min or overnight. The pellet was precipitated by centrifuging at 12000g at 4°C for 15 min, and resuspended with 25 μl DEPC H_2O. After the concentration was measured using a photometer, the transcribed mRNA was stored in aliquots of 1 μl at –80°C.

3.5.2.3 Anti-Sense Labeled RNA

Solutions

- 10X NTP Digoxigenin-UTP labeling mixture: 10 mM ATP, 10 mM CTP, 10 mM GTP, 6.5 mM UTP, 3.5 mM DIG-UTP, pH 7.5

- 10X NTP Fluorescein-12-UTP labeling mixture: 10 mM ATP, 10 mM CTP, 10 mM GTP, 6.5 mM UTP, 3.5 mM fluorescein-12-UTP, pH 7.5

The linearized plasmid cleaved by a specific endonuclease was used for preparation of anti-sense RNA probe. Alternatively, the plasmid DNA fragments of choice can be amplified by PCR and purified by agarose gel extraction. It should be mentioned that a promoter for SP6, T7 or T3 polymerase must be included in the amplified fragment by designing a pair of promoter-containing primers. The polyA tail special for *in vivo* stabilization is unnecessary. Depending on the purpose, either the fluorescein-12 or digoxigenin-coupled UTP was used to label the transcripts which were detected by antibodies against flourescein-12 or digoxigenin. A standard reaction was carried out in a volume of 20 μl consisting of 2 μl 10x transcription buffer (Roche, Mannheim, Germany), 2 μl digoxigenin or fluorescein labeling NTP mix, 0.5 μl RNase inhibitor, 1 μl SP6, T7 or T3 RNA polymerase and 1 μg linearized DNA filled with DEPC H_2O to the final volume. The mixture was incubated at 37°C for 2 hours. At the interval of 1 hour, additional 1 μl RNA polymerase was added to enhance the reaction. 2 μl DNase I was added and incubated at 37°C for 15 min to remove the DNA template. After adding 30 μl DEPC H_2O, the transcribed anti-sense RNA was purified by loading to a *G50* column. After centrifugation at 3000g for 1 min, 1500 μl hybridization buffer was added and mixed up. The probe was stored at -70°C for further use or boiled at 85°C for 5 min for direct use.

3.5.3 Whole Mount *in situ* Hybridization

Buffers and Solutions

- 20x SSC: 3 M NaCl, 300 mM sodium citrate (pH 7.0) in DEPC H_2O, stored at RT

- 50x Denhardt's: 1% BSA, 1% polyvinylpyrrolidone, 1% Ficoll in DEPC H_2O, stored at -20°C

- Antibodies: anti-digoxigenin-AP (1:2000 in blocking solution), anti-fluorescein-AP (1:2000 in blocking solution)

- Alkaline phosphate (AP) buffer: 1 ml 1 M Tris (pH 9.5), 500 μl 1 M $MgCl_2$, 200 μl 5 M NaCl, 100 μl 10% Tween, filled up to 10 ml with DEPC H_2O

- Blocking solution: 2% BMB, 0.05% Tween, 10% lamb serum in MAB, stored at -20°C

- BMB: 10% Boehringer Blocking Agent in MAB, autoclaved, stored at -20°C

- Heparin solution: 100 mg/ml in DEPC H_2O

- Hybridization buffer (50 ml): 25 ml formamide, 12.5 ml 20x SSC, 1 ml torula RNA sol., 50 μl heparin sol., 1 ml 50x Denhardt's, 500 μl 10% Tween, 500 μl 10% CHAPS, 500 μl 0.5 M EDTA, all contents must be RNase free

- Lamb serum: inactivated by boiling at 55°C for 30 minutes, stored at -20°C, filtered sterile before use
- MAB buffer: 100 mM maleic acid, 150 mM NaCl (pH 7.5), stored at 4°C
- Proteinase K stock solution: 20 mg/ml in TBST (working concentration: 10 μg/ml), stored at -20°C
- Staining solution: 4.5 μl NBT, 3.5 μl BCIP ad 1 ml AP buffer
- TBS: 25 mM Tris (pH 7.4), 137 mM NaCl, 5 mM KCl, 0.7 mM $CaCl_2$, 0.5 mM $MgCl_2$
- TBST: 0.1% Tween in TBS
- Triethanolamine: 0.1 M (pH 7-8) in distilled water, filtered sterile, stored at 4°C
- Torula RNA solution: 50 mg/ml torula RNA in DEPC H_2O, stored at -20°C

In situ hybridization, developed by Gall and Pardue in 1969, has been widely used to reveal the distribution of specific nuclear acids within cells and tissues. It was further developed by Harland in 1991 to be applied on whole embryos, and called whole mount *in situ* hybridization. The anti-sense RNA probe labeled with digoxigenin or fluorescein hybridized with embryonic mRNA complementarily and specifically, therefore the anti-digoxingenin-AP or anti-fluorescein-AP can detect the labeled double-stranded RNA. After a color reaction, the specific embryonic mRNA hybridized with the probe was visualized.

Fixing of Embryos

Embryos of different stages were fixed with MEMFA, and transferred stepwise to and stored in 100% ethanol for further use. The vitelline membrane of gastrula and neurula stage embryos was removed manually to allow for better staining.

Hybridization

The fixed embryos were rehydrated by passing through a series of ethanol solution, from 75% ethanol/25% DEPC H_2O, 50% ethanol/50% DEPC H_2O, 25% ethanol/75% DEPC H_2O to finally TBST, 5 min each step. After washing twice for 5 min with TBST, the embryos were incubated in 10 μg/ml Proteinase K in TBST 10 min for younger than stage 14 embryos or 15-30 min for older than stage 15 embryos. The embryos were then washed twice 5 min with 0.1 M triethanolamine, incubated in fresh triethanolamine spiked with 17.5 μl acetic anhydride in the volume of 7 ml for 5 min, and 5 more min in the solution supplemented with additional 17.5 μl acetic anhydride. After washing twice for 5 min with TBST, the embryos were post-fixed with MEMFA plus 0.1%Tween at RT for 30 min, followed by two washing steps for 5 min with TBST. TBST was completely removed and the embryos were briefly washed in 500 μl hybridization buffer before they were incubated in 500 μl fresh hybridization buffer at 60°C for 4 hours. For hybridization, the buffer was replaced by hybridization buffer containing 1 μg/ml whole mount RNA probe, and incubated at 60°C overnight. Before use the RNA probe was boiled at 85°C. Following hybridization the removed probe was saved for further use. The embryos were intensively washed with 1 ml hybridization buffer at 60°C for

20 min, twice for 20 min with 2x SSC plus 0,05% Tween and twice for 20 min with 0.2x SSC plus 0.05% Tween. Finally, the embryos were washed twice for 10 min with TBST at RT.

Antibody Incubation and Color Reaction

The embryos were incubated in 500 µl blocking solution at RT for 1 hour. The antibody diluted 1:2000 in 500 μl blocking solution was also preblocked at RT before the embryos were incubated with the antibody solution at RT for 4 hours or at 4°C overnight. After washing 6 times for 30 min in TBST, 2 times for 5 min in 1 ml AP buffer at RT, the embryos were incubated in the staining solution in a dark box by adding 4.5 μl NBT plus 3.5 μl BCIP to 1 ml AP buffer per sample. Staining process proceeded until the embryos reached the desired level of staining. The embryos were washed 2 times for 5 min in TBST, and post-fixed with MEMFA plus 0.1% Tween at RT for 2 hours or at 4°C overnight. The embryos could be stored in TBST at 4°C until 4 weeks or in 70% ethanol for a longer period. The endogenous pigment could be bleached in 70% methanol/10% hydrogen peroxide for at least 2 hours under sunlight or UV light.

Double Staining

- *Fast Red* Tablets: 1 tablet dissolved in 2 ml 100 mM Tris (pH 8.2)

The double staining was done to distinguish different marker genes based on the *in situ* hybridization as described above. The whole mount probes labeled with digoxigenin or flurorescein were prepared. The procedure before hybridization is the same as stated above. The hybridization with two whole mount probes can be done simultaneously by incubating the embryos in a mixture of two probes at 60°C overnight. Because the antibodies are coupled to alkaline phosphatase, the antibody incubation and color reaction have to be performed consecutively. Between the two antibody incubations and color reaction, the primary alkaline phosphatase must be denatured. The *Fast Red* staining is first performed because this staining is much more stable to heating than NBT/BCIP blue staining. After washing twice for 5 min in 0.1 M Tri-HCl pH 8.2, the embryos were incubated in 1ml *Fast Red* staining solution prepared by adding 1 *Fast red* tablet in 2 ml 100 mM Tris-HCl pH 8.2. The color reaction was frequently controlled until the embryos reached the desired level of staining. After washing twice for 5 min in TBST, the embryos were then heated in 1ml 5 mM EDTA at 65°C for 10 min to denature the primary alkaline phosphatase. The embryos were washed twice for 5 min in TBST at RT, and incubated with the secondary antibody followed by the NBT/BCIP color reaction as described above. It should be noted that methanol or ethanol treatment has to be avoided because *fast* red staining is sensitive to alcohol treatment. After post-fixation, the embryos were stored in TBST at 4°C or in 70% ethanol at −20°C.

3.6   3.6 Proteinbiochemical Methods

3.6.1   Cell and Embryo Lysates

Buffers:

- APBS: 103 mMNaCl, 2.7 mMKCl, 0.15 mM KH_2PO_4, 0.7 mMNa$_2$HPO$_4$, pH 7.5
- APBS/Ca^{2+}: 2 mM CaCl$_2$ in APBS
- NOP Lysis buffer: 150 mM NaCl, 10 mM Tris/HCl (pH 7.8), 1 mM MgCl$_2$, 0.75 mM CaCl$_2$, 2% Nonidet P40, stored at 4°C
- Protease inhibitors: 1 mM PMSF, 10 μg/ml Aprotinin, Leupeptin, Pepstatin A

To isolate cadherin proteins for Western blotting, NOP buffer lysates of cells or embryos were prepared which allows for the extraction of cytoplasmic proteins and membrane proteins even from cytoskeleton-bound fractions. This procedure must be performed at 4°C to avoid protease digestion.

A cell culture flask of cells was gently washed twice with 750 μl APBS/Ca^{2+}. The cells were scraped from the bottom twice with 750 μl APBS/Ca^{2+} using a rubber policeman. After transfer to a fresh eppendorf tube, the mixture was centrifuged at 12000g at 4°C for 5 min. To prepare embryo lysate, 20 embryos were collected in a reaction tube and the overlaying MBSH was removed. When immediately frozen in liquid nitrogen the embryos could be stored at -70°C for later use. For protein extraction, 150-200 μl NOP buffer were added to the cell pellets or embryos. Lysis was performed by sucking the solution through a pipette and a syringe with a needle (0.40 mm in diameter). Embryos older than stage 40 were homogenized with a sonifer. Lysates were kept on ice or gently rocked at 6-8°C for a while. Afterwards, an equal volume of freon was added to the lysates to remove yolk proteins which could react nonspecifically with antibodies during Western blotting. After vortexing and centrifugation at 12000g for 10 min for cell culture lysates or 2 min for embryonic lysates, the clear upper layer was transferred into a new tube. 1/4 volume of 1x SDS-PAGE sample buffer was added. The sample was boiled at 95°C for 5 min, and finally stored at -20°C for future use.

Enrichment of Glycoproteins

Buffers

- High Salt: 0.5 M NaCl, 10 mM Tris (pH 7.5), 2 mM CaCl$_2$
- Low Salt: 10 mM Tris (pH 7.5), 2 mM CaCl$_2$
- RIPA: 1% Triton, 150 mM NaCl, 0.5% Sodium deoxycholate, 0.2% SDS, 20 mM HEPES (pH 7.4)

Concanavalin A (Con A), first crystallized by Sumner and Howell (1936), is a lectin which has been shown to have a high affinity for terminal-D-mannopyranosyl and -D-glucopyranosyl

residues of glycoproteins, enzymes and membrane lipids. Con A is used for the enrichment of glycoproteins, e.g cadherins in NOP lysates.

50 μl of the suspension of Con A coupled with sepharose were suitable for 150 μl NOP lysate. To remove the preservatives, Con A sepharose was washed three times with the same volume of NOP buffer and spun at 550g for 3 min. Subsequently, a suitable volume of NOP lysates was added into Con A sepharose and the mixture was gently agitated on the rotator at 4°C for 90 min. After centrifugation at 550g for 3 min, the pellet was washed three times with RIPA, three times with High Salt and three times with Low Salt buffer at 4°C. After the last centrifugation, the pellet was resuspended in 1/4 volume (about 5 μl) of 1x SDS-PAGE sample buffer and then boiled at 95°C for 5 min. To remove the ConA-beads, a bottom punctured tube was placed in a fresh collecting tube, and then centrifuged at 20,000g to collect as much lysate as possible. Normally, 20 μl of Con A lysate can be obtained.

3.6.2 Western Blotting

Western blotting is a powerful method for identifying a specific protein in a complex mixture and for determining its molecular weight. The procedure consists of a series of steps.

First, the denatured proteins in the mixture were separated by polyacrylamide gel electrophoresis (PAGE).

Second, the separated proteins were transferred to a nitrocellulose membrane while retaining their relative position.

Third, the protein was detected by incubation of the membrane with a specific antibody and visualized with chemiluminescent reagent.

SDS-Polyacrylamide Gel Electrophoresis

Buffers and Solutions:

- Acrylamide stock solution: 24% (w/v) Acrylamide, 0.64% (w/v) Bisacrylamide
- APS: 10% Ammonium peroxodisulfate
- 5x Sample buffer: 0.5 M Tris/HCl (pH 6.8), 10% (w/v) SDS, 20% Glycerol,0.0025% Pyronin Y, 25% β-Mercaptopropanediol
- 5x Electrophoresis stock buffer: 125 mM Tris, 960 mM Glycine
- Gel Electrophoresis buffer: 1x Electrophoresis buffer with 0.1% (w/v) SDS
- Sol A: 24% Acrylamide, 0.64% Bisacrylamide
- Sol B: 1.5 M Tris (ph 8.8)
- Sol C: 10% SDS
- Sol D: 0.5 M Tris (pH 6.8)

Electrophoresis is the migration of charged molecules in an applied electric field. Their rate of migration depends on the strength of the field, the net charge, the size and shape of the molecules and also on the ionic strength, viscosity and temperature of the medium wherein

the molecules are moving. Sodium dodecyl sulphate (SDS) is an anionic detergent which can bind to hydrophobic regions of the protein molecules causing them to unfold into extended polypeptide chains. They also get released from other associated proteins or lipid molecules. Thus, the proteins are denatured. Due to the binding of the negatively charged SDS in a mass ratio of 1.4:1 to each protein, which overwhelms the protein's intrinsic charge, the proteins will migrate toward the anode when a voltage is applied. After treatment of the proteins with SDS, the denatured polypeptides turn into rods of negatively charged clouds with equal charges or charge densities per unit length. Consequently, the migration rate does not depend on the intrinsic charge of the polypeptide, but on its molecular weight. A highly crosslinked gel of polyacrylamide with desired pore size provides the support matrix in which the movement of large macromolecules is retarded or in some cases completely inhibited while smaller molecules can migrate freely. The gel pore size depends on the concentration of acrylamide, which is chosen with regards to the expected sizes of the analyzed polypeptide. In this work, a discontinuous pH electrophoresis consisting of two-gel system was used to improve the resolution of protein bands. In a discontinuous system, a non-restrictive large pore gel, called a stacking gel, is placed on top of a separating gel. Each gel is made with a different buffer, two units less in the upper (pH 6.8) than that (pH 8.8) in the lower. The ions in the buffer with which the stacking gel is made from migrate faster than the proteins, while the ions in the tank buffer migrate slower than the protein, so that between the leading and trailing ions there is a zone of lower conductivity with higher voltage gradient causing the protein to move faster and to concentrate at the boundary in the stacking gel. This will contribute to the higher resolution of protein separation in the separating gel.

Table of Gel Components

	Stacking Gel		Separating Gel		
Concentration	3%	6%	5%	7.5%	15%
Sol A	1.25 ml	1.8 ml	3.1 ml	4.8 ml	9.3 ml
Sol B	0	0	3.75 ml	3.75 ml	3.75 ml
Sol C	100 μl	100 μl	150 μl	150 μl	150 μl
Sol D	2.5 ml	2.5 ml	0	0	0
H2O	6.2 ml	5.6 μl	7.9 ml	6.2 ml	1.7 ml
TEMED	30 μl	30 μl	25 μl	25 μl	25 μl
APS	50 μl	50 μl	50 μl	50 μl	50 μl

The gel apparatus with two clean glass plates was set up, and the gel monomer was prepared by mixing the ingredients gently in the order shown above. TEMED and APS were added just prior to pouring the gel between the glass plates because polymerization reaction can start immediately. Pouring was done very carefully to avoid air bubble formation. The separation gel was overlaid with butanol to create a flat surface and to exclude air which inhibits polymerization. It took about 20 min at RT for the separating gel to polymerize.

Butanol was removed and the gel surface was washed with distilled water. The stacking gel solution was added on top of the separating gel, the comb was inserted and the gel is allowed to polymerize for 20 min. After removing the comb the wells were cleaned with distilled water using a syringe needle. The discontinuous gel was placed into the electrophoresis apparatus and was filled with electrophoresis buffer. After boiling for 5 min at 95°C, 5-10 μl of prepared samples as described above were loaded onto the gel with a micropipette, and the gel was run at 60V. Once the dye front entered the separating gel, the voltage was increased to 120 V and subsequently maintained until the dye front reached the bottom of the gel. The gel was then carefully removed.

Coomassie Staining

Solutions:

- Coomassie solution: 0.25% Coomassie Brilliant Blue G-250, 50% ethanol, 10% acetic acid
- Destaining solution: 10% acetic acid, 30% ethanol

Coomassie staining solution fixes the proteins in the gel and the dye is then bound to the proteins. After electrophoresis, the gel was incubated in Coomassie staining solution for 1 hour at RT. The staining solution was removed and the gel was destained by repeated washings in the destaining solution. The sensitivity of the Comassie staining is 0.1-0.5 μg protein per band.

Gel Drying

The gel was placed onto a piece of Whatman paper and wrapped in a piece of plastic membrane before drying in a vacuum gel dryer for 1 hour.

Autoradiography

The proteins generated by radioactive *in vitro* transcription and translation (TNT) containing ^{35}S-methionine were visualized by autoradiography. This was done by exposing the dried gel to an overlaying X-ray film (X-OMAT AR-5) overnight or even longer and finally developing the film with a developing machine (Amersham, Braunschweig, Germany).

Molecular Weight Determination

The size of the proteins of interest was determined in relation to the molecular weight standard maker. In this work, the high molecular weight standard used consists of Myosin (rabbit muscle, 205 kD), β-Galactosidase (*E. coli*, 116 kD), Phosphorylase b (rabbit muscle, 97 kD), Albumin (bovine, 66 kD), Albumin (egg, 45 kD), and Carbonic Anhydrase (Bovine erythrocytes, 29 kD).

Protein Transfer

Buffers and Solutions:

- PBS: 2.7 mM KCl, 137 mM NaCl, 6.5 mM Na_2HPO_4, 1.4 mM KH_2PO_4 (pH 7.2)
- PBS/Tween: 0.5%Tween in PBS
- Ponceau solution: 1:20 dilution of stock (Sigma)
- Transfer buffer: 25 mM Tris (pH 8.3), 192 mM Glycine, 10% (v/v) methanol

For immunologic protein detection, the proteins in the gel must be transferred to a nitrocellulose membrane. This can be achieved by tank blotting (Towbin et al., 1979). Four sheets of Whatman paper and one sheet of nitrocellulose paper were cut to the same size as the gel. Once the electrophoresis was finished, some transfer buffer was poured into a container, and 2 sheets of sponge, 4 sheets of Whatman paper, 1 sheet of nitrocellulose paper were equilibrated in transfer buffer. Between the plastic holder a blot sandwich of buffer-soaked sheets was arranged in the following order: from the cathode to anode, sponge, 2x Whatman paper, polyacrylamide gel, nitrocellulose paper, 2x Whatman paper, and sponge. To isolate the gel from the electrophoresis apparatus, one glass plate was carefully removed from the gel, from which the stacking gel was cut off. Afterwards the gel was inverted and placed onto the Whatman paper, and the remaining glass plate was removed. More importantly, during the arrangement of the blotting chamber each layer has to be kept wet and air bubbles have to be pressed out. Finally the sandwich was placed into the transfer tank, which was filled with transfer buffer and cooled by a block of ice. After ensuring that the nitrocellulose paper was facing the anode, the transfer took from 1 to 1.5 hours at 111V. Afterwards, the nitrocellulose paper was briefly stained in Ponceau solution to judge the transfer quality. Stain was washed out with PBS and the lanes and the molecular weight standard were marked on the nitrocellulose paper with a ball pen. If necessary, the lanes were cut into stripes for later incubation with different antibodies.

Immunological Detection of Proteins

Solution and Antibodies

- Blocking solution: 10% nonfat milk powder in 0.5% APBS/Tween
- Alkaline phosphate (AP) buffer: 100 mM NaCl, 100 mM Tris (pH 9.5)
- TBS: 25 mM Tris (pH 7.4), 137 mM NaCl, 5 mM KCl, 0.7 mM $CaCl_2$, 0.5 mM $MgCl_2$
- TBST: 0.1% Tween in TBS
- Primary Antibody Solutions: GFP monoclonal antibody (1:500 in APBS), Myc monoclonal antibody (1:500 in APBS), rabbit cadherin-6 polyclonal antibody against EC1 (1:40 in APBS), mouse anti-HA monoclonal antibody (1:2000 in APBS), mouse 10H3 monoclonal anti-XEcadherin antibody (1:2 in APBS)
- Secondary Antibody Solutions: GAM-POD (1:20000 in APBS), GAR-POD (1:20000 in APBS), GAM-AP (1:4000 in APBS), GAR-AP (1:4000 in APBS)

To avoid non-specific binding by the antibody, the nitrocellulose paper or stripes were placed into the blocking solution and incubated for 0.5 hour at RT or overnight at 4°C on a rocker. After 3 times washing with APBS/Tween, the paper or stripes were incubated with the primary antibody solution in a sealed plastic bag overnight at 4°C on a rotator. The primary antibody solution was removed, the filters were washed 2 times with APBS/Tween for 15 min each on a rocker and incubated with the secondary antibody for 2 hours at RT on a rotator. After removal of the antibody the filters were washed 4 times with APBS/Tween for 10 min each. Afterwards proteins were visualized either by chemiluminescence if the peroxidase-conjugated secondary antibodies were used or by color reaction if the alkaline phosphate-conjugated secondary antibodies were applied.

The *ECL*^{TM} Western blotting detection system works as follows: the horse radish peroxidase (GAM-POD, GAR-POD) combined with the secondary antibody can catalyze oxidation of luminol, cyclic diacylhydrazide, which generates acridinium ester under slight alkaline conditions. This acridinium ester in an excited state can produce a sustained, high intensity chemiluminescence with maximum emission at a wavelength of 430 nm. Therefore, after Western blotting the nitrocellulose paper or strips was incubated with *ECL*^{TM} for 1 min at RT, exposed in a dark container to a blue light sensitive film (Kodak X-OMAT AR 5 film) for 0.5-60 min depending on the strength of the signal. The film was developed with an automachine (Amersham, Braunschweig, Germany). Alternatively the signal on the filters was directly documented using a Diana camera detection system (Raytest, Straubenhardt, Germany). For color reaction, the filters were incubated in AP buffer 2 times for 5 min after washing 4 times for 10 min in TBST. The signal was detected by incubating the filters in the NBT/BCIP (Roche, Mannheim, Germany) solution (1 tablet dissolved in 10 ml AP buffer) until the staining reached the desired level. The reaction was terminated by washing 2 times in TBST.

Stripping the Blot for Reuse

Solutions

- 0.1 M Glycin pH 2.5-3.0
- 6 M Urea in APBS
- 3 M Urea in APBS

For reuse, all the antibodies bound to the nitrocellulose filter were removed by stripping. It included the following steps: incubation in 0.1 M glycine for 5-10 min at RT, washing with APBS/Tween for 20 min, renaturation of the blot by incubating in 6 M urea, 3 M urea, APBS alone for 15 min. The blot was then ready for reuse.

3.6.3 *In vitro* Transcription and Translation (*in vitro* TNT)

By the TNT^{TM} coupled reticulocyte lysate systems (Promega, Mannheim, Germany), a protein can be synthesized *in vitro* directly from a DNA template, and the yield of protein is 3-6 fold in a 1.5 hour reaction compared to the standard *in vitro* translation with RNA templates. In this work, the *in vitro* translated protein was used in Western blotting to examine the specificity of cadherin-6 polyclonal peptide antibodies and to test function of the new construct of the molecule by subcloning. By radioactive ^{35}S-methionine labeling, the TNT coupled reaction was proved successful. The reaction was done by mixing the components in 50 μl of reaction volume in a microcentrifuge tube as follows: 25 μl TNT rabbit reticulocyte lysate, 2 μl TNT reaction buffer, 1 μl RNase inhibitor (40 U/μl), 1 μl 1 mM amino acid mix minus methionine, 1 μl 1 mM amino acid mix minus leucine or 2 μl 10 mCi/ml ^{35}S-methionine, 2 μl circular DNA template (0.5 μg/μl), 1 μl TNT RNA polymerase (SP6, T3 or T7), finally filled up with DEPC H$_2$O to 50 μl. The components were mixed by pipetting gently, and incubated for 60-120 min at 30°C. 1/4 volume of SDS-PAGE sample buffer was added and the sample was heated for 5 min at 95°C, 3-5 μl of the sample were loaded onto the SDS-polyacrylamide electrophoresis gel per slot and separated as described above. In case of radioactive TNT translated proteins, after electrophoresis the gel was dried and the proteins were visualized by autoradiography as stated above.

3.6.4 Protein Quantification

UV Detection

Absorbance of UV irradiation by proteins is the quickest method to quantify protein solution, whereby the absorbance maximum at 280 nm is due to the presence of tyrosine and tryptophane. This method is very suitable for an estimation of the protein concentration during the elution steps of protein purification. The absorbance was measured versus a suitable control, e.g. the elution buffer.

3.7 Histological Methods

3.7.1 Fixation, Embedding and Sectioning

Fixatives and Solutions

- Agarose solution: 3% agarose dissolved in APBS/$^{Ca2+}$ by heating with a microwave

The first step of any histological procedure is always fixation. In this work, the embryos were fixed in paraformaldehyde for 2-3 hours at RT or overnight at 4°C. Before embedding, the embryos were transferred stepwise through a series of APBS buffer from 50%, 75% to 100%, 10 min for each step. The embryos were embedded with hot agarose solution (60°C), and orientated well with a hair needle for sectioning before agarose polymerization. After

being cut into an appropriate embryo-containing block, the agarose block was stuck to a metal stander with biological glue for sectioning. With the aid of a vibratome, 25-50 μm sections were performed, and collected with a pipette into a plastic well or mounted on a glass slide. The sections were then ready for the further analysis, such as immunostaining.

3.7.2 Histological Examination

Buffers and Solutions

- Carmin-Borat solution: 2-3 g Carmin, 4 g Borat, filled up with H_2O to 100 ml, heated up until completely dissolved. After cooling, 100 ml of 70% ethanol were added. The mixture stood for several weeks and shaken several times. Finally, it was cleared through a folded filter.
- Anillin-Orange solution: 0.5 g Anillin, 2 g Orange G, 2 g oxalic acid dihydrate ($C_2H_2O_4$ x $2H_2O$), filled up with H_2O to 100 ml, heated up, and cleared through a folded filter
- HCl-Ethonal: 70% ethanol plus 0.25-0.5% concentrated HCl

In this work, histological analysis was performed with Carmin and Anillin staining as previously described (Geis et al., 1998). For infiltration of paraffin, the fixed embryos were incubated as follows: 30 min in isopropanol, 30 min in 1:1 isopropanol/xylene at RT, 30 min in xylene by heating at 60-65°C. The embryos were immersed in paraffin at 60-65°C stepwise as follows: 1 hour in 1:1 paraffin/xylene, 1.5 hour in 2:1 paraffin/xylene, 3 times 1 hour in paraffin, finally in paraffin overnight. The embryos were embedded in paraffin within a mould, and allowed to harden for 1 day at RT. After orientation in a right position, the embryos were cut transversely into 10 μm sections by a microtome. The sections were stretched at 37°C overnight. Deparaffinization of the sections was performed by incubating 5 min in xylene, 5 min in Rotihistol, 2 min in ethanol from 96%, 90%, 80% to 60%, 5 min in 1x PBS. The specimens were stained in Carmin-Borat solution for 1 hour at RT. For clearance, the sections were incubated 5 min at RT in 70% ethanol plus 0.5% HCl, and the surplus dye was removed by washing in 70% ethanol, and 50% ethanol. After washing 5 min with H_2O, the sections were incubated for 37 min in 7% tungstophosphric acid hydrate to intensify the color. The sections were washed 2 times 5 min with H_2O, and stained with Anillin-Orange for 20 min. Afterwards, the sections were fixed 3 min in 96% ethanol. The dried slides were coverslipped with Canada-Balsam (Canada-Balsam: 2:1) and analyzed under a brightfield microscope (Axiovert200, Zeiss, Oberkochen, Germany, stated in the Materials).

3.7.3 Immunostaining of Sections

Solutions

- Blocking solution: 1% bovine albumin (BSA) in APBS, sometimes plus 20% fetal calf serum (FCS) in case of high background
- DAPI stock solution: 1 mg/ml DAPI in APBS (working solution 1:2500 in APBS), stored at 4°C

- Primary antibodies: rabbit *Xenopus* cad-6 antibody against EC1 (1:10 in APBS), mouse GFP monoclonal antibody (1:50 in APBS), rabbit anti-phospho-Histone H3 (1:200 in APBS), mouse 9E10 monoclonal anti-myc antibody (protein A purified antibody 1:50 in APBS), rabbit polyclonal anti-flag antibody (1:400 in APBS)
- Secondary antibodies: GAR-Cy2 (1:100 in APBS); GAM-Cy3 (1:400 in APBS), GAR-cy3 (1:400 in APBS), GAM-cy2 (1:200 in APBS)

To avoid unspecific binding, the embryo sections were incubated in blocking solution for 1 hour at RT on a shaker. After removal of the blocking solution, the sections were incubated with the primary antibody overnight at 4°C. The sections were rinsed 4 times 30 min with APBS plus 0.1%Triton to remove the primary antibody. The sections were then incubated with the secondary antibody for 2 hours at RT. Again the sections were washed 4 times 30 min with APBS plus 0.1%Triton. At this step, DAPI was sometimes used to label the cell nuclei by incubating the sections 2 min with DAPI working solution at RT. After 2 times washing, the sections were mounted on a glass slide and embedded in elvanol. The sections were then available for examination by a fluorescent microscope or a confocal laser scanning microscope.

3.7.4 TUNEL Assays

Most higher eukaryotic cells have the ability to self-destroy by an intrinsic cellular suicide mechanism, the so-called programmed cell death or apoptosis (Ellis et al., 1991; Steller, 1995). The morphological changes occurring in the nucleus of apoptotic cells are characterized by the generation of DNA fragments cleaved by endogenous endonucleases, typically a population of multimers of 180-200 bp fragments (Arends et al., 1990; Gavrieli et al., 1992). Digoxigenin-coupled UTP is incorporated at the 3'-OH DNA fragment ends using the enzyme Terminal deoxynucleotidyl Transferase (TdT). Thereby, the antibody against digoxigenin can detect the apoptotic cells. In this work, TUNEL assays were conducted as previously described (Hensey and Gautier, 1998). The fixed embryos were rehydrated twice for 20 min in PBS puls 0.2% Tween 20 at RT, washed 2 times 15 min in PBS, and equilibrated 2.5 hours in TdT buffer. The embryos were then incubated in 150 U/ml TdT (*Gibco* BRL, Karlsruhe, Germany), and 0.5 μM digoxigenin-coupled UTP (Roche, Mannheim, Germany) at RT overnight. The reaction was terminated by twice 1 hour incubating in PBS plus 1 mM EDTA at 65°C. After washing 4 times 1 hour in PBS, the embryos were blocked in PBS plus 0.1% Triton and 0.2% BSA (PBT-B) for 1 hour at RT, PBS plus 0.1% Triton and 2% BMP for 30 min, PBT-B plus 20% horse serum for 1 hour, respectively, followed by incubation with anti-digoxigenin antibody coupled to alkaline phosphatase (1:500 in PBT-B plus 20% horse serum) at 4°C overnight. After washing 4 times 30 min in PBT-B at RT, the embryos were equilibrated with AP buffer 2 times 20 min. The color reaction was done by

incubating in 20 μl NBT/BCIP stock solution/1 ml AP buffer until the embryos reached the desired level of staining. The reaction was inactivated by washing 2 min with H_2O. Following dehydration 5-10 min with 100% methanol, the embryos were viewed with a binocular microscope (MZFl III, Leica, Benzheim, Germany).

4 Results

4.1 Cloning and Characterization of two *Xenopus* Cadherin-6 Isoforms

4.1.1 Sequence Comparison of the Full-Length Transmembrane and Soluble Isoforms of Xcadherin-6 Reveals Alternative Splicing of Xcadherin-6 mRNA

Via a PCR cDNAs encoding two isoforms of *Xenopus* cadherin-6, full-length Xcad-6 and short-form Xcad-6 were isolated from stage 35 *Xenopus laevis* embryos. Sequence comparison of both isoforms indicates that full-length Xcadherin-6 as a member of type II classic cadherin subfamily structurally displays an extracellular domain with 5 specific cadherin-repeats (EC1-5), a transmembrane domain (TM) and a highly conserved intracellular domain (IC). The putative homophilic binding site consists of a QAV motif instead of the HAV motif present in classical type I cadherins. The short-form Xcadherin-6 only possesses the three extracellular repeats EC1-3 and only part of the EC4 lacking a transmembrane and cytoplasmic domain. The full-length Xcadherin-6 was then designated as the transmembrane isoform of Xcadherin-6 (Xcad-6) and the short-form as the putative soluble isoform of Xcadherin-6 (sXcad-6) (Fig. 4.1). This suggested that alternative splicing of the Xcadherin-6 mRNA probably occurs during embryonic development resulting in two different isoforms of Xcadherin-6 which could have different functions. Therefore, the in vivo presence of both isoforms was further investigated.

4.1.2 Two Isoforms Are Expressed during *Xenopus* Development

To figure out whether two isoforms of Xcad-6 are indeed expressed during embryogenesis, RT-PCR was applied to detect the different transcripts of Xcadherin-6 in embryogenesis. Using a pair of primers, which amplifies the fragment from the EC3 to the EC4 region containing the putative alternatively splicing site of Xcad-6 mRNA (Fig. 4.2 A) the RT-PCR revealed a single fragment at early tadpole embryos of stage 32, while two fragments appeared in tadpole embryos of stage 40 (Fig. 4.2 C). The two fragments amplified were of the expected size, full-length Xcad-6 of 304bp and sXcad-6 of 165bp when compared with the fragments generated from the corresponding plasmid DNA (Fig. 4.2 C). The results demonstrate that both isoforms are present as transcripts but the full-length transcript appears earlier and in higher amounts than the short form. The validity of the RT-PCR reactions was determined by amplification of histone 4 fragments of 200bp which appeared in the positive RT-PCR, but were undetectable in the negative RT-PCR. The latter reaction was performed without adding the reverse transcriptase (Fig. 4.2 B). When plasmids were used in PCR (Fig. 4.2 C), the purity of the reaction was demonstrated by a H_2O control. No contamination was observed (Fig. 4.2 C).
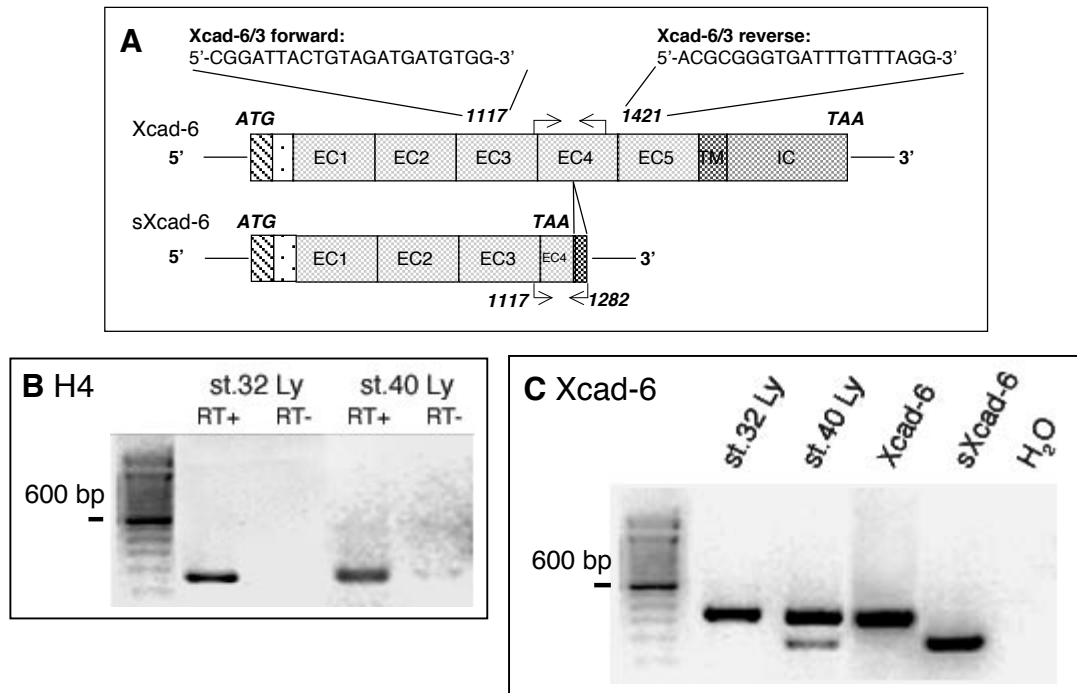
```
                                                                                                          EC1
Xcad-6 !!!!!!!!1!MRTFRCLILLTLWASQLQNSHTTPLPERTSPSTQPTAEEEQLKEDNEMERSRSKRSWMWN
sXcad-6!!!!!!!1!MRTFRCLILLTLWASQLQNSHTTPLPERTSPSTQPTAEEEQLKEDNEMERSRSKRSWMWN


Xcad-6!!!!!!!!61!QFFLLEEYTGSDYQYVGKLHSDQDKGDGSLKYILSGDGAGDLFVINENTGDIQATKRLDR
sXcad-6!!!!!61!QFFLLEEYTGSDYQYVGKLHSDQDKGDGSLKYILSGDGAGDLFVINENTGDIQATKRLDR
                                                                            EC2
Xcad-6!!!!!!!121!EEKPVYILRAQAVNRITGIPVEPKSEFVIKIHDINDNEPKFTQDLYTATVPEMSEVGAFV
sXcad-6!!!!121!EEKPVYILRAQAVNRITGIPVEPKSEFVIKIHDINDNEPKFTQDLYTATVPEMSEVGAFV


Xcad-6!!!!!!!181!VQVTANDADDPTYGNSARVVYSILQGQPYFSVESETGIIKTALPNMDRENREQYKVVIQA
sXcad-6!!!!181!VQVTANDADDPTYGNSARVVYSILQGQPYFSVESETGIIKTALPNMDRENREQYKVVIQA
                                                                        EC3
Xcad-6!!!!!!!241!KDMGGQLGGLSGTTVVNIALSDVNDNPPRFLQSTYQLRALESSPVGSSIGKIKANDTDEG
sXcad-6!!!!241!KDMGGQLGGLSGTTVVNIALSDVNDNPPRFLQSTYQLRALESSPVGSSIGKIKANDTDEG


Xcad-6!!!!!!!301!ENAETEYHISEGDESNMFDIITDRDTQEGVITVKKPLDFEKKKLYTLTVEAVNSHINPRF
sXcad-6!!!!301!ENAETEYHISEGDESNMFDIITDRDTQEGVITVKKPLDFEKKKLYTLTVEAVNSHINPRF
                                                                    EC4
Xcad-6!!!!!!!361!LDLGPFKDYATIRITVDDVDEPPVFNKPAYEFEVKEDAKMSTIIGTVLAQDPDAIRSPVK
sXcad-6!!!!361!LDLGPFKDYATIRITVDDVDEPPVFNKPAYEFEVKEDAKMSTIIGTVLAQDPDAIRSPVK


Xcad-6!!!!!!!421!YSLDRHTDMDRIFDIDSGNGSIYISKSLDRETVLWHNITVIATEISNPKQITRVPVFVKV
sXcad-6!!!!421!QS_____
                                EC5
Xcad-6!!!!!!!481!LDINDNAPELAMLYEIFVCENTKSEQVIHTISAIDKDDSFNGLQFSFALATPAASSPNFT
sXcad-6!!!!!!!!!  _____


Xcad-6!!!!!!!541!IKDNRDNTASILTRRNGYSRHEMSTYLLPVVISDYGYPIQSSTGTLTIRVCACDHRGNMQ
sXcad-6!!!!!!!!!  _____
                      TM                                                 IC
Xcad-6!!!!!!!601!SCTAEALIHPTGLSTGALIAILLCIIILLVTVVLFAALRRQRKKEPLIVSKEDIRDNIVS
sXcad-6!!!!!!!!!  _____


Xcad-6!!!!!!!661!YNDEGGGEEDTQAFDIGTLRNPEAIEDSKLRRDIVPETLFFPRRNQAARDNTDVRDFINQ
sXcad-6!!!!!!!!!  _____


Xcad-6!!!!!!!721!RLNDNDMDPTAPPYDSLATYAYEGNGSVAESLSSLESVTTDGDQDYDYLSDWGPRFKKLA
sXcad-6!!!!!!!!!  _____


Xcad-6!!!!!!!781!DMYGGADSDKDS!!!!!!!!!!!!!!!!!!!!!!!!!!!!!!!!!!!!!!!!!!!!!!!!!!!
sXcad-6!!!!!!!!!  _____!!!!!!!!!!!!!!!!!!!!!!!!!!!!!!!!!!!!!!!!!!!!!!
```

Fig.4.1 Comparison of amino acid sequences of full-length *Xenopus* cadherin-6 (Xcad-6) and the short, soluble isoform of *Xenopus* cadherin-6 (sXcad-6). Green letters point to the 5 extracellular domains EC1 to EC5, red letters within a black frame to the transmembrane domain TM, blue letters to the intracellular domain IC. A shaded QAV motif serves as homophilic binding site of type II classic cadherin.

Fig. 4.2 RT-PCR yielding the two isoforms of Xcad-6 mRNA in embryonic lysates. A: Schematic representation of *Xenopus* full-lengh Xcad-6 (top) and the soluble isoform, sXcad-6 (bottom). The boxes and horizontal lines indicate the coding and untranslated regions (UTR) from 5'- to 3'-terminus, respectively. The arrows point to the binding sites of the primers, Xcad-6/3 used for amplification of fragments containing the putative region of alternative splicing, while the numbers indicate the sequence position of the primers within the two Xcad-6 isoforms. Each box represents: hatched box, signal peptide; dotted box, prosequence; EC1-5, cadherin repeats 1-5; TM, transmembrane domain; IC, intracellular domain; black box, a part of 3'-UTR of the soluble isoform of Xcad-6, which binds with the reverse primer. ATG, TAA point to first methionine of translation and stop codon, repectively. B: Positive and negative controls of RT-PCR for histone 4 (H4). Amplified fragments from embryonic RNA with (RT+) or without (RT-) reverse transciptase. C: RT-PCR for Xcad-6 with Xcad-6/3 primers. Amplified fragments (304 bp and 165 bp) from embryonic RNA (Ly), the full-length Xcad-6 plasmid (Xcad-6) and the soluble isoform of Xcad-6 plasmid (sXcad-6) and H_2O control PCR reaction product were separated by gel electrophoresis. Standard molecular weight markers are on the left side corresponding to 100, 200, 300, 400, 500, 600, 700, 800, 900, 1000 and 1500bp.

Next, the question was addressed whether the short transcript is also translated into a protein. Therefore, immunoblots of glycoproteins enriched by Con A treatment from embryonic lysates of stage 40 were incubated with the polyclonal Xcad-6 antibody raised against the first EC1 domain which is present in both Xcadherin-6 isoforms. As seen in Fig. 4.3, two bands of about 120 KD and 75 KD corresponding to the expected transmembrane and soluble isoforms of Xcad-6 were detected. Taking together, the results form RT-PCR and immunoblotting demonstrate that the two isoforms of Xcadherin-6 are indeed expressed during embryo development. The identification of a putative soluble isoform of a cadherin in early development is striking and has not been observed before.
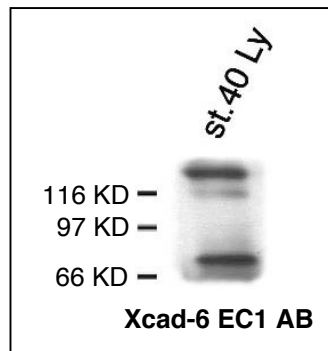
Fig. 4.3 Immunoblot for *Xenopus* cadherin-6 (Xcad-6). Concanavalin-treated embryonic lysates (Ly) of stage 40, equivalents of 4 embryos per lane were separated by SDS gel electrophoresis. Endogenous Xcad-6 was detected using a polyclonal antibody raised against Xcad-6 extracellular domain EC1 (Xcad-6 EC1 AB, 1:40 in APBS). Standard molecular weight markers are indicated by bars corresponding to 116, 97 and 66KD.

4.1.3   Transfection of H293 Cells Confirms the Secretion of the Soluble Isoform of Xcadherin-6

To answer the question whether the soluble form of Xcad-6 is secreted transfection of H293 cells (human embryonic kidney cell line) with cDNA of the soluble Xcad-6 tagged with GFP was performed. For comparison, cells were also tansfected with the full-length Xcadherin-6. Then the supernatant, which was centrifuged at the highest speed to remove cell fragments, and NOP whole cell-lysates were collected, and analysed by immunoblotting using a tag specific antibody. When the supernatants were analyzed a GFP signal was only found upon transfection of short-form Xcad-6-GFP but not of full-length Xcad-6-GFP. However, both protein isoforms were detected in the corresponding cell NOP lysates. As expected, the positive control Actin-GFP was only detected in cell NOP lysates and not in the supernatant. Also the negative controls, supernatant and cell lysate of untransfected cells did not show any GFP signal (Fig. 4.4). Taken together, the transfections experiments demonstrate that the short form of Xcadherin-6 is secreted and is soluble because it is found in the supernatant and not stuck to the outer cell surface. Remarkably, the soluble form appears slightly larger in size in the supernatant than in the NOP lysate. This might be due to a folding effect.
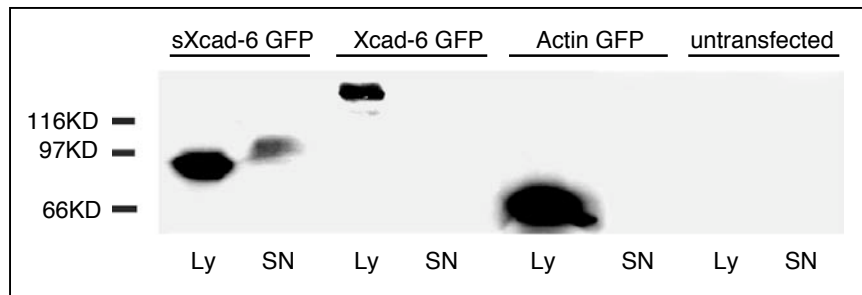
Fig. 4.4 Immunobot specific for green fluorescent protein (GFP) after transfection of *Xenopus* GFP tagged-cadherin-6 constructs into H293 cells. Transfection was done with either the full-length Xcad-6 GFP (Xcad-6 GFP) or the soluble isoform of Xcad-6 GFP (sXcad-6 GFP). Actin GFP plasmid served as a positive control for transfection. Transfected cell NOP lysates (Ly) and their corresponding culture supernatant (SN) were separated by SDS gel electrophoresis and detected using an anti-GFP antibody (1:250 in APBS). Standard molecular weight markers are indicated by bars corresponding to 116, 97 and 66KD.

4.2   Xcadherin-6 Protein Expression

To analyze the function of Xcadherin-6 isoforms, it is very necessary to elicit the spatiotemporal expression profiles of the proteins. A polyclonal Xcad-6 antibody directed against the EC1 domain was used to follow Xcad-6 expression during embryogenesis.

4.2.1   Xcadherin-6 Proteins are Expressed from Late Neurula Onwards

As shown by immunoblotting using the EC1-Xcad-6 antibody, Xcad-6 was detectable at expected size of about 120 KD from late neurula stage 20 embryos onwards and gradually increased until tadpole stage 40, the latest stage that was analyzed. A lower band of 75 KD appeared from stage 25 tailbud embryos. With further development, the lower band was also intensified (Fig. 4.5). The size of this band corresponds to that of the sXcad-6 (compare also with sXcad-6-GFP in Fig. 4.4) while the faint band about 100 KD in size might represent the typical cadherin degradation product.
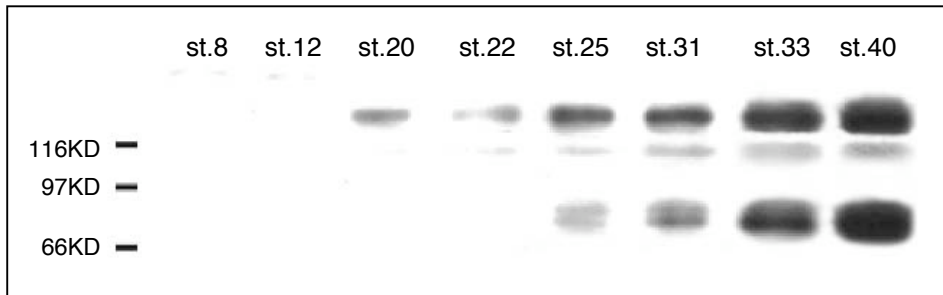
Fig. 4.5 Immunoblot showing the temporal expression profiles of Xcad-6 protein during early embryonic development. Glycoprotein-enriched Concanavalin A embryo lysates of different stages, equivalent to 5 embryos were separated by SDS gel electrophoresis and incubated with a polyclonal antibody against the extracellular domain EC1 (1:50 in APBS). The expression was analyzed from midblastula transition (MBT) of stage 8 embryo to tadpole of stage 40 embryo according to the standard stage table of (Nieuwkoop and Faber, 1975). The bars indicate the standard molecular weight marker corresponding to 116KD, 97KD and 66KD.

4.2.2 Xcadherin-6 Proteins are Restricted to the Nervous system and Developing Eye

When the spatial expression pattern of Xcad-6 was analyzed by immunostaining a distinction between the membrane integrated and the soluble protein was not possible because the antibody against the intracellular domain failed to react in immunostainings. Xcadherin-6 was found in the central and peripheral nervous system (CNS and PNS) and developing eye predominantly in neurites.

Xcad-6 proteins initially appear in the fiber tract of mid- and hindbrain and the root of trigeminal nerve in early tailbud embryos (stage 22) (Fig. 4.6 A). Xcad-6 was detectable in the optic cup in late tailbud embryos (stage 28) with restriction to the inner- and outer limiting membranes of the optic cup (Fig. 4.6 D-G). The expression gradually extended to the entire CNS, eye and in the PNS excluding the two hypobranchial nerves until late tadpole embryos (stage 42) (Details in Table 4.1).

4.2.2.1 Brain expression

Xcad-6 was localized at the processes but not the cell bodies of neuroepithelial cells in different brain compartments showing a positive signal from the ventricle zone to the marginal zone of the brain (Fig. 4.6 B, H, S). However, Xcad-6 expression was not equally distributed throughout the brain. A stronger signal occurred particularly at places where nerves accumulate and fasciculate for entering or leaving the brain (Fig. 4.6 M-R, T, U). Xcad-6 was detectable in the neurites of neurons in the CNS, which form fibers in fiber tracts of the brain (Fig. 4.6 F).

Xcad6 positive tissues at serial stages
during development detected by section immunostaining

				St.22	St.28	St.33	St.37	St.42
CNS	Brain							
		PrC (TelC./DiC.)			FTs		TelC: neurites,+	TelC/PrC: neurites,+
		MeC		Ventral longitudial FTs,+	FTs	Ventral longitudial FTs,+	posterior DiC/anterior MeC: neurites,+	Ventral longitudial FTs,+
		RhC (MetC./MyC)		Ventral longitudial FTs, +	FTs	-	neurites,+	Posterior MeC/anterior RhC: neurites, +; Ventral longitudial FTs,+
		Sp. Cord		-		-	neurites,+	neurites,+
PNS	Cranial N.	Olfactory						
		placode			some labeled cell bodies			
		neurites		-	FTs	+	+	+
		Profundal/Trigeminal (V)						
		ganglion		-	both G, +	profundal G,+	+	+
		neurites		r of V,+	profundal, +	r of v,+	+	trigeminal V,+
		Epibranchial VII						
		ganglion		-		+	+	+
		neurites		-		+	ventral r, +	+
		Epibranchial IX						
		ganglion		-		+	+	+
		neurites		-		-	+	+
		Epibranchial X1						
		ganglion		-		-	+	+
		neurites		-		-	+	+
		Epibranchial X2,3						
		placode		-		-	X3,+	-
		ganglion		-		-	+	+
		neurites		-		-	r, also intestinal branches, +	r, also intestinal branches,+
		Otic V.						
		ganglion		-		+	+	+
		neurites		-		-	+	-
		Eye		-	OLM + ILM	neurites,+	neurites and some neuronal bodies +	-
		Optic N		-		-	+	+
		Anterodorsal LL						
		ganglion		-		+	+	+
		neurites		-		+	+	+
		Anteroventral LL						
		ganglion		-		+	+	+
		neurites		-		+	dorsal r, +	+
		Middle LL						
		ganglion		-		+	+	+
		neurites		-		-	+	+
		Posterior LL						
		ganglion		-		-	+	+
		neurites		-		-	+	+
		Supratemporal LL						
		ganglion		-		-	+	+
	Spinal N.			-		-	Ventral r of 1st sp.N.,+	Dorsal r of 2nd sp.N.,+

Table 4.1 Summary of Xcad-6 positive tissues in developing embryos revealed by immunostaining of sections with a polyclonal Xcad-6 antibody. From late neurula embryo of stage 22 until tadpole embryo of stage 42, Xcad-6 location was restricted to the nervous system, the central- (CNS) and peripheral nervous system (PNS) including placodally derived lateral line nerves. In this table, the CNS and PNS were subdivided into different detailed components. "+" points to detectable for Xcad-6; "-" undetectable. Abbreviations: refer to Fig. 4.6.

4.2.2.2   Cranial and spinal nerves expression

Xcad-6 was also localized in the neurites rather than cell bodies of the peripheral nerves. Importantly, Xcad-6 was not seen in cells residing in placodes. Instead it was only present in cells that leave and send out neurites with the exception of few cells in olfactory at stage 28 and epibranchial placodes at stage 37 that had already sent out neurites.

Olfactory nerve

Some Xcad-6 labeled cell bodies were detected in the olfactory placode as early as late tailbud embryo (stage 28). Meanwhile the first fiber of olfactory nerve originating from placode expresses Xcad-6 (Fig. 4.6 B).

Lateral line nerves

All five lateral line nerves (anterodorsal-, anteroventral-, middle-, posterior and supratemporal lateral lines) start to express Xcad-6 from early tadpole embryo (stage 33) onwards. Xcad-6 localization was confined to the neurites of ganglial cells and the corresponding lateral line nerves (Fig. 4.6 A, D, H, I, M-T). However, all five neurogenic lateral line placodes were Xcad-6 negative although they exclusively contribute to the development of lateral line nerves (Schlosser and Northcutt, 2000). Also, the neuromast of lateral line nerves, such as sensory ridges or migratory primordial do not express Xcad-6 during development of lateral line nerves.

Otic nerve

The otic nerve originating from the neurogenic otic placode was Xcad-6 positive (Fig. 4.6 O).

Profundal nerve

Xcad-6 was found in profundal ganglia and neurites in late tailbud embryos (stage 28) (Fig. 4.6 C, D) and remained present in both structures until late tadpole embryos (stage 42).

Branchiomeric nerves

Xcadherin-6 was found in trigeminal-, facial epibranchial-, glossopharyngeal epibranchial- and vagal epibranchial nerves which are derived from both neural crests and neurogenic placodes (Schlosser and Northcutt, 2000). Temporally, the trigeminal nerve expressed Xcad-6 earlier (stage 22, Fig. 4.6 A) while the staining in the vagal epibranchial nerve appeared later (stage 37, Fig. 4.6 N-R). Xcad-6 was detected in the facial epibranchial- and glossopharyngeal nerves of early tailbud embryos (stage 33) and their ganglia and neurites (Fig. 4.6 M-O). Due to fusions of ganglia and nerves, it was difficult to decide whether the Xcad-6 labeling was observed on neurites from neural crest and placodally derived sensory cells or motor neurons, or whether it predominated in one subpopulation. However, some placodally derived Xcad-6 stained neurites were seen to emerge from epibranchial placodes (Fig. 4.6 R). Additionally, some Xcad-6 positive cells were found in the third vagal epibranchial placode (Fig. 4.6 R).

Spinal nerves

Starting with stage 37 tadpole embryos) Xcad-6 was found restricted to both the dorsal- and ventral roots, indicating that in the trunk some neural crest derived neurites and motor neurons were also Xcad-6 positive (not shown).
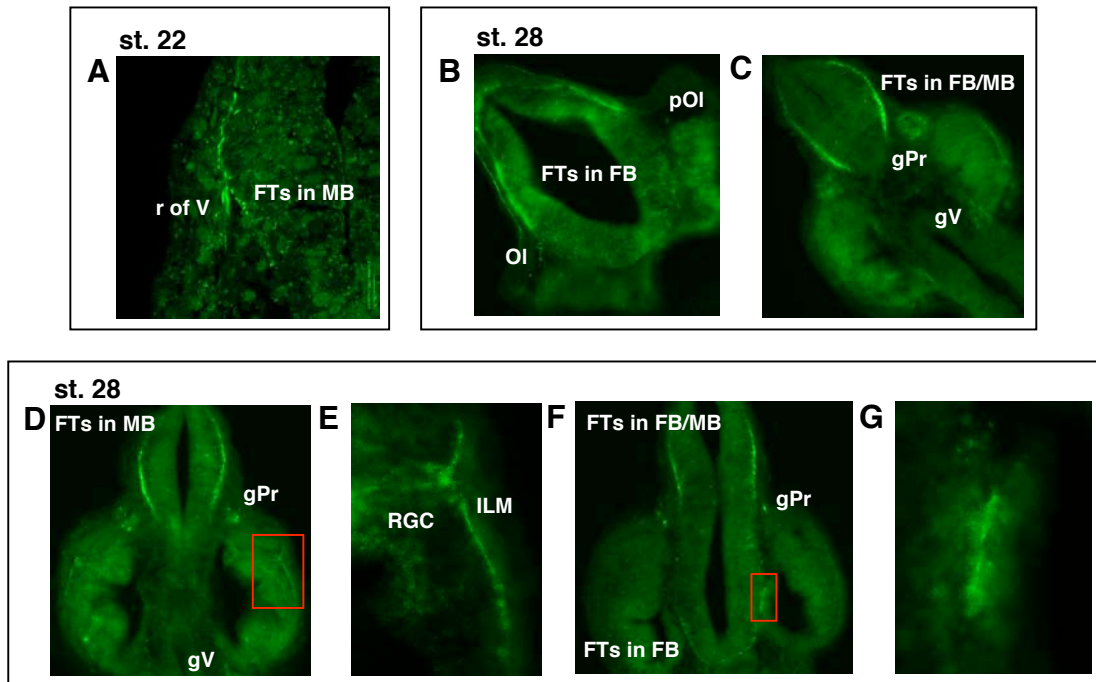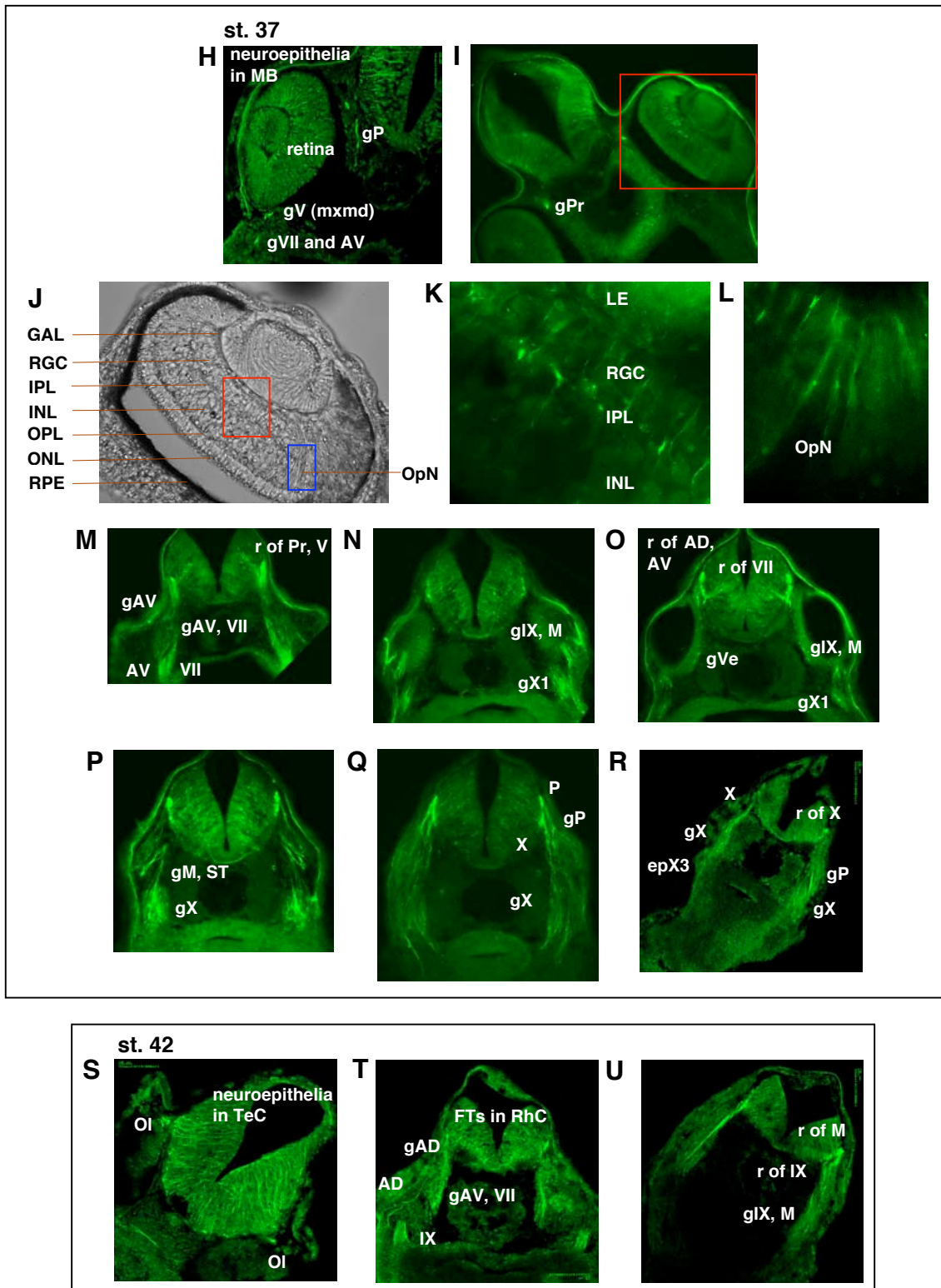
Fig. 4.6 Stage 22 to 28 (A-G): Xcad-6 immunostaining of 40 μm vibratome cross sections of different developmental stage, displayed by conventional fluorescence microscopy (B-G) or confocal laser microscopy (A). Developmental stage is indicated with the number on the left side of each black frame. Within each black frame the cross sections are arranged in a rostal-caudal direction. The area within red frame was magnified as the following image to indicate Xcad-6 positive tissue. Abbreviations: AD, anterodorsal lateral line nerve; AV, anteroventral lateral line nerve; DiC: diencephalons; epX3, third vagal epibranchial placode; FB, forebrain; FTs, fibre tracts; ILM, inner limiting membrane; INL, inner nuclear layer; IPL, inner plexiform layer; IX, glossopharyngeal nerve; LE, Lens epithelium; M, middle lateral line nerve; MeC: mesencephalon; MetC: metencephalon; MB, midbrain; MyC: myelencephalon; Ol, olfactory nerve; OpN, optic nerve; P, posterior lateral line nerve; pOl, olfactory placode; Pr, profundal nerve; PrC: prosencephalon; GAL, ganglion axon layer; gAD, anterodorsal lateral line ganglion: gAV, anteroventral lateral line ganglion; gIX, M: fused ganglia of glossopharyngeal nerve and middle lateral line nerve; gM, ST: fused ganglia of middle lateral line nerve and supratemporal lateral line nerve; gP, posterior lateral line ganglion; gPr, profundal ganglion; gV, trigeminal ganglion; gVe, Vestibulocochlear ganglion; gVII, facial ganglion; VII, facial nerve; gX1, the first vagal ganglion; gX, vagal nerve ganglion; OLM, outer limiting membrane; ONL, outer nuclear layer; OPL, outer plexiform layer; r, root; RGC, retinal ganglion cell; RhC, rhobencephalon; RPE, retinal pigment epithelium; TeC, telencephalon; V, trigeminal nerve; TelC: telencephalon; X, vagal nerve.

Fig. 4.6 Stage 37 to 42 (H-U): Xcad-6 immunostaining of 40 µm vibratome cross sections of different developmental stage, displayed by conventional fluorescence microscopy (I, K-Q) or confocal laser microscopy (H, R-U). The area within red frame in I was magnified as bright field image in J to illustrate the histological structure of the eye. High magnifications of neural retina (red frame) and optic fibres (blue frame) are shown in K and L.

4.2.2.3 Developing eye

Xcad-6 was detectable at both inner- and outer limiting membranes and inner retinal ganglion cells (RGCs) (Fig. 4.6 D-G) adjacent to the lens placode as early as tailbud stage 28. With further development, Xcad-6 expression was progressively intensified and extended into deeper zones of the neural retina (NR). In tadpole embryos of stage 37, Xcad-6 was detected in the retinal ganglial axon layer (not shown), the neurites of RGCs, the inner- (IPL) and outer plexiform layer (OPL), the inner nuclear layer (INL) and some optic fibers (Fig. 4.6 I) forming a network of neuronal connection in the NR. The high magnification images of red- and blue frames in (Fig. 4.6 J) display the neurites of RGCs, IPL and INL and optic nerve (Fig. 4.6 K, L). The histological eye structure of stage 37 is illustrated in the bright images (Fig. 4.6 J).

4.3 Xcadherin-6 Is Required for Epithelial Organization in Optic Cup Formation

4.3.1 Xcad-6 Knockdown Leads to Eye Defects in Optic Cup Formation

Initially, overexpression of Xcad-6 by microinjection of cDNA PCR fragments into 4-cell stage embryos did not emerge any significant phenotype (not shown). However, in a loss-of-function study Xcad-6 knockdown by Xcad-6 morpholino microinjection into the dorsal blastomere of 4-cell stage embryos resulted in severe eye defects in a dose dependent manner. Xcad-6 morpholino oligonucleotide (MO) was designed to target the start codon region of Xcad-6 by complementary binding, which should specifically block translation of Xcad-6 proteins. In contrast, the control morpholino (CoMO) displays a completely different nucleotide sequence compared to the Xcad-6MO targeting region (Fig. 4.7 A). To prove the efficiency and specificity of the designed Xcad-6MO the presence of endogenous Xcad-6 protein was examined by immunoblotting with the Xcad-6 antibody after morpholino injections into embryos. As seen in Fig. 4.7 (B: the upper blot), the endogenous Xcad-6 protein was absent from early tadpole embryos of stage 31/32 after Xcad-6MO application. In contrast, embryos injected with CoMO and uninjected embryos still expressed Xcad-6 protein (Fig. 4.7 B: the upper blot). After stripping the immunoblot the same nitrocellulose was re-incubated with anti-XEcadherin antibody. The immunoblot revealed that the expression level of endogenous XEcadherin was not altered either in Xcad-6 morpholino- or the control morpholino tretated and uninjected embryos (Fig. 4.7 B: the lower blot). The results show that Xcad-6 MO specifically suppressed Xcadherin-6 mRNA translation in *Xenopus* embryos.

A

B
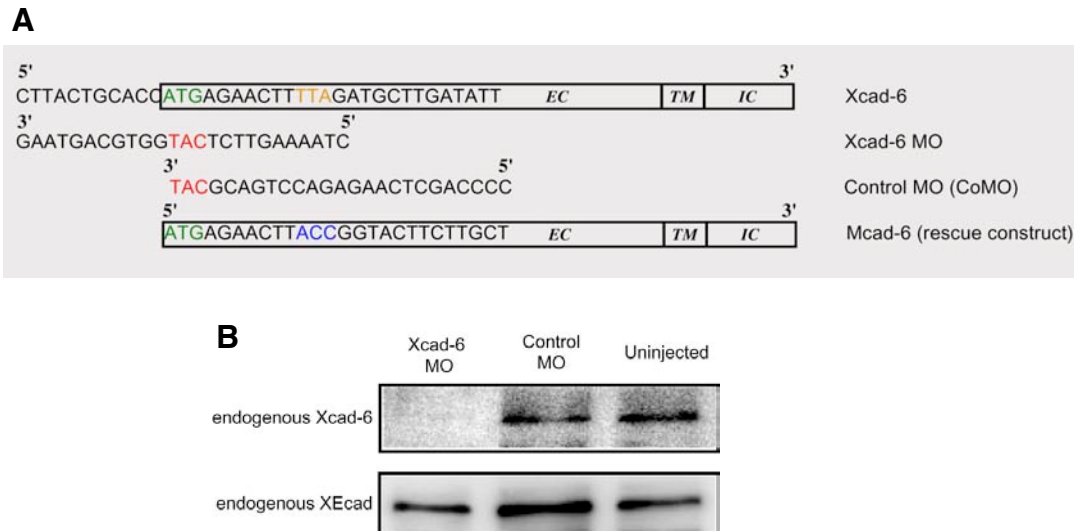
Fig. 4.7 Anti-sense Xcad-6 morpholino and its efficiency to block Xcad-6 translation. A: Nucleotide sequences of Xcad-6, Xcad-6 MO, CoMO, and mcad-6 showing the strategy of Xcad-6 knockdown and its rescue in the loss-of-function study. Xcad-6 MO was designed to be complementary to Xcad-6 fragment around the start codon region (green), while the rescue construct, mcad-6 is shown to have at least three different bases (blue) in this start codon region. With an obviously different sequence, CoMO serves as the control morpholino for Xcad-6 during this study. B: Immunoblot testing the efficiency of Xcad-6 MO on the endogenous protein. Concanavalin A lysates of late tailbud embryos of stage 31/32 injected with Xcad-6 MO and CoMO into 2 dorsal blastomeres of 4-cell stage at $8\mu M$, respectively were loaded on SDS gel electrophoresis and incubated with a polyclonal Xcad-6 antibody (1:50 in APBS) used in Fig.4.5 (the upper blot). After stripping, the same blot was stained with anti-XEcad antibody (1:2 in APBS) serving as loading control (the low blot). The uninjected embryonic lysates of the same stage act as positive controls. Abbreviations: MO, morpholino; CoMO, control morpholino; mcad-6, murine cad-6; XEcad, *Xenopus* E-cadherin.

Embryos co-injected with 4 μM Xcad-6 morpholino and GFP-myc mRNA exhibited defects in the eye (54.5%) in tadpole embryos of stage 40, such as

- missing eye (6.3%),
- abnormal eye with aberrant retina structure and smaller eye in size (29.9%),
- reduced eye with only smaller eye in size (27.5%),
- or normal eye (45.5%, n=284) (Fig. 4.8 A, C).

If supplemented with a murine homologue of cadherin-6 (mcad-6), which shares 73.9% identity with Xcad-6 (David and Wedlich, 2000) but does not bind to Xcad-6 morpholino (Fig. 4.7 A), the percentage of defect eye phenotype was reduced to 0.6% for missing eye, 4.9% abnormal eye and 12.9% reduced eye, while the incidence of normal eye phenotype was increased up to 81.6% (n=326) (Fig. 4.8 C). The rescued phenotype in eye by mcad-6 showed a normal retina structure on the injected side compared to the non-injected side. The
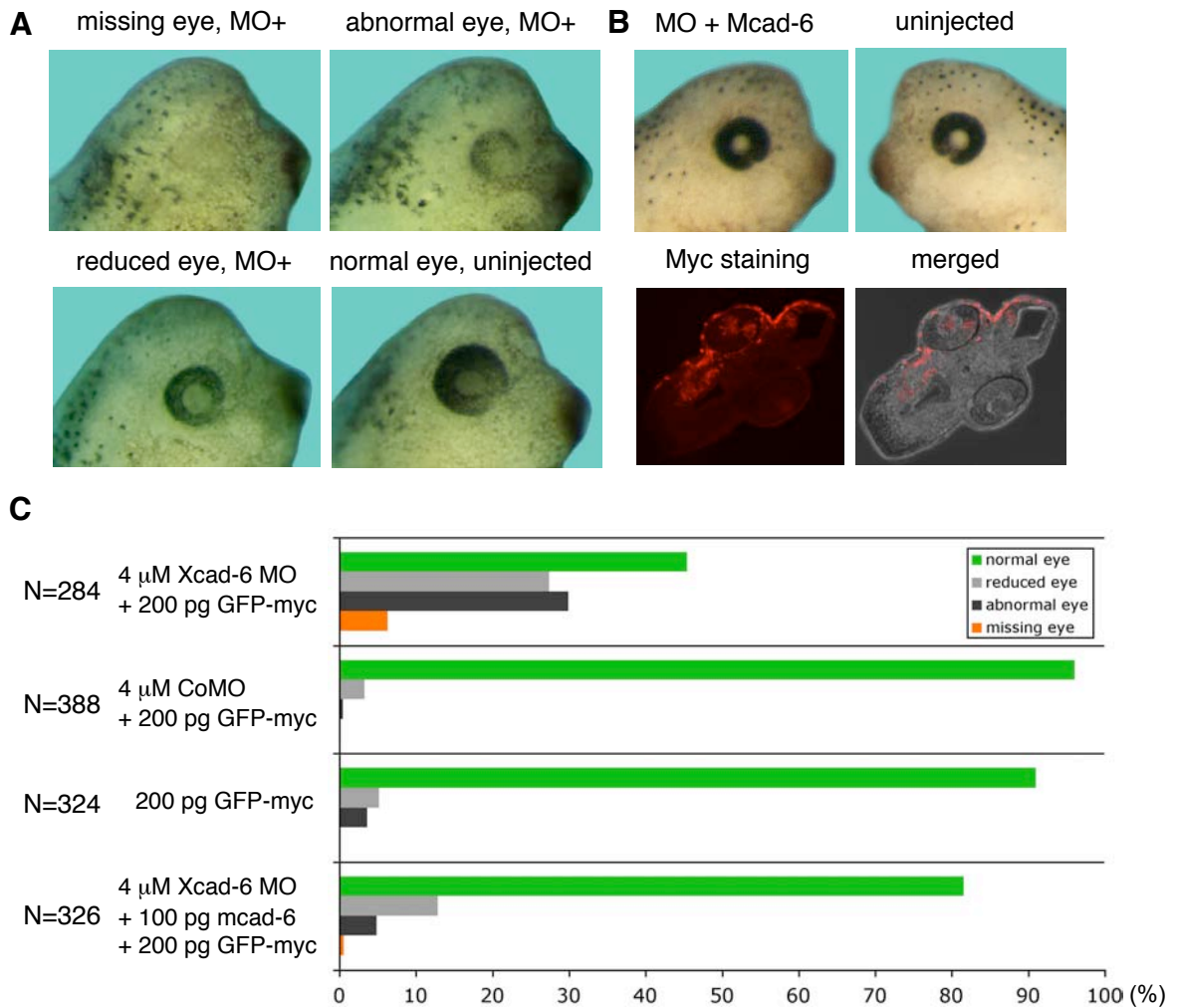
Fig. 4.8 A. Bright light images of tadpole embryos of stage 39/40 coinjected with 4μM Xcad-6 MO and 200 pg GFP-myc mRNA into 1 dorsal blastomere of 4-cell stage embryos. The success of Xcad-6 MO injection was traced by the coinjection of GFP, which produces green fluorescence labeling on the injected site. The morpholino phenotypes of eye defects were defined in 3 categories: missing eye (complete loss of eye structure), abnormal eye (smaller eye with abnormal structure), reduced eye (smaller eye without abnormal structure). is: injected side; nis, non injected side.

B. Rescue effect of mcad-6. Bright light images of the tadpole embryo of stage 39/40 coinjected with 4 μM Xcad-6 MO, 100pg mcad-6 cDNA and 200 pg GFP-myc mRNA into 1 dorsal blastomere of 4-cell stage embryo showing the rescue effect of Xcad-6 MO phenotypes by mcad-6 cDNA (the upper panel). The successful injection of Xcad-6 MO and mcad-6 was traced by the expression of GFP fluorescence on the injected site of the whole-mount embryo, and by the myc immunostaining of section (red) on the same embryo (fluorescent- and merged images on the lower panel).

C. Statistic histogram of eye defects indicating Xcad-6 MO phenotypes at 4μM, the rescue effect by coinjection of mcad-6 cDNA, CoMO, as well as the injection control of GFP-myc mRNA. The eye defects were determined as shown in A. Except for the embryos with eye defects, the rest was classified as the group of normal eye phenotype.

myc tag immunostaining of sections of the rescued embryos confirmed that the embryos were single sided injected (Fig. 4.8 B). In contrast, the co-injection of CoMO and GFP-myc mRNA or GFG-myc alone injection led to embryos displaying up to 96.1% (n=388) and 91% (n=324) normal eye phenotypes, respectively. In these control injections the missing eye phenotype was not observed (Fig. 4.8 C). Taken together, the Xcad-6 MO-caused Xcad-6 knockdown specifically resulted in eye defects during embryo development which could be rescued by the murine homologue of cadherin-6.

4.3.2 Xcadherin-6 Knockdown Does Not Affect the Early Eye Development

The Xcad-6 knockdown did not influence the early eye development, such as eye field induction and separation as revealed by in situ hybridization for XRx1. XRx1, an early eye marker gene which is initially expressed in the anterior neural plate of embryos between stage 12 and 13. The XRx1-expressing domain gives rise to the eye field and the ventral hypothalamus (Casarosa et al., 1997). As shown, Xcad-6 morpholino injection did not change XRx1 expression in the anterior neural plate of stage 13 embryos. It also did not affect the separation of the eye field stage 18 embryos (Fig. 4.9 A). This suggests that Xcadherin-6 is not required in the establishment and separation of the eye field. To confirm whether Xcad-6 is expressed in the eye field of such embryos between stage 12 and 13, RT-PCR for Xcad-6 with isolated anterior neural plates was performed. As seen in Fig. 4.9 B) Xcad-6 transcripts were exclusively detected in the eye field and not in the residual embryos. In parallel, XRx1 and ET1, two early eye marker genes were proved to be expressed in these explants but not in the residual embryos, which confirmed the correct selection of isolated material. All the genes used in this RT-PCR analysis were expressed in the whole embryos as expected (Fig. 4.9 B).

4.3.3 Xcad-6 Is Required for Development and Maintenance of the Orientated Epithelial Structure in the Eye

With the invagination of the optic vesicle the optic cup is formed consisting of an inner layer, the future neural retina, and an outer layer which later give rise to retina pigmented epithelium (RPE). This process of optic cup formation is obviously disturbed upon Xcad-6 knockdown. As seen in Fig. 4.10 A, late tailbud embryos of stage 27 co-injected with Xcad-6 MO and GFP-myc mRNA still displayed a normal polarized structure of the injected site (Fig. 4.10 A). However, later in development at stage 30 embryos showed a disrupted retinal architecture (Fig. 4.10 B). Differentiation of the RPE was also inhibited in the later development of stage 33. The lens induction was not affected in weak (Fig. 4.10 C), but in strong phenotypes. In some strong phenotypes the whole optic cup was observed to be formed inside the embryos of stage 37 and 39, lacking the contact with the overlaying lens
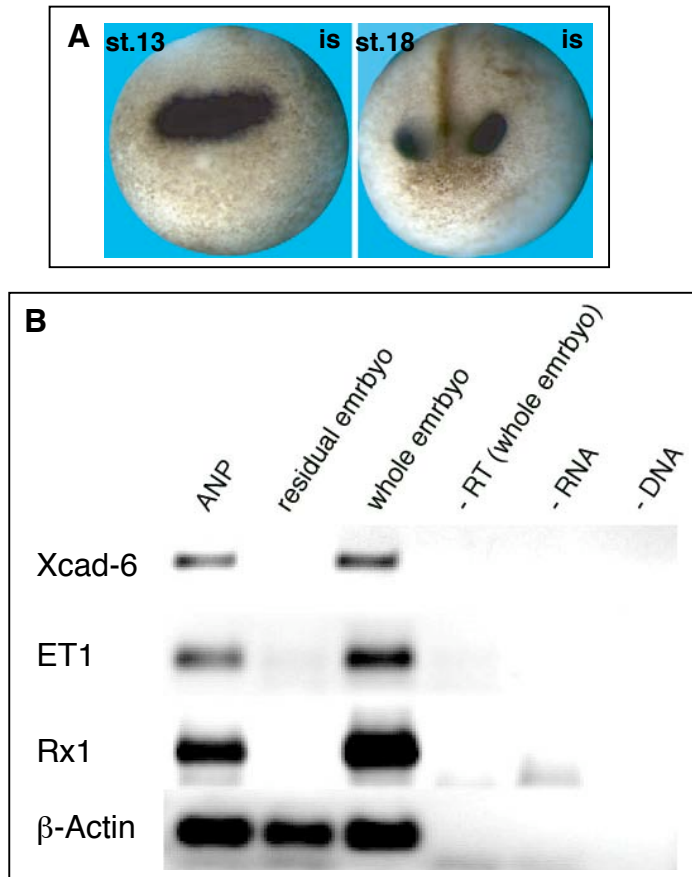
Fig. 4.9 A: Whole mount in situ hybridization for XRx1 in neurula-stage embryos co-injected with 4 *µ*M Xcad-6 MO and 200 pg GFP-myc mRNA into 1 dorsal blastomere of 4-cell stage embryos. GFP fluorescence labeling allows to detect the MO injected side (is). B: RT-PCR for Xcad-6 (the primers: Xcad-6/2) with different isolated embryonic region of early neurula embryo of stage 13 investigating tissue-specific Xcad-6 expression. XET1 and Rx1 serve as most anterior neural plate (ANP) marker genes, while β-Actin as loading control gene.

(Fig. 4.10 D, F). Embryos with reduced eyes displayed the normal structures such as laminar neural retina and lens while the RPE was lost (Fig. 4.10 E), suggesting that the RPE seems to be more sensitive for loss of Xcadherin-6 function than the other retinal structures.

Double immunostaining for Xcad-6 and GFP-myc revealed that Xcad-6MO treated embryos with abnormal eyes has lost Xcad-6 expression and normal laminar structure of the neural retina. They exhibited stronger aberration in ventral RPE which is formed later in development (Fig. 4.10 F).
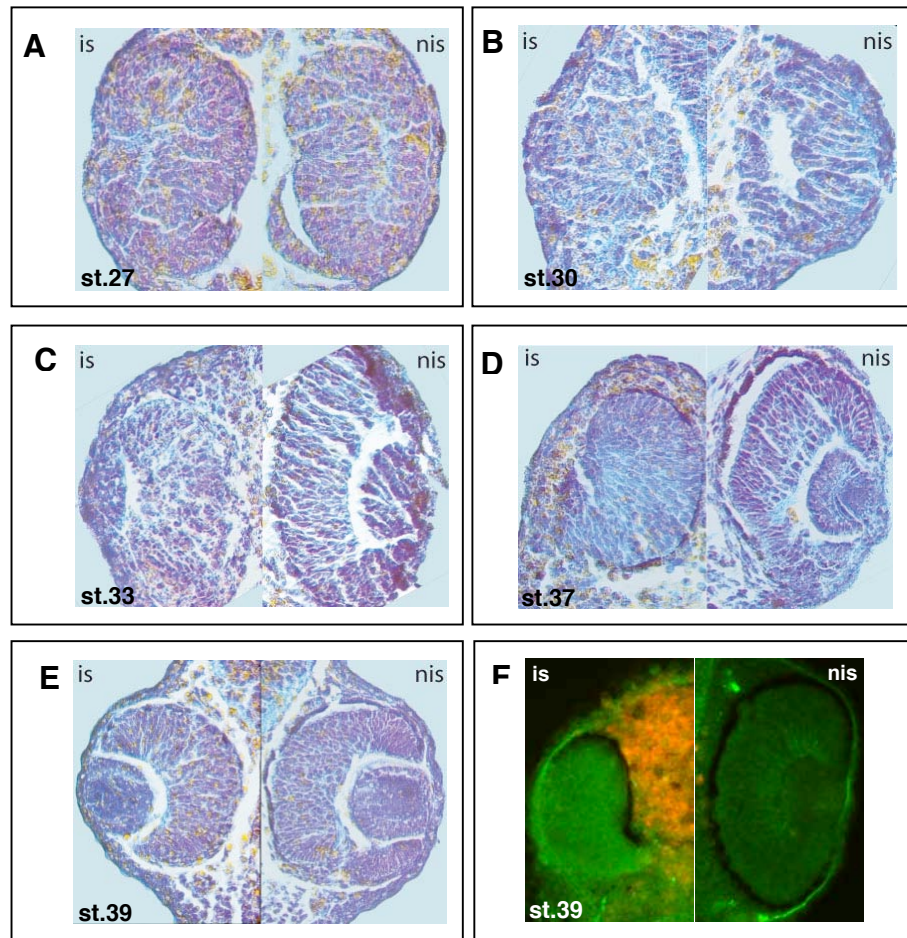
Fig. 4.10 Histological analysis indicating the laminar structure of the developing retina following co-injection of 4 μM Xcad-6 MO and 200 pg GFP-myc mRNA into 1 dorsal blastomere of 4-cell stage embryos. GFP fluorescence labeling allows the detection of the MO injected side (is). The non-injection side (nis) serves as control. A-E: Histological staining of 10 μm paraffin sections passing through the central eye region of different stage embryos. F: Double immunostaining of 40 μm vibratome sections passing through the central eye region of stage 39 embryos. The MO injected side was indicated with myc staining in red and Xcad-6 location was labeled by Xcad-6 staining in green.

4.3.4 Xcadherin-6 Is Required to Maintain the Epithelial Organization of the Retina during Optic Cup Formation

In an attempt to clarify the mechanism underlying the Xcad-6 MO-caused eye defects, part of the eye fields were transplanted (Fig. 4.9 B) when injected embryos reached early neurula stage 13. For transplantation, the DsRed2-flag construct (DsRed) was first created by PCR amplification of the 680 bp DsRed2 insert from the DsRed2-N1 plasmid (Clontech, Palo Alto, USA) with the restriction sites (5' Eco RI, 3' XhoI; primer sequences: ref. to 2. MATERIALS). The amplified fragment was subcloned into a pCS2-flag vector. In the transplantation experiments, the parts of the eye field from donor embryos injected with Xcad-6 MO plus GFP-myc or the CoMO plus GFP-myc were isolated and transferred to the corresponding
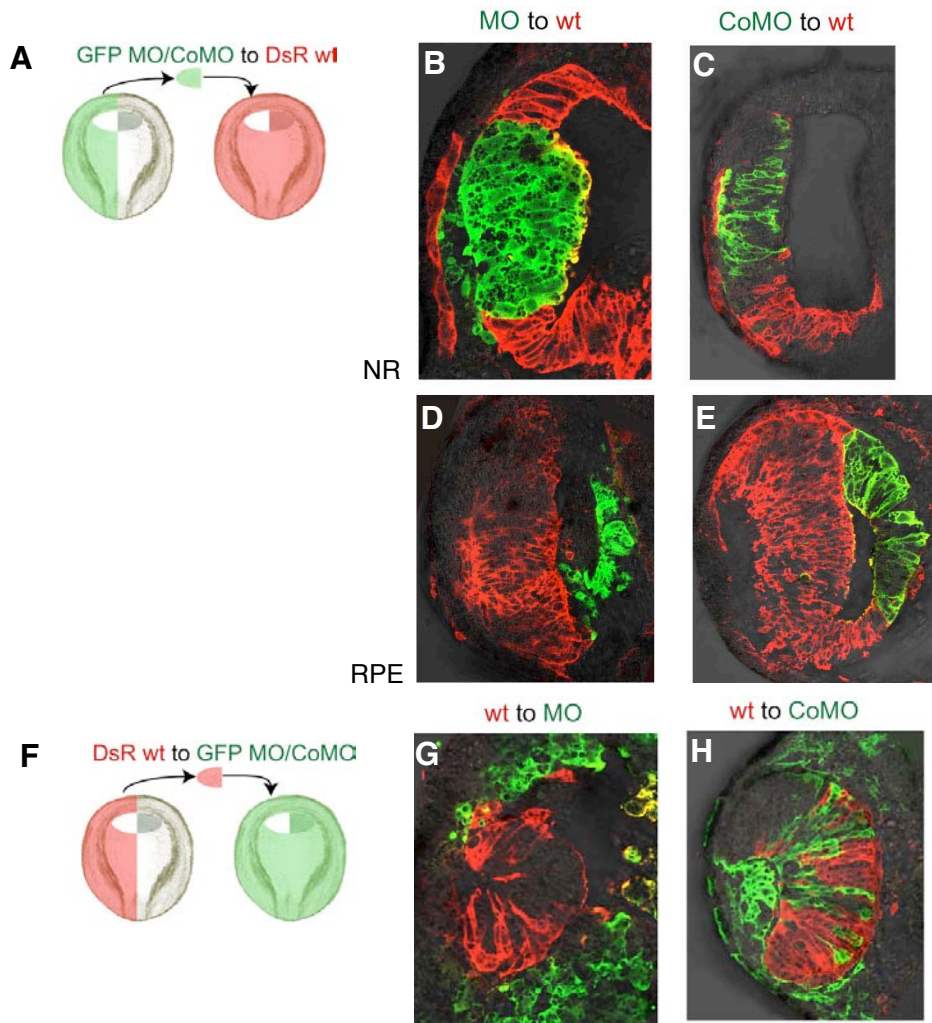
Fig. 4.11 A-E: Double-labeling transplantation of eye field in the direction from the 8 μM Xcad-6 MO injected embryos to the wild type embryos. As demonstrated in the diagram A, the prospective eye field, the most anterior neural plate of early neurula embryo of stage 13 co-injected with Xcad-6 MO and 200 pg GFP-myc mRNA into 1 dorsal blastomere of 4-cell stage embryo was dissected and transferred into the corresponding cavity of 400 pg DsRed mRNA injected embryos at 4-cell stage. After cultivating until early tadpole of stage 31/32, the graft was analyzed by GFP green fluorescence on the whole-mount view and myc immunostaining of sections passing through the transplant in red. MO transplants (green) of NR (B) and RPE (D) show aberrant epithelial polarization as compared with the corresponding CoMO transplants (C, E). F-H: Double-labeling transplantation of eye field in the direction from the 400 pg DsRed mRNA injected embryos to the 8 μM Xcad-6 MO or CoMO injected embryos. As demonstrated in the diagram F, the most anterior neural plate of early neurula embryo of stage 13 injected with 100 pg DsRed mRNA into 1 dorsal blastomere of 4-cell stage embryo was dissected and transferred into the corresponding cavity of 8 μM Xcad-6 MO and 200 pg GFP-myc mRNA or 8 μM CoMO and 200 pg GFP-myc mRNA co-injected embryos at 4-cell stage. In MO injected host (green), the DsRed-labeling eye field gives rise to a normal retinal structure (G, red) as compared with the CoMO injected host (H, green) in which the wild-type eye field (red) develops a normal retina.

cavity of host embryos injected with DsRed mRNA (Fig.4.11 A). The different fluorescence markers served to distinguish between donor and host tissue. After transplantation the embryos were cultivated until early tadpole of stage 31/32 before they were analyzed by fluorescence microscopy from outside and by immunostaining of vibratome sections using the myc antibody. When Xcad-6 MO containing transplants in wild-type host embryos were analyzed they showed a loss of polarization in the neural retina (Fig.4.11 B) and a disorganization of the epithelial structure in the RPE (Fig.4.11 D). Of 14 analyzed transplants from MO to wild type, none could develop a normal structure of the optic cup (Table 4.2). In contrast, the CoMO containing transplants revealed a normally polarized epithelium in the neural retina and in the RPE (Fig.4.11 C, E), and all of them formed normal optic cup (Table 4.2). When the transplants from the DsRed donor embryos were inserted into Xcad-6 MO or CoMO injected host embryos (Fig.4.11 F), the grafts showed a normally organized neural retina and RPE even in a tissue environment disturbed by Xcad-6 knockdown (Fig.4.11 G, H). Of 18 analyzed grafts from wild type to MO, more than half of the grafts displayed a normal optic cup (Table 4.2). Taken together, the results of the transplantation experiments revealed that Xcad-6 functions in maintaining the polarization of retinal epithelia during optic cup formation in cell autonomous manner.

Table 4.2

Direction of Transplantation	Number of analyzed transplants at stage 14	Number of normal optic cups at stage 32	Number of transplants visible from outside at stage 32
Xcad-6MO to wt	14	0	3
CoMO to wt	4	4	4
wt to Xcad-6MO	18	10	18
wt to CoMO	3	2	3

Table 4.2 Summary of eye field transplantation. Out of 14 analyzed transplants from MO to wild type with immunostaining of section, none gave rise to a normal optic cup. Only 3 grafts were visualized under GFP green fluorescence on the whole mount view. In contrast, CoMO transplants all developed normal retina and can been seen from outside. Of 18 analyzed grafts from wild type to MO host, 10 wild-type eye fields formed normal optic cup in MO enviroment. The transplants either from wild type to MO or to CoMO were all seen under fluorescence.

An important difference was observed when Xcad-6 MO transplants in wild type hosts were compared with the inverse situation, wild type transplants in Xcad-6 MO injected hosts. 78.6% (11 out 14) Xcad-6 MO transplants were not seen from outside at later stages (Fig.4.12 A and Table 4.2) whereas 100% (18 out 18) wild type transplants could be followed from outside during the eye development (Table 4.2). All the Xcad-6 MO transplants were analyzed by double immunostaining on sections. The immunostaining showed that Xcad-6

MO grafts which could not been seen from outside exhibited scattered spots within wild type tissue. All other types of transplants were found integrated as tissues pieces in the neural retina or in the RPE (Fig. 4.12 B and Table 4.2). This indicates, that Xcad-6 MO grafts with disturbed epithelial structure might be degraded.
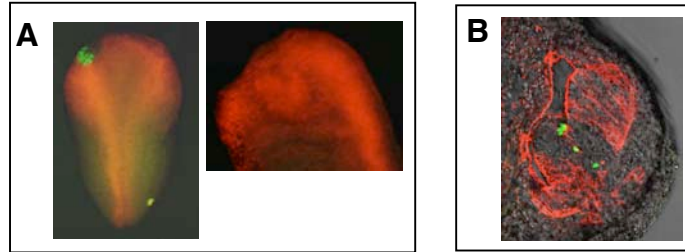

Fig. 4.12 Eye field transplants traced by whole mount fluorescence and double immunostaining. A: View from outside: Xcad-6 MO eye field (green) was successfully transplanted into wild-type host (red) at stage 14. B: Double immunostaining of sections: MO transplant (green) within wild-type host (red) at stage 31 analyzed by confocal microscopy.

4.3.5 Xcadherin-6 Promotes Cell Proliferation and Prevents Retinal Cell from Undergoing Apoptosis

To find out why Xcad-6 MO led to reduction or missing of the eyes, anti-phospho Histone 3 (PH 3) immunostaining was performed to detect dividing cells. During embryonic development, the PH 3-positive cells were detectable mostly in the anterior neural plate starting with late neurula of stage 18 embryos. Specifically in eye development increasing proliferation was observed from stage 25 embryo onwards when the optic cup has been formed. The maximum of cell proliferation in the developing eye and nervous system was reached around stage 31/32 revealed by PH 3 immunostaining on whole mount (WM) embryos (data not shown). Following 8 μM Xcad-6 MO injection, the PH3 staining cells were analyzed until tadpole of stage 33 by WM immunostaining and subsequent sectioning (Fig. 4.13 A, B and C). The myc tag staining labeled the injected side, while the DAPI staining for nuclei showed the total amount of nuclei (Fig. 4.13 B and C). Scoring was done by counting the PH 3-labeled cells and setting the noninjected side as reference to 100%. In total, 10 sections per embryo and 4 embryos per developmental stage were analyzed. At stage 26 the proliferation was nearly equal between the injected side and the noninjected side, 98.6% (standard error 7.7%) (Fig. 4.13 B, D). With further development, the number of PH 3-positive cells gradually decreased to 55.5% (standard error 18.4%) on the MO-injected eye region until stage 33 (Fig. 4.13 C, D). Furthermore, the localization of the PH3-positive cells was severely disrupted in the MO-injected embryo. The dividing cells were found ubiquitously distributed and not restricted to the ciliary marginal zone (CMZ) and the outer nuclear layer

(ONL) which is the case in wild type embryos (Fig. 4.13 C). In summary, the data indicate that Xcad-6 knockdown lead to reduction in cell proliferation in the eye region.
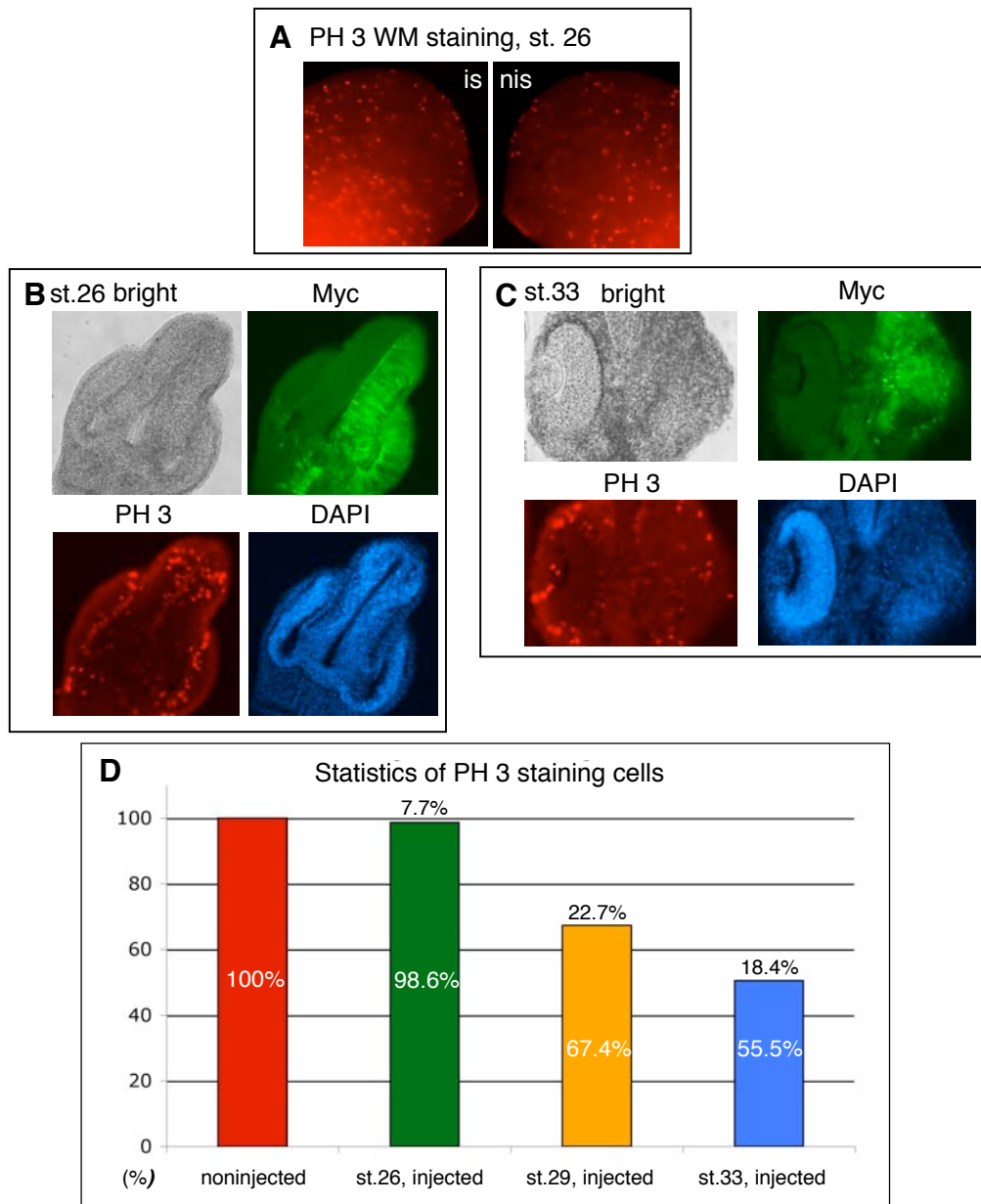

Fig. 4.13 Anti-phospho Histone 3 (PH 3) immunostaining showing cell proliferation in the eye region of Xcad-6 MO-injected embryos. A: At tailbud of stage 26, 8 μM Xcad-6 MO-injected embryos were used for whole mount (WM) immunostaining for PH 3. The mitotic cells were visualized in the eye region on the injected (is) and noninjected side (nis) of the WM embryos in red by fluorescence microscopy. B and C: Sections of embryos after whole mount staining for PH3 of stage 26 (B) and stage 33 (C). bright: bright field; green: myc staining to identify the injected side; red: PH3 positive cells; blue: DAPI staining. D: Quantification of PH 3-labeled cells from the noninjected side and the injected side. Stained- cells were counted in the eye region of single sections, normalized to the noninjected side, which was set as reference to 100%. The average percentage from 10 single sections per embryo out of 4 injected embryos was obtained. The number inside the column is average of mitotic cells in the eye region, while the number above the column represents the standard error.

To prove whether Xcad-6 morpholino explants undergo programmed cell-death as assumed by the transplantation assay, a TUNEL assay was carried out with embryos co-injected with Xcad-6 MO and GFP-myc mRNA. The physiological situation of apoptosis during embryonic development was first tested with wild type embryos between tailbud stage 24 and early tadpole stage 31. Apoptosis did not occur during the period from stage 24 and 31 (data not shown). Serving as control, the injection of GFP-myc mRNA alone did not result in any significant apoptosis on the injected side within this analyzed period as exemplarily shown for stage 27 (Fig. 4.14 A). However, 30 % of Xcad-6 MO-coinjected embryos (21 out of 58) displayed apoptotic cells on the injected side compared to the non-injected side (Fig. 4.14 B). After sectioning, the apoptotic signals were found localized in the neural retina but not restricted to a specific region. The Xcad-6 MO injected side was traced by myc immunostaining (Fig. 4.14 C).
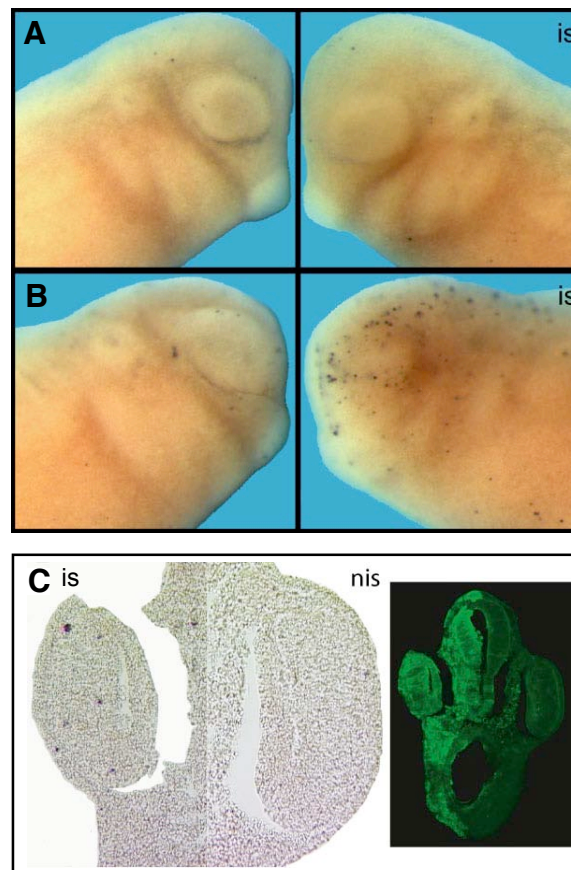
Fig. 4.14 TUNEL assay revealing apoptosis after Xcad-6 knockdown caused by MO. A: Normal amount of apoptotic cells in eye and brain in tailbud embryo of stage 27 (left). Injection of GFP-myc mRNA alone serving as control did not lead to increased apoptosis (right). B: Increase of apoptotic cells following injection of 8 μM Xcad-6 MO detected at stage 27. C: Section analysis of the MO injected embryos (bright field image on the left side), blue spots: apoptotic cells. Right insert: immunostaining for myc tag to show the injected side. Abbreviations: is, injected side; nis, non injected side.

Taken together, Xcad-6 knockdown might reduce cell proliferation and trigger apoptosis within the developing retina which lead to the reduced and missing eye observed in Xcad-6 MO injected embryos.

4.4 Xcadherin-6 Seems Involved in Neurite Fasciculation and Fiber Net Formation

4.4.1 Xcadherin-6 Knockdown Does not Affect Neural Differentiation

As Xcadherin-6 was found expressed in the peripheral nervous systems, the question was addressed whether Xcadherin-6 plays a role in axon growth, axon pathfinding or fiber formation. Since overexpression of Xcadherin-6 did not give any obvious effects on the pattern of neural tissue-specific markers, the loss-of-function phenotype by anti-sense Xcadherin-6 morpholino injection was investigated. The effects of Xcadherin-6 knockdown on the neural marker genes were studied by *in situ* hybridization at different developmental stages.

At late neurula stage 19, transcripts of the neural marker genes XPax2, Otx2, XMyT1, and XDelta1 were still detected in midbrain and in neurogenic placodes (olfactory-, profundal-, trigeminal-, lateral line-, epibranchial- and otic placodes) and only slightly reduced in expression (Fig. 4.15 A-C, E). Quantification showed that 38.6% of 44 MO-injected embryos displayed a reduction for XPax2, 55.3% of 47 for Otx2, 65.2% of 23 for XMyT1, and 67.7% of 31 for XDelta1. However, at tadpole stage 32 when neural differentiation has progressed the former slight reduction of neural marker gene expression was no longer observed (Fig. 4.15 A-C, E). Transcripts of XNeuroD were found slightly reduced at tailbud stage 25 but unchanged in their localization (Fig. 4.15 D). These data indicate that the precursor neurons derived from the neuroepithelium of the midbrain and the neurogenic placodes differentiate properly in absence of Xcadherin-6.
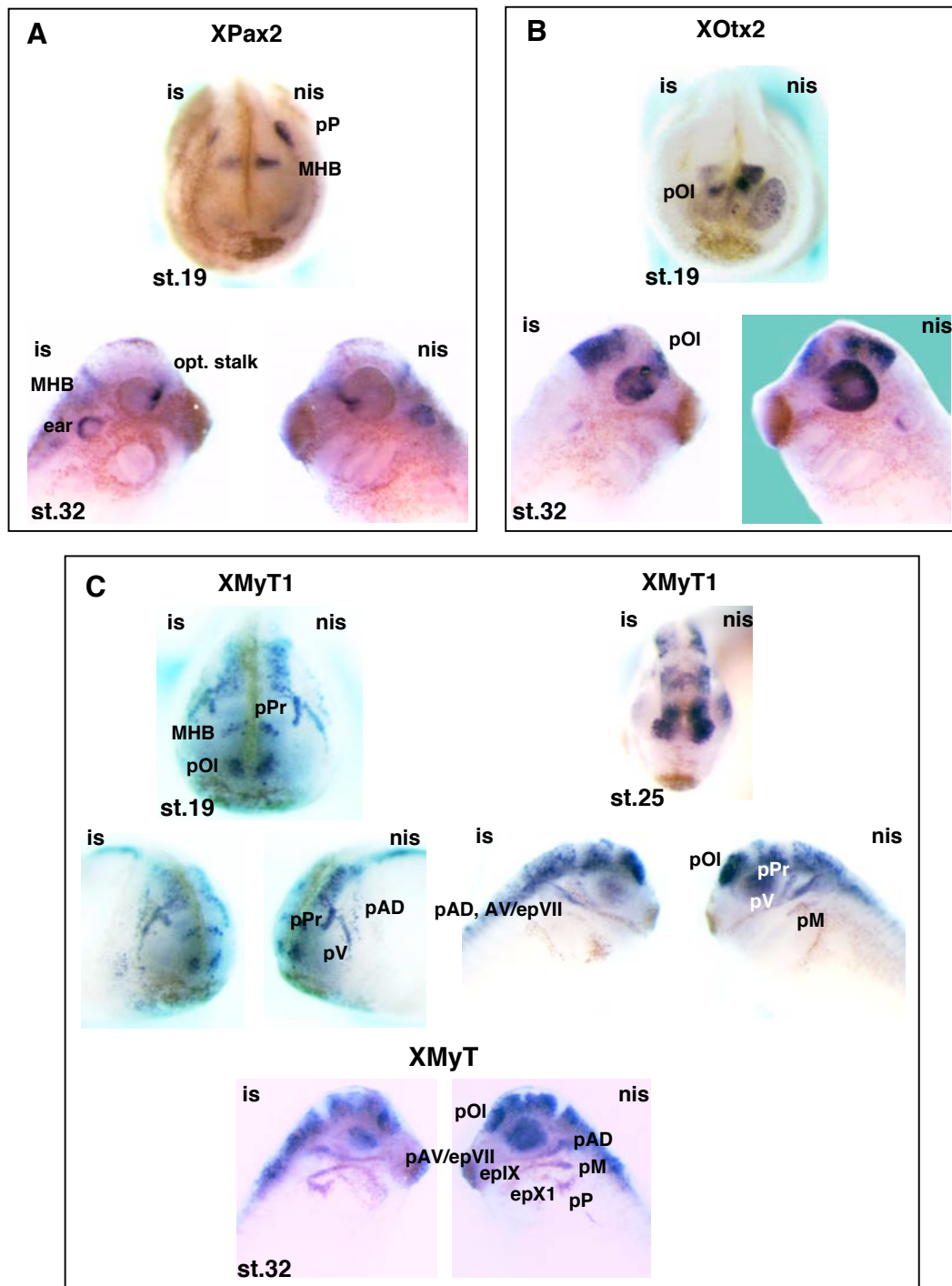
Fig.4.15 XPax2 and XOtx2 for brain, XMyT1 for brain, cranial ganglia and nerves (A-C): Whole mount *in situ* hybridization for neural tissue-specific marker genes of embryos co-injected with 4μM Xcad-6 MO and 200 pg GFP-myc mRNA demonstrating the effects of Xcad-6 knock-down. GFP fluorescence labeling was used for sorting out the injected site of the embryo (left vs right side). is, injected side; nis, non-injected side.
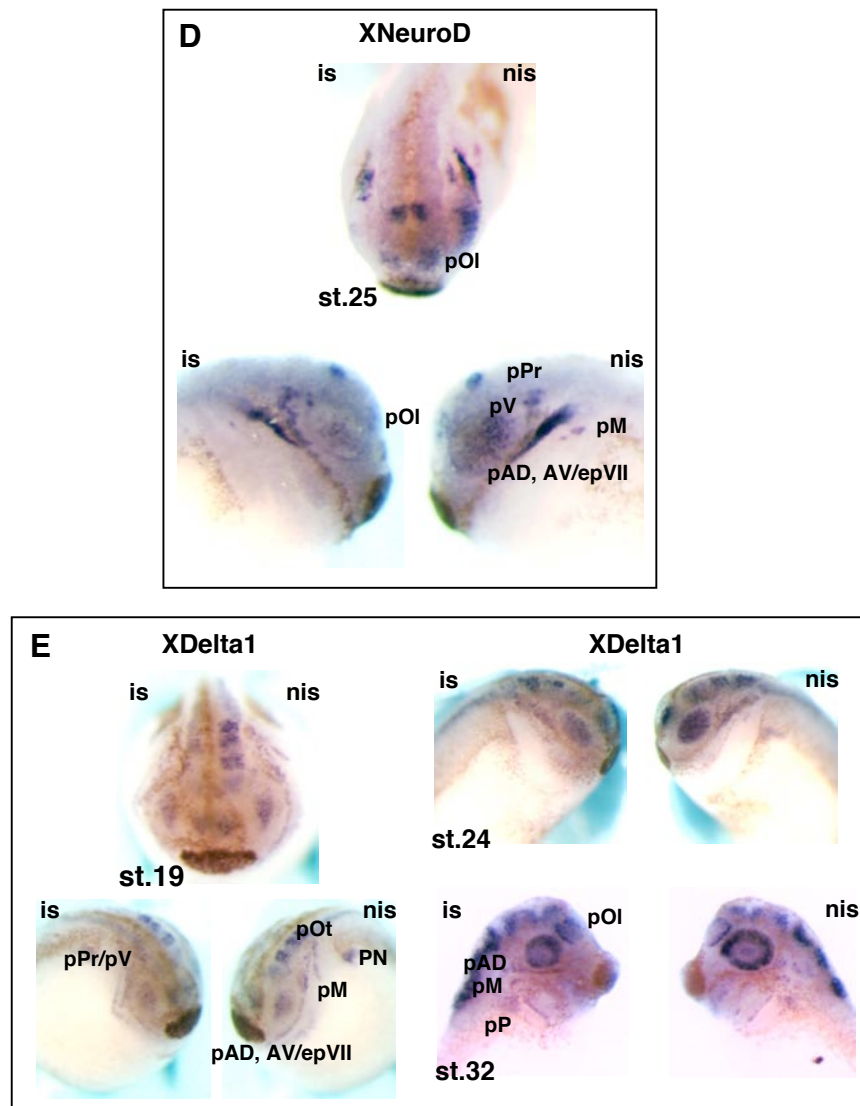
Fig. 4.15 XNeuroD and XDelta1 for brain, cranial ganglia and nerves (D, E): Whole mount *in situ* hybridization for neural tissue-specific marker genes of embryos co-injected with 4μM Xcad-6 MO and 200 pg GFP-myc mRNA demonstrating the effects of Xcad-6 knock-down. Abbreviations: epIX, glossopharyngeal epibranchial placode; epVII, facial epibranchial placode; epX1, the first vagal epibranchial placode; MHB, midbrain-hindbrain boundary; opt. stalk, optic stalk; pAD, anterior dorsal placode; pAV, anterior ventral placode; pM, middle lateral line placode; PN, pronephros; pOl, olfactory placode; pOt, otic placode; pP, posterior placode; pPr, profundal placode; pV, trigeminal placode.

4.4.2 Xcadherin-6 Knockdown Results in Fasciculation Defects of Nerve Fibers

Double immunostaining for Xcad-6 and myc tag revealed that Xcad-6 protein was still present at the Xcad-6 MO injected side compared to the non-injected side (Fig. 4.16 A-C). However, the pattern of neurites in brain (A) and fiber fasciculation in cranial nerves (B-C) were severely disturbed at stage 39/40, as seen by Xcad-6 immunostaining in green. This

indicates that Xcad-6 could play a role in outgrowth or pathfinding of neurites and in fiber fasciculation. To prove this idea an explant tissue cultivation assay was established.
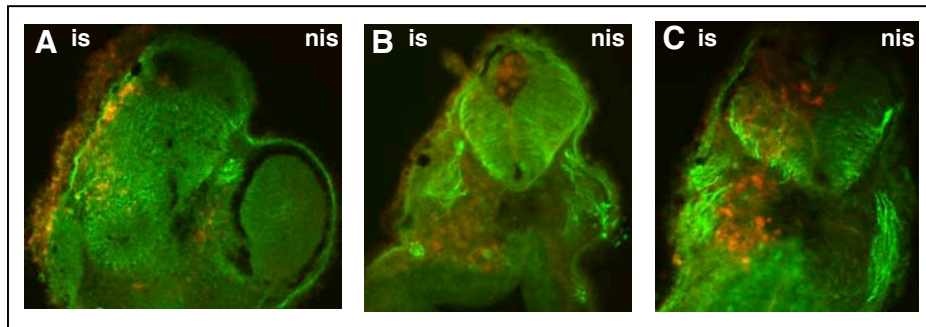
Fig. 4.16 Double immunostaining showing routes of neurites in brain and cranial nerves. The analysis was done on 40 μm vibratome cross sections of stage 39 embryos co-injected with 4 μM Xcad-6 MO and 200 pg GFP-myc mRNA. Immunostaining of Xcad-6 in green. Myc staining to distinguish the MO injected side in red (is). The non-injection side (nis) serves as control. A: through midbrain and eye region; B. posterior to the eye; C: posterior to the ear.

4.4.3   Xcad-6 Is Required for Fiber Network Formation in Neuralized Animal Caps

To clarify the possible role of Xcad-6 in the development of neurites animal caps (ACs) neuralized by injection with truncated BMP-receptor (tBR) were cut and cultivated for 56 hours, equivalent to stage 40 noninjected embryos. The explants of neuralized ACs, called wild type (wt) neuralized ACs were able to send out neurites from the edge of the explants. This behavior was not observed in Xcad-6 MO-coinjected neuralized ACs, called MO ACs (Fig. 4.17 A). Quantification of the number and length of the outgrowing neurites revealed that Xcad-6 knockdown led to a significant reduction in the density of neurites. For quantification the number of neurites within an explant margin length of 1 mm were scored in 4 different length categories and compared to the wt neuralized ACs. Furthermore, the extending of the neurite was disrupted because the neurites with the length more than 100 μm were hardly seen in the MO neuralized ACs, e.g. in categories of 100-200 μm and >200 μm (Fig. 4.17 B).
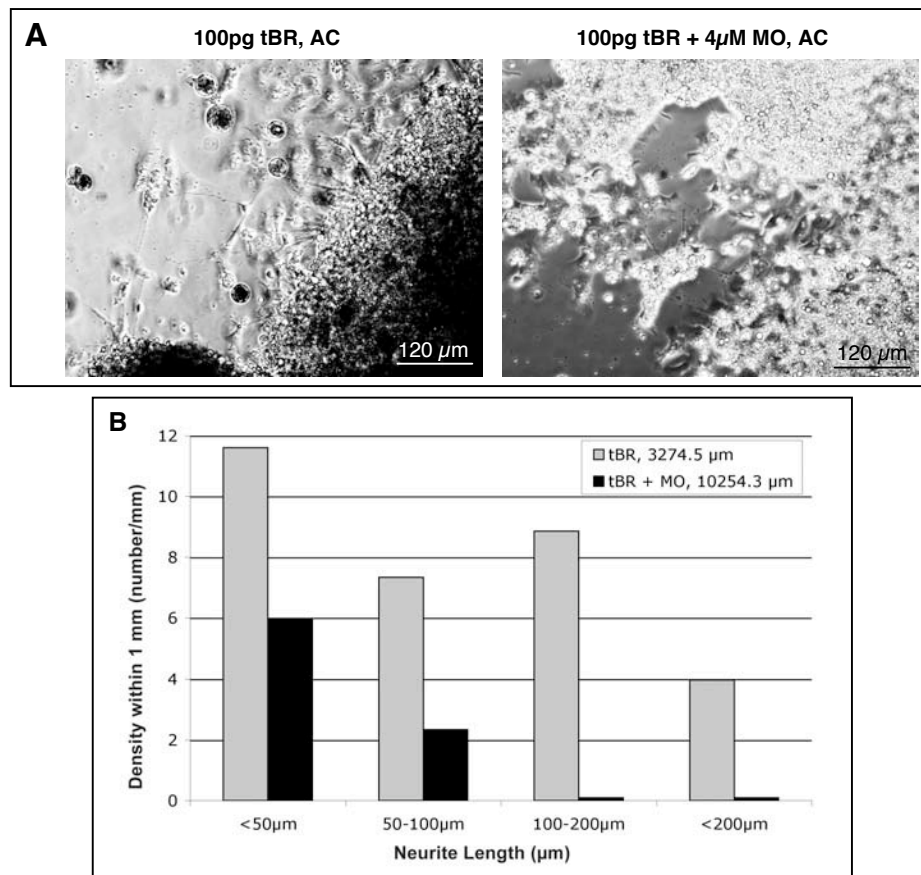
Fig. 4.17 Effect of Xcad-6 MO on formation of the neurites of the neuralized animal caps (ACs) after 3days of cultivation. 100 pg truncated BMP-receptor (tBR) with or without 4 μM Xcad-6 MO was injected. A: Bright field view of neuralized wt AC and MO AC. B: Neurites along the margin of AC explants were counted and grouped into 4 categories in terms of length: <50 μm, 50-100μm, 100-200 μm and >200 μm. Simultaneously, the margin length of the explant was measured in μm. The density of neurites within 1 mm was obtained by dividing the total number of the neurites in each category by the total margin length of the AC explant. The total margin lengths of the AC explants analyzed were 3274.5 μm for the wt AC and 10254.3 μm for the MO AC, respectively.

N-CAM immunostaining further confirmed that wt neuralized ACs formed a fiber network and tended to fasciculate the neurites into fibers. In contrast, the MO neuralized ACs did not form a fiber network and neurites were rarely seen (Fig. 4.18 A). Similar observations were found in another experiment (Fig. 4.18 B). Taken together, the differentiation of animal cap cells into nerve cells was not blocked by Xcad-6 knockdown as seen in the N-CAM signal, however, neurite formation, fiber fasciculation and the establishment of a fiber network were inhibited in the absence of Xcadherin-6.
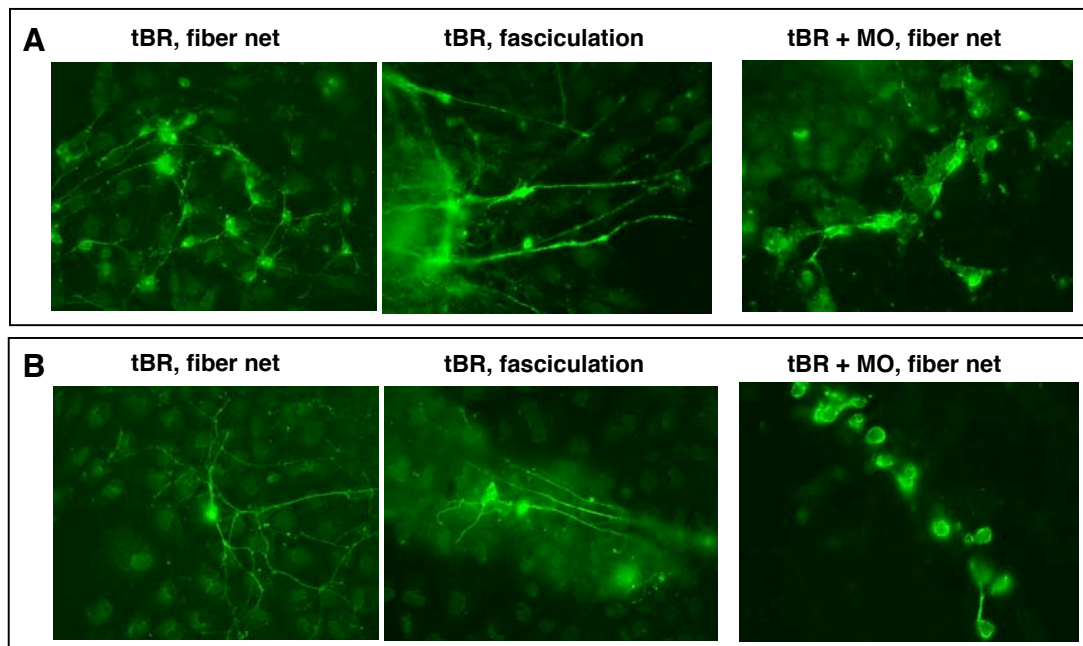
Fig. 4.18 N-CAM immunostaining demonstrating the Xcad-6 MO effects on fasciculation of the neurites and fiber network formation in neuralized AC after 56 hours cultivation. A: 1st experiment. The neural cells and neurites of the wt and MO AC were stained with mouse monoclonal N-CAM antibody (1:100 in APBS/Ca^{2+}) and visualized using a fluorescence microscope. B: 2nd experiment.

5   Discussion

At the beginning of this work only the expression pattern of Xcadherin-6 (Xcad-6) was known and antibodies raised against peptides of the protein were generated.

Using the latter the protein pattern of Xcad-6 was explored revealing its predominant presence on neurites and nerve fibers in the PNS and in the CNS including the eye.

Morpholino (MO)-induced loss-of-function studies showed that Xcad-6 takes over two different functions in neural development: it is required for proper epithelial organization of the eye cup and for the development of interneuronal connections. As shown by transplantation experiments the eye defects are explained by a disturbed epithelial organization of the presumptive retina layers during invagination of the eye vesicle. It turned out that this disorganization resulted in reduced proliferation and increase in apoptosis of the neural retina and the RPE. Animal cap explants neuralized by injection of truncated BMP receptor and depleted of Xcad-6 confirmed a role of this cadherin in outgrowth and fasciculation of neurites. Both functions of Xcad-6 are in concordance with the expression profile.

In addition to the membrane integrated Xcad-6, a soluble isoform (sXcad-6) was identified. During embryonic development it is expressed along with full-length Xcad-6 starting from tailbud of stage 25 onwards. In cell transfections it was found to be secreted into the supernatant. Unfortunately no molecular tools are available to prove its presence and possible function in *Xenopus* development.

Isoforms of Cadherins Are Rarely Observed

Cadherine are integral transmembrane glycoproteins mostly mediating Ca^{2+}-dependent homophilic binding between neighboring cells. However, cadherin isoforms lacking a certain domain or consisting of an unusual fragment generated by proteolysis or alternative splicing of the mRNA is observed in rare cases. In addition to mature forms of cadherins, proteolytic cleavage generates soluble fragments of cadherins lacking the intracellular domain. For instance, soluble E-cadherin (sE-cad) and soluble P-cadherin (sP-cad) are detectable in the serum and urine of certain human carcinoma patients serving as a prognostic marker. sE- and sP-cadherin were also found in healthy people suggesting that shedding of cadherins is a normal event (Soler et al., 2002). Alternative spliced isoforms of cadherins have been reported for classical type II cadherins, such as PB-cadherin, and cadherin-11, both of which are transmembrane proteins with different truncated intracellular domains (Sugimoto et al.,

1996; Kawaguchi et al., 1999). More recently, the soluble isoform of chicken cadherin-7 generated by alternative splicing was reported to lack the transmembrane and intracellular domains. The soluble cadherin-7 inhibits full-length cadherin-7-mediated cell adhesion in aggregation and immunoprecipitation assays (Kawano et al., 2002). Several isoforms of cadherin-6 have been found in embryonic brain and kidney in rat and human by Northern blot analysis also probably due to alternative splicing of mRNA (Xiang et al., 1994; Paul et al., 1997). However, there are no experimental data about the existence of the soluble form of a cad-6 protein. When Xcad-6 was cloned a short form with a polyA signal following the EC-4 domain was isolated (David unpublished results) In this work, it was first shown using the polycolonal Xcad-6 antibody against the first extracellular domain (EC1) that *Xenopus* soluble cad-6, most likely derived from alternative splicing, is expressed from stage 25 onwards along with full-length Xcad-6 during embryogenesis. Immunoblot of stage 40 lysates using a polyclonal Xcad-6 antibody against the intracellular domain (IC) indirectly confirmed the presence of a sXcad-6 because it was not recognized by the IC-antibody (Ruan, 2003). The short form of Xcad-6 is secreted as shown in transfections assays. Surprisingly, the Xcad-6 soluble isoform secreted in the supernatant displayed 5 more KD in size compared to the one detected in NOP cell lysates. This could be due to different folding or glycosylation of the soluble form when it is expressed in human cells. Since there are no molecular tools available to distinguish sXcad-6 from the full-length form by specific antibodies one may speculate it functions to antagonize the full-length Xcad-6.

The Cadherin-6 Expression Pattern Is Conserved Among the Vertebrates

Xcad-6 protein appears from late neurula stage onwards and is restricted to the CNS and PNS, strongly in the placode-derived cranial nerves and the developing eye. This further proved Xcad-6 transcripts in previous data (David and Wedlich, 2000). In vertebrates, neurons are generated from three sources: the neuroepithelium of the neural tube, neural crest and neurogenic placodes. The neural tube will give rise to the brain anteriorly and the spinal cord posteriorly (Gilbert and Raunio, 1997). The neural crest is a population of migratory, pluripotent cells that detach from the dorsal neural tube, delaminate in a rostrocaudal fashion and eventually develop into numerous cell types including neurons and glia of the PNS, cranial cartilage and pigment cells (Le Dourain and Kalcheim, 1999). The neurogenic placodes are transient specialized regions of the cranial ectoderm of vertebrate embryos giving rise to sensory neurons as well as to other nonepidermal cell types (Schlosser, 2003). Based on the location in the embryo and the fate in the adult, several types of neurogenic placodes can be distinguished in the rostrocaudal and dorsoventral way:

the olfactory placode forming the primary sensory neurons of the olfactory nerve; the profundal and trigeminal placodes giving rise to the neurons of the profundal and trigeminal ganglia; a series of epibranchial placodes developing into the ganglia of the facial, glossopharyngeal and vagal nerves; the otic placode forming the inner ear and the neurons of the otic ganglion; a series of lateral line placodes developing into individual sense organs, the so-called neuromasts, and the neurons of lateral line nerves that innervate the neuromasts; finally the hypobranchial placodes giving rise to neurons without any contribution so far. During neurulation, differentiated neurons sort themselves out, aggregate and migrate to form functional subdivisions and neural circuits. In brain, confocal microscope analysis revealed that Xcad-6 proteins were localized in the neurites but not in the cell body of the neuroepithelia within the subpopulations where nerves leave and enter. In some cases, the axons of the neurons are certainly Xcad-6 positive. This suggests a similarity of expression with cad-6 and R-cadherin (Cdh4) in mouse developing brain (Inoue et al., 2001) where a unique expression pattern of cadherins is restricted to brain compartment boundaries, thereby postulating that a cadherin code specifies the brain architecture (Redies and Takeichi, 1996). In spinal cord, Xcad-6 was detected in the NC-derived dorsal roots and motor neuron-derived ventral roots of the spinal nerves. This indicates that Xcad-6 is involved in the neural development originating from the three sources of neural tube, neural crest and neurogenic placodes. Obviously, intensive expression of Xcad-6 was observed in cranial ganglia connecting the Xcad-6-expressing neurites of the brain with the cranial nerves, which does extend the idea that cadherins, a system of potentially adhesive cues play a role in the formation of neural nets from embryonic CNS divisions (Redies et al., 2003). Except for two hypobranchial placodes, all the other placode-derived cranial ganglia express Xcad-6. This suggests that Xcad-6 is a candidate for a marker gene for the cranial nerves originating from neurogenic placodes because Xcad-6 was confirmed not to be expressed in the NC cells (David and Wedlich, 2000). Both placodally derived cells and neural crest cells contribute neurons to the profundal and trigeminal ganglia, the glossopharyngeal ganglion and the vagal ganglion (Schlosser and Northcutt, 2000). Thus, in this work it is difficult to distinguish the sources of cranial ganglia by Xcad-6 immunostaining. However, in combination with the transcripts of Xcad-6 confined to the neurogenic placodes but not to the neural crest (David and Wedlich, 2000), it may be postulated that Xcad-6 contributes to the development of placodally derived cranial nerves. Amphibians in contrast to higher vertebrates develop an expanded placodally derived lateral line system by the head epidermis. This may explain why Xcadherin-6 is not found in the neural crest. With the reduction of the lateral line system during evolution the neural crest has to compensate this source of nerve cells and cadherin-6 might get required in the crest.

Xcadherin-6 Is Involved in Neurite Outgrowth and Fasciculation

Although the expression of cadherins in the brain has extensively been studied little is known about their function because functional experiments are missing. Conclusions mostly rely on changes in expression. For example, R-cad expression was found intensified during axon outgrowth and synaptogenesis, suggesting a role of R-cad in development and maintenance of neuronal connection (Liu et al., 1999). Chicken N-cad transfected cell lines, such Neuro 2a or L cells can induce outgrowth of chicken embryonic optic axons, indicating that N-cad is a guide molecule for migration of optic axons on cell surfaces (Matsunaga et al., 1988b). The functions of cadherins in axon elongation and neurites fasciculation are discussed to be realized mostly via homophilic binding. This work seems to confirm this idea. Xcad-6 protein is localized on the neurites of the neuroepithelium, on the axons of the neuron, and on the fiber tract in the developing brain as well as the nerve fibers in the PNS. Xcad-6 seems not to be required for the induction and specification of the neural fate since the neural cells still appeared in MO-injected embryos as revealed by *in situ* hybridization (Fig.4.15) and N-CAM immunostaining of ACs (Fig.4.18). With the establishment of an animal cap culture of neuralized cells it was possible to perform functional assays and to show that Xcad-6 is required for the formation and fasciculation of neurites (Fig.4.18). These results confirmed the observation of unfold fiber tracts in Xcad-6 MO-injected embryos (Fig.4.16).

In summary, these data suggest that Xcad-6 is involved in the formation and fasciculation of neurites during interneuronal connection.

Xcadherin-6 Is Required for Proper Eye Formation

The vertebrate eye development has long been studied during embryogenesis and also in adult. In embryo stage, the process of eye development is basically clarified by classic methods, especially transplant experiments revealing inductive interactions among different tissues, such as neuroectoderm, epidermis and mesenchyme during early eye development (Gilbert and Raunio, 1997; Jean et al., 1998; Sivak and Sivak, 2000; Zhang et al., 2002; Mu et al., 2003; Nakagawa et al., 2003). The process of the early eye development is divided into 3 phases: first, the neuroectoderm of diencephalons bilaterally evaginates forming a bulge structure called optic vesicle; second, when the optic vesicle contacts the overlying surface ectoderm, the latter is induced to become thickened and form a structure termed as lens placode which gives rise to the lens vesicle later on. Concomitantly, the optic vesicle invaginates inwards to form a two-layer structure, known as optic cup; third, the above eye progenitors start differentiation. The lens vesicle differentiates into the lens, while the optic

cup further develops into the retina, the part of affiliated eye structures and optic stalk as well. The outer layer of the optic cup close to the optic stalk gives rise to the retinal pigment epithelium (RPE) with a certain cell polarity, while the inner layer of the optic cup forms the neural retina (NR) with a 7-type-cell forming laminar structure. The peripheral region of the optic cup gives rise to a part of the ciliary body except for the muscular system, and a part of the iris. The optic stalk further develops into optic nerve and optic chiasm. The first layer of mesenchyme develops into the choroid, the muscular and vascular part of the ciliary body and the anterior ocular region of the iris as well. The second layer forms the sclera and cornea. Several cadherins are implicated in vertebrate eye development and basically divided into two groups: neural cadherins, N-cad (Cdh2) and R-cad (Cdh4); and epithelial cadherins, E-cad and P-cad. N-cad was detected in the developing eye of chicken, mouse and zebrafish (Matsunaga et al., 1988; Xu et al., 2002; Liu et al., 2001). It is first widely expressed in the undifferentiated retina, then confined to the neural retina, especially in the optic nerve fiber layer and the plexiform layers, but disappeared from RPE. Additionally, N-cad was found in the lens placode, the lens vesicle as well as the epithelial cells and fiber cells of the mature lens in mouse developing eye. R-cad is expressed in the RGC and inner INL in the zebrafish developing eye (Liu et al, 1999). E-cad is expressed in the epithelia of the cornea, eyelid and Harderian gland, and the lens epithelium in mouse as well. Atypically, E-cad was also detected in some retinal ganglion neurons (Xu et al., 2002). P-cad is an epithelial cadherin but not identical to E-cad expression. P-cad was found in the surface ectoderm except for lens region. RPE cells express P- but not E-cad, while lens epithelia express E- but not P-cad (Xu et al., 2002).

Functional study of cadherins involved in vertebrate eye development is not widely reported yet. Counteraction of a polyclonal chicken N-cad antibody showed dissociation of the undifferentiated retina and severely morphological alteration of the differentiated retina (Matsunaga et al., 1988). More recently, in zebrafish null N-cad mutants, N-cad mutations directly perturb outgrowth of the amacrine neurites and in turn retinal lamination, in which excessive and misdirected outgrowth of amacrine neurites failed to form a correct laminae. Also, dislocation of the dividing cells in the retina was observed. Other defects in RGC axon guidance and maturation of lens fiber cells were detected as well (Masai et al., 2003). Taken together, N-cad plays a role in maintenance of tissue integrity of the differentiated retina, the formation of laminar structure as well as in the axon outgrowth in the developing eye by cell sorting and cell movement via homophilic adhesion activity.

Although the first morphological event in vertebrate eye development is evagination of bilateral diencephalic neuroectoderm forming the optic vesicle, it has been acknowledged so long that the prospective eye field does exist in the anterior neural plate (ANP) prior to optic vesicle formation in the salamander and *Xenopus laevis* as revealed by explant assays (Lopashov and Stroeva, 1964; Li et al., 1997). Modern molecular analyses also identified a dozen of transcription factors that are expressed in the presumptive eye field as the eye field is specified at the anterior neural plate, including ET, Rx1, Pax6, Six3, Lhx2, tll, Optx2 (also known as Six6) (Wawersik and Maas, 2000). Furthermore, mutations of these transcription factors led to abnormal eyes or no eyes in vertebrates (Jean et al., 1998; Wawersik and Maas, 2000; Hanson, 2001; Zuber et al., 2003). Rx1 is a paired-like homeobox gene identified in *Xenopus*, mouse, chicken, zebrafish and human and proved to be an early eye marker gene. It is initially expressed in the entire anterior neural plate of *Xenopus* developing embryo circumscribed by cells expressing the neuronal determination gene X-ngnr-1 and the neurogenetic gene X-Delt-1. The Rx1-expressing domain in anterior neural plate will give rise to eye field and ventral hypothalamus. Overexpression of Xrx1 induces cell proliferation in the anterior neural plate. (Zhang et al., 2003; Jean et al., 1998; Andreazzoli et al., 2003). Xcad-6 is expressed in the ANP of stage 13 embryos as revealed by RT-PCR, although both immunostaining and *in situ* hybridization did not detect Xcad-6 at this stage. This raised the question of whether Xcad-6 is required for specification and separation of the eye field. *In situ* hybridization showed the normal XRx1 expression pattern on the MO-injected side of stage 13 embryos. This ruled out the role of Xcad-6 in defining the eye field in the ANP and in the subsequent splitting of the eye field.

Inductive interactions between different tissues in the developing vertebrate eye have been confirmed to be common events. Contacting with the overlying ectoderm, the optic vesicle is pushed in to form the bilayered optic cup probably by the lens placode invagination. Lhx2 and Pax6 mutants demonstrated that the lack of a developing lens placode leads to the end of optic cup formation (Jean et al., 1998), indicating that the formation of the optic cup is a passive process. However, the molecular mechanism underlying the process of optic vesicle invagination is so far little known. In this work, Xcad-6 was found to demarcate the ILM, the interface between the inner layer and the lens placode. Also, Xcad-6 is confined to the OLM of the outer layer opposite to the mesenchymal tissues when the optic vesicle folds inwards (Fig.4.6 D-G). This Xcad-6 localization may contribute to the invagination of the optic vesicle by maintaining a certain tension via homophilic binding, particularly to the development of the ventral neural retina which normally forms later during eye development (Holt, 1980). A transplantation assay seems to prove the role for Xcad-6 during the invagination of the optic

vesicle, in which the MO-injected primordial ventral neural retina was often found not integrated into the neural retina. This observation was made in the CoMO transplants (Fig.4.11 D and E). This suggests that the optic vesicle invagination may be an active process, in which the optic vesicle folds inwards via cell adhesive strength.

Zebrafish N-cad mutants display perturbed outgrowth of the amacrine neurites and subsequent defect in the retinal lamination by promoting excessive and misdirected outgrowth of the amacrine neurites (Masai et al., 2003). Xcad-6 MO-initiated defects were observed before the stage when the laminar structure develops, which is earlier than Zebrafish N-cad mutation. Xcad-6 MO-injected embryos did not form a correct epithelial structure of the neural retina and the RPE after normal invagination of the optic vesicle indicated in histological analysis (Fig.4.10 B). Transplantation experiments proved this observation, in which the Xcad-6 MO transplants could not develop a proper columnar epithelium either in the neural retina or the RPE. Because the formation of the epithelium in the developing eye already happens when the neuroepithelium of the diencephalons evaginates, Xcad-6 is not involved in the process of the epithelial specification of the eye as revealed in histological analysis earlier than stage 27 (Fig.4.10 A). Therefore, it can be postulated that Xcad-6 expression is essential to preserve the columnar epithelial structure of the outer and inner layer of the optic cup during invagination.

It has been shown by cadherin-6 antibody blockage and mutation that in the kidney cad-6 is required for the early aggregation of induced mesenchymal cells and their subsequent conversion to epithelium in mouse, in which the metanephric mesenchymal cells aggregate and become polarized to generate a primitive, proliferating epithelial vesicle that ultimately generates the glomerular, proximal tubular and distal tubular epithelium (Cho et al., 1998; Mah et al., 2000). In this work, this idea does fit to the function of Xcad-6 in the developing eye in which Xcad-6 is required for maintenance of cell polarization and columnar epithelial structure during formation of the optic cup revealed by transplantation and double immunostaining because cell polarization and the columnar epithelial structure were disturbed in the MO-injected eye region. Furthermore, Xcad-6 functions in a cell autonomous pattern during the invagination of the optic vesicle because the control MO transplants still developed proper retinae even in Xcad-6 MO-caused disrupted environments (Fig.4.11).

Furthermore, it was observed that Xcad-6 MO-injected embryos exhibited phenotypes like reduced eye, abnormal eye or even missing eye. Moreover, transplantation and double immunostaining indicated scattered tissue pieces of MO transplants in the developing host

which could not be visualized from outside of the embryo under a fluorescence microscope. These data provide evidence that the MO transplants collapse. Our finding confirmed this idea because Xcad-6 knockdown showed diminished proliferation from stage 29 onwards, when the invaginated optic cup starts to differentiate. Also, the distribution of the proliferating cells was disrupted in the MO-injected eye region. For instance, the proliferating cells were reduced to 55.5% and dislocated on the MO-injected side of stage 33 embryos compared with the noninjected side (Fig.4.13 C). Xcad-6 morpholino injection also resulted in an increase of apoptosis observed in the Xcad-6 MO-injected developing eye starting from stage 27. 30% of MO-injected embryos showed in the TUNEL assay apoptotic cells that were not restricted to a certain subpopulation (Fig.4.14 C). Apoptosis was hardly detected in the developing eye of the wild type embryos, which is contrary to previous results (Hensey and Gautier, 1998) where the programmed cell death is a regular event. This might be due to supplement of additional blocking treatments to avoid unspecific antibody binding in our TUNEL protocol (see in the Methods). It has been found that the misguided migratory cells in the developing nervous system undergo cell death (Burek and Oppenheim, 1996). It is most likely that the retinal cells losing epithelial architecture revealed by histological examination and PH3 immunostaining adopt apoptotic cell fate within the optic cup when Xcad-6 is insufficient due to MO injection. Therefore, reduction of mitosis and increase of apoptosis may contribute to the defect phenotypes, such as the reduced, abnormal and missing eye as well as the degradation of Xcad-6MO grafts of the eye field in the transplantation assay.

In this work, it was initially found that overexpression of different Xcad-6 constructs, such as the full length Xcad-6, the soluble Xcad-6, Xcad-6 mutant lacking the homophilic binding site, did not show any significant phenotype. Either RT-PCR or in situ hybridization analysis did not indicate any effect of Xcad-6 overexpression on expression of the neural marker genes (XDelt1, XMyT1, XNeuroD, and XEya1) during early neural development (not shown). However, Xcad-6 knockdown induced by microinjection of Xcad-6 MO resulted in significant phenotype exhibiting eye defects (Fig.4.8 A and C). Surprisingly, in situ hybridization revealed that the expression patterns of the neural marker genes, like XMyT1, XNeuroD, XDelt1, XPax2 and XOtx2 remained unchanged in Xcad-6 MO injected embryos analyzed from late neurula of stage 18 to tadpole of stage 32. The XNeuroD and XMyT1 are shown to be expressed in all neurogenic placodes and their deriving neurons, suggesting their importance in early steps of neuronal differentiation in primary neurons in *Xenopus*. It also holds true for XDelt1 which is expressed in the neurogenic placodes and involved in lateral inhibition in the neural plate of *Xenopus* (Schlosser and Northcutt, 2000). XOtx2, a *Xenopus* homeobox gene is expressed in anterior neuroectoderm and required for cement gland and

anterior neural determination (Pannese et al., 1995; Gammill and Sive, 2001). XPax2, a *Xenopus* paired box gene is detectable in the midbrain-hindbrain boundary (MHB) and the developing optic disk and involved in development of the MHB and the optic vesicle (Ristoratore et al., 1999; Ziman et al., 2001). Thus, the in situ hybridization data indicate that Xcad-6 knockdown seems not to influence neuronal differentiation because the neural fate cells still remained in the right localization.

6 Summary

The aim of this work was to clarify the function of *Xenopus* cadherin-6 (Xcad-6), a classical type II cadherin during embryogenesis.

Using a polyclonal anti-peptide antibody raised against the first extracellular domain (EC1), the Xcad-6 protein expression was first analyzed. Xcad-6 protein- was detected from late neurula stage 20 embryos onwards and restricted to the neurites and axons in subpopulations of the central nervous system, the developing eye and prominently in the neurogenic placode-derived cranial nerves including lateral line nerves. In the developing eye, Xcad-6 is initially confined to the inner- and outer limiting membrane, both of which are the interfaces between the invaginating optic vesicle and the surrounding tissues, like the overlying lens placode and the mesenchyme. Later, Xcad-6 expression extends to the other parts of the retina but still demarcates the neurites and axons of the neural retinal cells.

By microinjection of anti-sense morpholino oligonucleotides (MO), an initial morphological disorganization was identified which led to defects in the developing eye. Injection of Xcad-6 MO resulted in reduced eye, abnormal eye and missing eye observed at tadpole stage 40. Murine cadherin-6 was able to rescue these eye defects. RT-PCR and *in situ* hybridization assays excluded a role of Xcad-6 either in induction or separation of the eye field although Xcad-6 is exclusively expressed in the prospective eye field of the anterior neural plate of stage 13 embryos. However, histological examination identified disrupted epithelial structure of the neural and pigmented retina at tailbud stage 27. Transplantations of eye fields revealed defects in the process of epithelial polarization of the retina in a cell autonomous manner. PH3 immunostaining and TUNEL assay revealed a reduction of mitosis and an increase of apoptosis in the developing eye after microinjection of Xcad-6 MO, which probably contribute to smaller eye, missing eye and degradation of Xcad-6 MO transplants. Thus, it is concluded that Xcad-6 preserves epithelial structure and promotes growth of the presumptive neural and pigmented retina during the invagination of the optic vesicle.

Animal cap (AC) cultivation and N-CAM immunostaining revealed that Xcad-6 is involved in neurite formation and fiber fasciculation during interneuronal connections. Xcad-6 MO injected neuralized AC cells could not form neurites and a fiber network. Also, in *in vivo* embryos, cranial fibers deficient for Xcad-6 could not bundle properly. This suggests a role of Xcad-6 in interneuronal connections.

7 References

Alberts, B., Bray, D., Lewis, J., Raff, M., Roberts, K., and Watson, J. D. (1994). Molecular Biology of the Cell. 3rd ed. Garland Publishing, New York London, pp. 949-1009.

Andreazzoli, M., Gestri, G., Cremisi, F., Casarosa, S., Dawid, I. B., and Barsacchi, G. (2003). Xrx1 controls proliferation and neurogenesis in Xenopus anterior neural plate. Development *130*, 5143-5154.

Andrews, G. L., and Mastick, G. S. (2003). R-cadherin is a Pax6-regulated, growth-promoting cue for pioneer axons. J Neurosci *23*, 9873-9880.

Angst, B. D., Marcozzi, C., and Magee, A. I. (2001). The cadherin superfamily: diversity in form and function. J Cell Sci *114*, 629-641.

Arends, M. J., Morris, R. G., and Wyllie, A. H. (1990). Apoptosis. The role of the endonuclease. Am J Pathol *136*, 593-608.

Arndt, K., and Redies, C. (1996). Restricted expression of R-cadherin by brain nuclei and neural circuits of the developing chicken brain. J Comp Neurol *373*, 373-399.

Arndt, K., and Redies, C. (1998). Development of cadherin-defined parasagittal subdivisions in the embryonic chicken cerebellum. J Comp Neurol *401*, 367-381.

Bahjaoui-Bouhaddi, M., Padilla, F., Nicolet, M., Cifuentes-Diaz, C., Fellmann, D., and Mege, R. M. (1997). Localized deposition of M-cadherin in the glomeruli of the granular layer during the postnatal development of mouse cerebellum. J Comp Neurol *378*, 180-195.

Beesley, P. W., Mummery, R., and Tibaldi, J. (1995). N-cadherin is a major glycoprotein component of isolated rat forebrain postsynaptic densities. J Neurochem *64*, 2288-2294.

Benson, D. L., and Tanaka, H. (1998). N-cadherin redistribution during synaptogenesis in hippocampal neurons. J Neurosci *18*, 6892-6904.

Berx, G., Staes, K., van Hengel, J., Molemans, F., Bussemakers, M. J., van Bokhoven, A., and van Roy, F. (1995). Cloning and characterization of the human invasion suppressor gene E-cadherin (CDH1). Genomics *26*, 281-289.

Birnboim, C. A., and Doley, J. A. (1979). Rapid alkaline extraction procedure for screening recombinant plasmid DNA. Nucleic Acids Res., *7*, 1513–1523.

Bixby, J. L., Lilien, J., and Reichardt, L. F. (1988). Identification of the major proteins that promote neuronal process outgrowth on Schwann cells in vitro. J Cell Biol *107*, 353-361.

Bixby, J. L., and Zhang, R. (1990). Purified N-cadherin is a potent substrate for the rapid induction of neurite outgrowth. J Cell Biol *110*, 1253-1260.

Blaschuk, O. W., Sullivan, R., David, S., and Pouliot, Y. (1990). Identification of a cadherin cell adhesion recognition sequence. Dev Biol *139*, 227-229.

Borchers, A., David, R., and Wedlich, D. (2001). Xenopus cadherin-11 restrains cranial neural crest migration and influences neural crest specification. Development *128*, 3049-3060.

Bradley, R. S., Espeseth, A., and Kintner, C. (1998). NF-protocadherin, a novel member of the cadherin superfamily, is required for Xenopus ectodermal differentiation. Curr Biol *8*, 325-334.

Brieher, W. M., Yap, A. S., and Gumbiner, B. M. (1996). Lateral dimerization is required for the homophilic binding activity of C-cadherin. J Cell Biol *135*, 487-496.

Broders, F., and Thiery, J.-P. (1995a). Contribution of Cadherins to Directional Cell Migration and Histogenesis in Xenopus Embryos. Cell Adhesion and Communication *3*, 419-440.

Broders, F., and Thiery, J. P. (1995b). Structure and Function of Cadherins. Organization of the Vertebrate Embryo Edited by N Zagris et al, Plenum Press, New York, 183-208.

Bullock, W. O., Fernandez, J. M., and Short, J. M. (1987). Xl-1-blue: A high efficiency plasmid transforming recA *E. coli* strain with β-galactosidase selection. Biotechniques *5*, 376-379.

Burek, M. J., and Oppenheim, R. W. (1996). Programmed cell death in the developing nervous system. Brain Pathol *6*, 427-446.

Casarosa, S., Andreazzoli, M., Simeone, A., and Barsacchi, G. (1997). Xrx1, a novel Xenopus homeobox gene expressed during eye and pineal gland development. Mech Dev *61*, 187-198.

Chitaev, N. A., and Troyanovsky, S. M. (1997). Direct Ca2+-dependent heterophilic interaction between desmosomal cadherins, desmoglein and desmocollin, contributes to cell-cell adhesion. J Cell Biol *138*, 193-201.

Cho, E. A., Patterson, L. T., Brookhiser, W. T., Mah, S., Kintner, C., and Dressler, G. R. (1998). Differential expression and function of cadherin-6 during renal epithelium development. Development *125*, 803-812.

Daniel, J. M., and Reynolds, A. B. (1995). The tyrosine kinase substrate p120[cas] binds directly to E-cadherin but not to the adenomatous polyposis coli protein or alpha-catenin. Mol Cell Biol *15*, 4819-4824.

David, R., and Wedlich, D. (2000). Xenopus cadherin-6 is expressed in the central and peripheral nervous system and in neurogenic placodes. Mech Dev *97*, 187-190.

Drazba, J., and Lemmon, V. (1990). The role of cell adhesion molecules in neurite outgrowth on Muller cells. Dev Biol *138*, 82-93.

Ellis, R. E., Yuan, J. Y., and Horvitz, H. R. (1991). Mechanisms and functions of cell death. Annu Rev Cell Biol *7*, 663-698.

Espeseth, A., Johnson, E., and Kintner, C. (1995). Xenopus F-cadherin, a novel member of the cadherin family of cell adhesion molecules, is expressed at boundaries in the neural tube. Mol Cell Neurosci *6*, 199-211.

Fannon, A. M., and Colman, D. R. (1996). A model for central synaptic junctional complex formation based on the differential adhesive specificities of the cadherins. Neuron *17*, 423-434.

Fannon, A. M., Sherman, D. L., Ilyina-Gragerova, G., Brophy, P. J., Friedrich, V. L. J., and Colman, D. R. (1995). Novel E-cadherin-mediated adhesion in peripheral nerve: Schwann cell architecture is stabilized by autotypic adherens junctions. J Cell Biol *129*, 189-202.

Faulkner-Jones, B. E., Godinho, L. N., and Tan, S. S. (1999). Multiple cadherin mRNA expression and developmental regulation of a novel cadherin in the developing mouse eye. Exp Neurol *156*, 316-325.

Fredette, B. J., Miller, J., and Ranscht, B. (1996). Inhibition of motor axon growth by T-cadherin substrata. Development *122*, 3163-3171.

Frixen, U. H., Behrens, J., Sachs, M., Eberle, G., Voss, B., Warda, A., Lochner, D., and Birchmeier, W. (1991). E-cadherin-mediated cell-cell adhesion prevents invasiveness of human carcinoma cells. J Cell Biol *113*, 173-185.

Gall, J. G., and Pardue, M. L. (1969). Formation and detection of RNA-DNA hybrid molecules in cytological preparations. Proc Natl Acad Sci U S A *63*, 378-383.

Gammill, L. S., and Sive, H. (2001). otx2 expression in the ectoderm activates anterior neural determination and is required for Xenopus cement gland formation. Dev Biol *240*, 223-236.

Ganzler, S. I., and Redies, C. (1995). R-cadherin expression during nucleus formation in chicken forebrain neuromeres. J Neurosci *15*, 4157-4172.

Garrod, D. R., Merritt, A. J., and Nie, Z. (2002). Desmosomal cadherins. Curr Opin Cell Biol *14*, 537-545.

Gavrieli, Y., Sherman, Y., and Ben-Sasson, S. A. (1992). Identification of programmed cell death in situ via specific labeling of nuclear DNA fragmentation. J Cell Biol *119*, 493-501.

Geis, K., Aberle, H., Kuhl, M., Kemler, R., and Wedlich, D. (1998). Expression of the Armadillo family member p120[cas]1B in Xenopus embryos affects head differentiation but not axis formation. Dev Genes Evol *207*, 471-481.

Gilbert, S. F., and Raunio, A.M. (1997). Amphibians. In *Embryology* Sinauer Associates, Inc., Sunderland, pp. 421-7.

Gorman, C. (1985). High efficiency gene transfer into mammalian cells. In DNA cloning: a practical approach. / D. M. Glover (Ed.), vol.2, IRL Press, Oxford, United Kingdom, pp. 143-190.

Grunwald, G. B. (1993). The structural and functional analysis of cadherin calcium-dependent cell adhesion molecules. Curr Opin Cell Biol *5*, 797-805.

Gumbiner, B. M. (1996). Cell adhesion: the molecular basis of tissue architecture and morphogenesis. Cell *84*, 345-357.

Hadeball, B., Borchers, A., and Wedlich, D. (1998). Xenopus cadherin-11 (Xcadherin-11) expression requires the Wg/Wnt signal. Mech Dev *72*, 101-113.

Hanson, I. M. (2001). Mammalian homologues of the Drosophila eye specification genes. Semin Cell Dev Biol *12*, 475-484.

Harland, R. M. (1991). In situ hybridization: An improved whole-mount method for *Xenopus* embryos. Methods Cell Biol., *36*, 685–695.

Hatta, K., Nose, A., Nagafuchi, A., and Takeichi, M. (1988). Cloning and expression of cDNA encoding a neural calcium-dependent cell adhesion molecule: its identity in the cadherin gene family. J Cell Biol *106*, 873-881.

Hensey, C., and Gautier, J. (1998). Programmed cell death during Xenopus development: a spatio-temporal analysis. Dev Biol *203*, 36-48.

Hilschmann, N., Barnikol, H. U., Barnikol-Watanabe, S., Gotz, H., Kratzin, H., and Thinnes, F. P. (2001). The immunoglobulin-like genetic predetermination of the brain: the protocadherins, blueprint of the neuronal network. Naturwissenschaften *88*, 2-12.

Hirano, S., Kimoto, N., Shimoyama, Y., Hirohashi, S., and Takeichi, M. (1992). Identification of a neural alpha-catenin as a key regulator of cadherin function and multicellular organization. Cell *70*, 293-301.

Hirano, S., and Takeichi, M. (1994). Differential expression of alpha N-catenin and N-cadherin during early development of chicken embryos. Int J Dev Biol *38*, 379-384.

Hoffmann, I., and Balling, R. (1995). Cloning and expression analysis of a novel mesodermally expressed cadherin. Dev Biol *169*, 337-346.

Holt, C. (1980). Cell movements in Xenopus eye development. Nature *287*, 850-852.

Honjo, M., Tanihara, H., Suzuki, S., Tanaka, T., Honda, Y., and Takeichi, M. (2000b). Differential expression of cadherin adhesion receptors in neural retina of the postnatal mouse. Invest Ophthalmol Vis Sci *41*, 546-551.

Honjo, Y., Nakagawa, S., and Takeichi, M. (2000). Blockade of cadherin-6B activity perturbs the distribution of PSD-95 family proteins in retinal neurones. Genes Cells *5*, 309-318.

Hunt, S. P., and Kunzle, H. (1976). Observations on the projections and intrinsic organization of the pigeon optic tectum: an autoradiographic study based on anterograde and retrograde, axonal and dendritic flow. J Comp Neurol *170*, 153-172.

Hyafil, F., Morello, D., Babinet, C., and Jacob, F. (1980). A cell surface glycoprotein involved in the compaction of embryonal carcinoma cells and cleavage stage embryos. Cell *21*, 927-934.

Inoue, A., and Sanes, J. R. (1997). Lamina-specific connectivity in the brain: regulation by N-cadherin, neurotrophins, and glycoconjugates. Science *276*, 1428-1431.

Inoue, T., Chisaka, O., Matsunami, H., and Takeichi, M. (1997). Cadherin-6 expression transiently delineates specific rhombomeres, other neural tube subdivisions, and neural crest subpopulations in mouse embryos. Dev Biol *183*, 183-194.

Inoue, T., Tanaka, T., Suzuki, S. C., and Takeichi, M. (1998). Cadherin-6 in the developing mouse brain: expression along restricted connection systems and synaptic localization suggest a potential role in neuronal circuitry. Dev Dyn *211*, 338-351.

REFERENCES

Inoue, T., Tanaka, T., Takeichi, M., Chisaka, O., Nakamura, S., and Osumi, N. (2001). Role of cadherins in maintaining the compartment boundary between the cortex and striatum during development. Development *128*, 561-569.

Ivanov, D. B., Philippova, M. P., and Tkachuk, V. A. (2001). Structure and functions of classical cadherins. Biochemistry (Mosc) *66*, 1174-1186.

Jean, D., Ewan, K., and Gruss, P. (1998). Molecular regulators involved in vertebrate eye development. Mech Dev *76*, 3-18.

Kawaguchi, J., Takeshita, S., Kashima, T., Imai, T., Machinami, R., and Kudo, A. (1999). Expression and function of the splice variant of the human cadherin-11 gene in subordination to intact cadherin-11. J Bone Miner Res *14*, 764-775.

Kawano, R., Matsuo, N., Tanaka, H., Nasu, M., Yoshioka, H., and Shirabe, K. (2002). Identification and characterization of a soluble cadherin-7 isoform produced by alternative splicing. J Biol Chem *277*, 47679-47685.

Kemler, R. (1992). Classical cadherins. Semin Cell Biol *3*, 149-155.

Kemler, R. (1993). From cadherins to catenins: cytoplasmic protein interactions and regulation of cell adhesion. TIG *9*, 317-321.

Kemler, R., Babinet, C., Eisen, H., and Jacob, F. (1977). Surface antigen in early differentiation. Proc Natl Acad Sci U S A *74*, 4449-4452.

Kemler, R., Ozawa, M., and Ringwald, M. (1989). Calcium-dependent cell adhesion molecules. Curr Opin Cell Biol *1*, 892-897.

Kim, S.-H., Yamamoto, A., Bouwmeester, T., Agius, E., and De Robertis, E. M. (1998). The role of Paraxial Protocadherin in selective adhesion and cell movements of the mesoderm during Xenopus gastrulation. Development *125*, 4681-4691.

Kimura, Y., Matsunami, H., Inoue, T., Shimamura, K., Uchida, N., Ueno, T., Miyazaki, T., and Takeichi, M. (1995). Cadherin-11 expressed in association with mesenchymal

morphogenesis in the head, somite, and limb bud of early mouse embryos. Dev Biol *169*, 347-358.

Kimura, Y., Matsunami, H., and Takeichi, M. (1996). Expression of cadherin-11 delineates boundaries, neuromeres, and nuclei in the developing mouse brain. Dev Dyn *206*, 455-462.

King, I. A., Angst, B. D., Hunt, D. M., Kruger, M., Arnemann, J., and Buxton, R. S. (1997). Hierarchical expression of desmosomal cadherins during stratified epithelial morphogenesis in the mouse. Differentiation *62*, 83-96.

Knudsen, K. A., and Wheelock, M. J. (1992). Plakoglobin, or an 83-kD homologue distinct from beta-catenin, interacts with E-cadherin and N-cadherin. J Cell Biol *118*, 671-679.

Kohmura, N., Senzaki, K., Hamada, S., Kai, N., Yasuda, R., Watanabe, M., Ishii, H., Yasuda, M., Mishina, M., and Yagi, T. (1998). Diversity revealed by a novel family of cadherins expressed in neurons at a synaptic complex. Neuron *20*, 1137-1151.

Kuhl, M., and Wedlich, D. (1996). Xenopus cadherins: sorting out types and functions in embryogenesis. Dev Dyn *207*, 121-134.

Kuroda, H., Inui, M., Sugimoto, K., Hayata, T., and Asashima, M. (2002). Axial protocadherin is a mediator of prenotochord cell sorting in Xenopus. Dev Biol *244*, 267-277.

Le Dourain, N. M., and Kalcheim, C. (1999). *The Neural Crest*. 2nd ed. Cambridge University Press, Cambridge.

Letourneau, P. C., Shattuck, T. A., Roche, F. K., Takeichi, M., and Lemmon, V. (1990). Nerve growth cone migration onto Schwann cells involves the calcium-dependent adhesion molecule, N-cadherin. Dev Biol *138*, 430-442.

Li, H., Tierney, C., Wen, L., Wu, J. Y., and Rao, Y. (1997). A single morphogenetic field gives rise to two retina primordia under the influence of the prechordal plate. Development *124*, 603-615.

Liu, Q., Babb, S. G., Novince, Z. M., Doedens, A. L., Marrs, J., and Raymond, P. A. (2001). Differential expression of cadherin-2 and cadherin-4 in the developing and adult zebrafish visual system. Vis Neurosci *18*, 923-933.

Liu, Q., Sanborn, K. L., Cobb, N., Raymond, P. A., and Marrs, J. A. (1999). R-cadherin expression in the developing and adult zebrafish visual system. J Comp Neurol *410*, 303-319.

Lodish, H., Berk, A., Zipursky, S. L., Matsudaira, P., Baltimore, D., and Darnell, J. E. (1999). *Molecular Cell Biology*. 4th ed. W H Freeman & Co, New York, pp. 969-976.

Lopashov, G. V., and Stroeva, O. G. (1964). Development of the eye: experimental studies. Jerusalem: Israel Program for Scientific Translations.

Madara, J. L. (1987). Intestinal absorptive cell tight junctions are linked to cytoskeleton. Am J Physiol *253*, C171-175.

Madara, J. L., Stafford, J., Barenberg, D., Carlson, S. (1988). Functional coupling of tight junctions and microfilaments in T84 monolayers. Am J Physiol *254*, G416-423.

Mah, S. P., Saueressig, H., Goulding, M., Kintner, C., and Dressler, G. R. (2000). Kidney development in cadherin-6 mutants: delayed mesenchyme-to- epithelial conversion and loss of nephrons. Dev Biol *223*, 38-53.

Manabe, T., Togashi, H., Uchida, N., Suzuki, S. C., Hayakawa, Y., Yamamoto, M., Yoda, H., Miyakawa, T., Takeichi, M., and Chisaka, O. (2000). Loss of cadherin-11 adhesion receptor enhances plastic changes in hippocampal synapses and modifies behavioral responses. Mol Cell Neurosci *15*, 534-546.

Marcozzi, C., Burdett, I. D., Buxton, R. S., and Magee, A. I. (1998). Coexpression of both types of desmosomal cadherin and plakoglobin confers strong intercellular adhesion. J Cell Sci *111*, 495-509.

Masai, I., Lele, Z., Yamaguchi, M., Komori, A., Nakata, A., Nishiwaki, Y., Wada, H., Tanaka, H., Nojima, Y., Hammerschmidt, M*., et al.* (2003). N-cadherin mediates retinal lamination, maintenance of forebrain compartments and patterning of retinal neurites. Development *130*, 2479-2494.

Matsunaga, M., Hatta, K., Nagafuchi, A., and Takeichi, M. (1988b). Guidance of optic nerve fibres by N-cadherin adhesion molecules. Nature *334*, 62-64.

Matsunaga, M., Hatta, K., and Takeichi, M. (1988). Role of N-cadherin cell adhesion molecules in the histogenesis of neural retina. Neuron *1*, 289-295.

Mbalaviele, G., Nishimura, R., Myoi, A., Niewolna, M., Reddy, S. V., Chen, D., Feng, J., Roodman, D., Mundy, G. R., and Yoneda, T. (1998). Cadherin-6 mediates the heterotypic interactions between the hemopoietic osteoclast cell lineage and stromal cells in a murine model of osteoclast differentiation. J Cell Biol *141*, 1467-1476.

Miyatani, S., Shimamura, K., Hatta, M., Nagafuchi, A., Nose, A., Matsunaga, M., Hatta, K., and Takeichi, M. (1989). Neural cadherin: role in selective cell-cell adhesion. Science *245*, 631-635.

Mooseker, M. S., Bonder, E. M., Conzelman, K. A., Fishkind, D. J., Howe, C. L., and Keller, T. C. (1984). Brush border cytoskeleton and integration of cellular functions. J Cell Biol *99*, 104s-112s.

Mu, H., Ohta, K., Kuriyama, S., Shimada, N., Tanihara, H., Yasuda, K., and Tanaka, H. (2003). Equarin, a novel soluble molecule expressed with polarity at chick embryonic lens equator, is involved in eye formation. Mech Dev *120*, 143-155.

Nagafuchi, A., and Takeichi, M. (1988). Cell binding function of E-cadherin is regulated by the cytoplasmic domain. Embo J *7*, 3679-3684.

Nagar, B., Overduin, M., Ikura, M., and Rini, J. M. (1996). Structural basis of calcium-induced E-cadherin rigidification and dimerization. Nature *380*, 360-364.

Nakagawa, S., and Takeichi, M. (1998). Neural crest emigration from the neural tube depends on regulated cadherin expression. Development *125*, 2963-2971.

Neugebauer, K. M., Tomaselli, K. J., Lilien, J., and Reichardt, L. F. (1988). N-cadherin, NCAM, and integrins promote retinal neurite outgrowth on astrocytes in vitro. J Cell Biol *107*, 1177-1187.

Nieuwkoop, P. D., and Faber, J. (1975). *Normal table of Xenopus laevis (Daudin).* North Holland Publishing Co., Amsterdam.

Nollet, F., Kools, P., and van Roy, F. (2000). Phylogenetic analysis of the cadherin superfamily allows identification of six major subfamilies besides several solitary members. J Mol Biol *299*, 551-572.

Nose, A., Tsuji, K., and Takeichi, M. (1990). Localization of specificity determining sites in cadherin cell adhesion molecules. Cell *61*, 147-155.

Oda, H., Uemura, T., Harada, Y., Iwai, Y., and Takeichi, M. (1994). A Drosophila homolog of cadherin associated with armadillo and essential for embryonic cell-cell adhesion. Dev Biol *165*, 716-726.

Ozawa, M., Ringwald, M., and Kemler, R. (1990). Uvomorulin-catenin complex formation is regulated by a specific domain in the cytoplasmic region of the cell adhesion molecule. Proc Natl Acad Sci U S A *87*, 4246-4250.

Pannese, M., Polo, C., Andreazzoli, M., Vignali, R., Kablar, B., Barsacchi, G., and Boncinelli, E. (1995). The Xenopus homologue of Otx2 is a maternal homeobox gene that demarcates and specifies anterior body regions. Development *121*, 707-720.

Paul, R., Ewing, C. M., Robinson, J. C., Marshall, F. F., Johnson, K. R., Wheelock, M. J., and Isaacs, W. B. (1997). Cadherin-6, a cell adhesion molecule specifically expressed in the proximal renal tubule and renal cell carcinoma. Cancer Res *57*, 2741-2748.

Peters, A., Palay, S. L., and Webster, H. d. F. (1991). The Fine Structure of the Nervous System: Neurons and Their Supporting Cells (New York: Oxford University Press).

Pouliot, Y. (1992). Phylogenetic analysis of the cadherin superfamily. Bioessays *14*, 743–748.

Redies, C. (1995). Cadherin expression in the developing vertebrate CNS: from neuromeres to brain nuclei and neural circuits. Exp Cell Res *220*, 243-256.

Redies, C. (1997). Cadherins and the formation of neural circuitry in the vertebrate CNS. Cell Tissue Res *290*, 405-413.

Redies, C. (2000). Cadherins in the central nervous system. Prog Neurobiol *61*, 611-648.

Redies, C., Inuzuka, H., and Takeichi, M. (1992). Restricted expression of N- and R-cadherin on neurites of the developing chicken CNS. J Neurosci *12*, 3525-3534.

Redies, C., and Takeichi, M. (1993). N- and R-cadherin expression in the optic nerve of the chicken embryo. Glia *8*, 161-171.

Redies, C., and Takeichi, M. (1996). Cadherins in the developing central nervous system: an adhesive code for segmental and functional subdivisions. Dev Biol *180*, 413-423.

Redies, C., Treubert-Zimmermann, U., and Luo, J. (2003). Cadherins as regulators for the emergence of neural nets from embryonic divisions. J Physiol Paris *97*, 5-15.

Reynolds, A. B., Daniel, J., McCrea, P. D., Wheelock, M. J., Wu, J., and Zhang, Z. (1994). Identification of a new catenin: the tyrosine kinase substrate p120[cas] associates with E-cadherin complexes. Mol Cell Biol *14*, 8333-8342.

Rimm, D. L., Koslov, E. R., Kebriaei, P., Cianci, C. D., and Morrow, J. S. (1995). Alpha 1(E)-catenin is an actin-binding and -bundling protein mediating the attachment of F-actin to the membrane adhesion complex. Proc Natl Acad Sci U S A *92*, 8813-8817.

Ristoratore, F., Carl, M., Deschet, K., Richard-Parpaillon, L., Boujard, D., Wittbrodt, J., Chourrout, D., Bourrat, F., and Joly, J. S. (1999). The midbrain-hindbrain boundary genetic cascade is activated ectopically in the diencephalon in response to the widespread expression of one of its components, the medaka gene Ol-eng2. Development *126*, 3769-3779.

Ruan, G. (2003). Generation of polyclonal antibodies directed against *Xenopus* cadherin-6 and *Xenopus* cadherin-11. Dissertation, Medizinische Fakultät, Universität Ulm.

Ruan, G., Wedlich, D., and Köhler, A. (2004). How cell-cell adhesion contributes to early embryonic development. In *The Vertebrate Organizer / Horst Grunz (Ed.)* Springer-Verlag, Berlin Heidelberg New York, pp. 201-218.

Rubenstein, J. L., and Rakic, P. (1999). Genetic control of cortical development. Cereb Cortex *9*, 521-523.

Sanger, F., Nicklen, S., and Coulson, A. R. (1977). DNA sequencing with chain terminating inhibitors. Proc. Natl. Acad. Sci. USA, *74*, 5463–5467.

Sano, K., Tanihara, H., Heimark, R. L., Obata, S., Davidson, M., St John, T., Taketani, S., and Suzuki, S. (1993). Protocadherins: a large family of cadherin-related molecules in central nervous system. Embo J *12*, 2249-2256.

Schlosser, G. (2003). Hypobranchial placodes in Xenopus laevis give rise to hypobranchial ganglia, a novel type of cranial ganglia. Cell Tissue Res *312*, 21-29.

Schlosser, G., and Northcutt, R. G. (2000). Development of neurogenic placodes in Xenopus laevis. J Comp Neurol *418*, 121-146.

Shapiro, L., Fannon, A. M., Kwong, P. D., Thompson, A., Lehmann, M. S., Grubel, G., Legrand, J. F., Als-Nielsen, J., Colman, D. R., and Hendrickson, W. A. (1995). Structural basis of cell-cell adhesion by cadherins. Nature *374*, 327-337.

Shibamoto, S., Hayakawa, M., Takeuchi, K., Hori, T., Miyazawa, K., Kitamura, N., Johnson, K. R., Wheelock, M. J., Matsuyoshi, N., Takeichi, M., and et al. (1995). Association of p120, a tyrosine kinase substrate, with E- cadherin/catenin complexes. J Cell Biol *128*, 949-957.

Shimoyama, Y., Gotoh, M., Terasaki, T., Kitajima, M., and Hirohashi, S. (1995). Isolation and sequence analysis of human cadherin-6 complementary DNA for the full coding sequence and its expression in human carcinoma cells. Cancer Res *55*, 2206-2211.

Shimoyama, Y., Tsujimoto, G., Kitajima, M., and Natori, M. (2000). Identification of three human type-II classic cadherins and frequent heterophilic interactions between different subclasses of type-II classic cadherins. Biochem J *349*, 159-167.

Simonneau, L., Broders, F., and Thiery, J. P. (1992). N-cadherin transcripts in Xenopus laevis from early tailbud to tadpole. Dev Dyn *194*, 247-260.

Simonneau, L., Kitagawa, M., Suzuki, S., and Thiery, J. P. (1995). Cadherin 11 expression marks the mesenchymal phenotype: towards new functions for cadherins? Cell Adhes Commun *3*, 115-130.

Sivak, B., and Sivak, J. (2000). Vertebrate eye development and refractive function: An overview. In *Vertebrate Eye Development / M. Elizabeth Fini (Ed.)* Springer-Verlag, Berlin Heidelberg, pp. 1-14.

Soler, A. P., Russo, J., Russo, I. H., and Knudsen, K. A. (2002). Soluble fragment of P-cadherin adhesion protein found in human milk. J Cell Biochem *85*, 180-184.

Spacek, J., and Harris, K. M. (1998). Three-dimensional organization of cell adhesion junctions at synapses and dendritic spines in area CA1 of the rat hippocampus. J Comp Neurol *393*, 58-68.

Stappert, J., and Kemler, R. (1994). A short core region of E-cadherin is essential for catenin binding and is highly phosphorylated. Cell Adhes Commun *2*, 319-327.

Steinberg, M. S., and Takeichi, M. (1994). Experimental specification of cell sorting, tissue spreading, and specific spatial patterning by quantitative differences in cadherin expression. Proc Natl Acad Sci U S A *91*, 206-209.

Steller, H. (1995). Mechanisms and genes of cellular suicide. Science *267*, 1445-1449.

Stone, K. E., and Sakaguchi, D. S. (1996). Perturbation of the developing Xenopus retinotectal projection following injections of antibodies against beta1 integrin receptors and N-cadherin. Dev Biol *180*, 297-310.

Sugimoto, K., Honda, S., Yamamoto, T., Ueki, T., Monden, M., Kaji, A., Matsumoto, K., and Nakamura, T. (1996). Molecular cloning and characterization of a newly identified member of the cadherin family, PB-cadherin. J Biol Chem *271*, 11548-11556.

Sumner, J., and Howell, S. (1936). The identification of hemagglutinin of the jack bean with Concanavalin A. J. Bacteriol., *32*, 227.

Suzuki, S., Sano, K., and Tanihara, H. (1991). Diversity of the cadherin family: evidence for eight new cadherins in nervous tissue. Cell Regul *2*, 261-270.

Suzuki, S. C., Inoue, T., Kimura, Y., Tanaka, T., and Takeichi, M. (1997). Neuronal Circuits Are Subdivided by Differential Expression of Type-II Classic Cadherins in Postnatal Mouse Brains. Mol Cell Neurosci *9*, 433-447.

Suzuki, S. T. (1996). Structural and functional diversity of cadherin superfamily: are new members of cadherin superfamily involved in signal transduction pathway? J Cell Biochem *61*, 531-542.

Takeichi, M. (1988). The cadherins: cell-cell adhesion molecules controlling animal morphogenesis. Development *102*, 639-655.

Takeichi, M. (1990). Cadherins: a molecular family important in selective cell-cell adhesion. Annu Rev Biochem *59*, 237-252.

Takeichi, M. (1991). Cadherin cell adhesion receptors as a morphogenetic regulator. Science *251*, 1451-1455.

Takeichi, M. (1995). Morphogenetic roles of classic cadherins. Curr Opin Cell Biol *7*, 619-627.

Takeichi, M., Hatta, K., Nose, A., and Nagafuchi, A. (1988). Identification of a gene family of cadherin cell adhesion molecules. Cell Differ Dev *25 Suppl*, 91-94.

Tanaka, H., Shan, W., Phillips, G. R., Arndt, K., Bozdagi, O., Shapiro, L., Huntley, G. W., Benson, D. L., and Colman, D. R. (2000). Molecular modification of N-cadherin in response to synaptic activity. Neuron *25*, 93-107.

Tang, L., Hung, C. P., and Schuman, E. M. (1998). A role for the cadherin family of cell adhesion molecules in hippocampal long-term potentiation. Neuron *20*, 1165-1175.

Towbin, H., Staehelin, T., and Gordon, J. (1979). Electrophoretic transfer of proteins from polyacrylamide gels to nitrocellulose sheets: procedure and some applications. Proc. Natl. Acad. Sci. USA, *76*, 4350–4354.

Uchida, N., Honjo, Y., Johnson, K. R., Wheelock, M. J., and Takeichi, M. (1996). The catenin/cadherin adhesion system is localized in synaptic junctions bordering transmitter release zones. J Cell Biol *135*, 767-779.

Uchida, N., Shimamura, K., Miyatani, S., Copeland, N. G., Gilbert, D. J., Jenkins, N. A., and Takeichi, M. (1994). Mouse alpha N-catenin: two isoforms, specific expression in the nervous system, and chromosomal localization of the gene. Dev Biol *163*, 75-85.

Vestweber, D., and Kemler, R. (1985). Identification of a putative cell adhesion domain of uvomorulin. Embo J *4*, 3393-3398.

Vleminckx, K., Vakaet, L., Jr., Mareel, M., Fiers, W., and van Roy, F. (1991). Genetic manipulation of E-cadherin expression by epithelial tumor cells reveals an invasion suppressor role. Cell *66*, 107-119.

Volk, T., and Geiger, B. (1986). A-CAM: a 135-kD receptor of intercellular adherens junctions. I. Immunoelectron microscopic localization and biochemical studies. J Cell Biol *103*, 1441-1450.

Wawersik, S., and Maas, R. L. (2000). Vertebrate eye development as modeled in Drosophila. Hum Mol Genet *9*, 917-925.

Wohrn, J. C., Nakagawa, S., Ast, M., Takeichi, M., and Redies, C. (1999). Combinatorial expression of cadherins in the tectum and the sorting of neurites in the tectofugal pathways of the chicken embryo. Neuroscience *90*, 985-1000.

Wu, Q., and Maniatis, T. (1999). A striking organization of a large family of human neural cadherin-like cell adhesion genes. Cell *97*, 779-790.

Xiang, Y. Y., Tanaka, M., Suzuki, M., Igarashi, H., Kiyokawa, E., Naito, Y., Ohtawara, Y., Shen, Q., Sugimura, H., and Kino, I. (1994). Isolation of complementary DNA encoding K-cadherin, a novel rat cadherin preferentially expressed in fetal kidney and kidney carcinoma. Cancer Res *54*, 3034-3041.

Xu, L., Overbeek, P. A., and Reneker, L. W. (2002). Systematic analysis of E-, N- and P-cadherin expression in mouse eye development. Exp Eye Res *74*, 753-760.

Yagi, T., and Takeichi, M. (2000). Cadherin superfamily genes: functions, genomic organization, and neurologic diversity. Genes Dev *14*, 1169-1180.

Yamagata, K., Andreasson, K. I., Sugiura, H., Maru, E., Dominique, M., Irie, Y., Miki, N., Hayashi, Y., Yoshioka, M., Kaneko, K.*, et al.* (1999). Arcadlin is a neural activity-regulated cadherin involved in long term potentiation. J Biol Chem *274*, 19473-11979.

Yamamoto, A., Amacher, S. L., Kim, S. H., Geissert, D., Kimmel, C. B., and De Robertis, E. M. (1998). Zebrafish paraxial protocadherin is a downstream target of spadetail involved in morphogenesis of gastrula mesoderm. Development *125*, 3389-3397.

Zhang, L., El-Hodiri, H. M., Ma, H. F., Zhang, X., Servetnick, M., Wensel, T. G., and Jamrich, M. (2003). Targeted expression of the dominant-negative FGFR4a in the eye using Xrx1A regulatory sequences interferes with normal retinal development. Development *130*, 4177-4186.

Zhang, S. S., Fu, X. Y., and Barnstable, C. J. (2002). Tissue culture studies of retinal development. Methods *28*, 439-447.

Ziman, M. R., Rodger, J., Chen, P., Papadimitriou, J. M., Dunlop, S. A., and Beazley, L. D. (2001). Pax genes in development and maturation of the vertebrate visual system: implications for optic nerve regeneration. Histol Histopathol *16*, 239-249.

Zuber, M. E., Gestri, G., Viczian, A. S., Barsacchi, G., and Harris, W. A. (2003). Specification of the vertebrate eye by a network of eye field transcription factors. Development *130*, 5155-5167.

8.1 Acknowledgements

8.2 Publication

Papers

1. **Ruan, G.**, David, R., Schlosser, G., and Wedlich, D. (2004). Xcadherin-6 is required for development of nervous system during *Xenopus laevis* development. (In preparation)

2. **Ruan, G.**, Wedlich, D., and Köhler, A. (2004). Xcadherin-6 is required in epithelial organization of neural and pigmented retina during optic cup formation. (In preparation)

3. **Ruan, G.**, Wedlich, D., Köhler, A. (2004). How cell-cell adhesion contributes to early embryonic development. In The Vertebrate Organizer / Horst Grunz (Ed.) Springer-Verlag, Berlin Heidelberg New York, pp. 201-218.

4. **Ruan, G.**, Chen, D. X., Liu, S., et al. (1998). The changes of the endothelium in peripheral microvessel induced by hypercholesteral diet and pretected by antioxidant vitamins in rabbit ear. Acta Academiae Medicinae Sinicae, *20(2)*, 94.

5. Chen, D. X., Yang, T., Song, F. J., **Ruan, G.**, et al. (1997). The inhibitory effects of antioxidant vitamins on serum oxLDL and experimental atherosclerosis of rabbit. Acta Academiae Medicinae Sinicae, *19(6)*, 451-5.

6. **Ruan, G.**, Liu, S., Zhao, H. Q., et al. (1997). Effects of smoking on microcirculation-mediated by lipid peroxidation and protected by free radical scavengers. Chinese Journal of Microcirculation, *7(4)*, 3-4.

7. **Ruan, G.**, Liu, S., Zhao, H. Q., et al. (1996). Angiogenesis and behaviors of relevant cells and tissues during wound healing process. Chinese Journal of Pathophysiology, *12(5)*, 558-9.

8. **Ruan, G.** (1996). Angiogenesis and its regulation. Chinese Journal of Microcirculation, *6(2)*, 35-7.

9. Zhang, S. L., and **Ruan, G.** (1994). Applicable methods for experimental and clinical studies on vascular endothelium. Chinese Journal of Microcirculation, *4(2)*, 4-6.

Invited Oral Presentation

- **Ruan, G.**, Köhler, A., David, R., and Wedlich, D.: *Xenopus* Cadherin-6 (Xcad-6) is required for retinogenesis during optic cup formation. 4th German-Italian *Xenopus* Meeting, Villa Vigoni (Loveno di Menoggio) Italy, October 2003

Posters

- **Ruan, G.**, Köhler, A., David, R., Schlosser, G., and Wedlich, D.: Xcadherin-6 is required for the formation of the eye and nervous system in *Xenopus* development. Annual Meeting of Cell Biology and Development (Deutsche Gesellschaft für Zellbiologie) 2003, Bonn, March 2003
- Völker, D., **Ruan, G.**, Wedlich, D., Kriebel, M., Hollemann, T., and Schlosser, G.: Role of *Xenopus* eya genes in placode development. 9th International Xenopus Conference, Hemerton College, Cambridge, UK, August 2002
- David, R., **Ruan, G.**, and Wedlich, D.: Misexpression of Cadherin-6 (Xcad-6), a type II cadherin, perturbs PNS-formation in *Xenopus* embryos. 14th Symposium of the Society of Developmental Biology (Gesellshcaft für Entwicklungsbiologie), Ulm, March 2001
- Wang, W. Y., Zhuang, F. Y., **Ruan, G.,** et al.: Controlled therapy of liver oxygen supply by imaging of functionalstructures in tissue. Saratov Fall Meeting'99 – Biophysics, Russia, October 1999